Extracellular Vesicles: Mechanisms of Cargo Selection and Cell-Cell Communication

By

Jessica J. Abner

Dissertation

Submitted to the Faculty of the

Graduate School of Vanderbilt University

In partial fulfillment of the requirements

for the degree of

DOCTOR OF PHILOSOPHY

in

Biological Sciences

May 14, 2021

Nashville, TN

Approved:

Katherine L. Friedman, PhD

James G. Patton, PhD

Robert J. Coffey, MD

Barbara Fingleton, PhD

Jared Nordman, PhD

Julie Rhoades, PhD

To my daughter, Jada,

Always remember that with dedication, hard work, and perseverance,

you can do anything you put your mind to

ACKNOWLEDGMENTS

This work would not have been possible without the financial support from Vanderbilt University Department of Biological Sciences and the Initiative for Maximizing Student Diversity. I am extremely grateful to my mentor, Dr. James G. Patton, for his guidance, support, and mentorship throughout my scientific career. Although unexpected circumstances brought me to your lab, I am thankful to have completed my graduate work under your supervision. Thank you for believing in me and always pushing me to think critically. I am a better scientist because of you. Thank you to my committee members and the many collaborators I've worked with especially Drs. Jeffrey Franklin, Kasey Vickers, Qi Liu, Robert Coffey, and Alissa Weaver, for your patience, guidance, and scientific discussions. I would also like to acknowledge past and present members of the Patton lab for their assistance, constant discussions, and scientific critiques throughout my graduate school experience, especially Dr. Scott Hinger and Margaret Clement.

In addition to the scientific community, I would like to thank my friends, both near and far, who kept me sane throughout this entire process. I am eternally grateful to my family who has always supported me, especially my mom and sister who continue to inspire me and push me to be the best I can be. Lastly, I would like to thank my husband, Kevin, and my daughter, Jada, for their constant love and support, and for providing daily inspiration to finish what I started.

This work was supported by grants from the National Institutes of Health, U19 CA179514 and PO1 CA229123.

TABLE OF CONTENTS

LIST OF TABLES

Table Page

LIST OF FIGURES

Figure Page

Chapter 1

Introduction

Cell-cell communication is critical for all organisms, and allows the exchange of information by direct interaction or through the secretion of soluble factors. This information can also be exchanged via extracellular vesicles (EVs), and the release of EVs by cells can impact local and distant cells. Interestingly, EVs were first thought to be cellular debris with no real significance until Raposo and colleagues described a role for EVs in stimulating adaptive immune responses (Raposo et al., 1996). They demonstrated that exosomes derived from B lymphocytes contained major histocompatibility complex (MHC) class II molecules on their surface, and presented antigens to T cells (Raposo et al., 1996). Zitvogel and co-authors expanded on this knowledge by showing that exosomes from dendritic cells also express MHC class II molecules, and tumor peptide-pulsed exosomes could suppress tumor growth *in vivo* (Zitvogel et al., 1998). Less than 10 years later, exosomes from primary mast cells and mast cell lines were found to contain and transfer RNA, including the presence of small RNAs (Valadi et al., 2007). This study, for the first time, showed exosomal transfer of mRNAs that could be functionally translated in recipient cells (Valadi et al., 2007). Together, these studies set the stage for EVs to serve as biologically relevant mediators of intercellular communication. Cell-cell communication via EVs has since been shown to play important roles in many physiological processes including development, immune function, and drug resistance (Colombo et al., 2014). For cancer, EVs are thought to be

critical for the establishment and maintenance of the tumor microenvironment, especially in promoting proliferation and metastasis, evading growth suppressors, inducing angiogenesis, and modulating immune responses (Kalluri, 2016, Han et al., 2019).

Advances over the last few years have increased our knowledge of EVs, especially in regards to cell-cell communication, impact on disease, and elucidation of EV biogenesis and cargo. However, much remains to be discovered. Key questions include quantitation of the effects of transfer of EV cargo on recipient cells, mechanisms that control the loading of cargo, and how EVs might be used for therapeutic approaches. This dissertation will focus on the regulation of EV cargo loading, focusing mostly on RNA, and the role of EVs in cancer emphasizing tumor microenvironment interactions.

Extracellular Vesicles

Extracellular vesicles (EVs) are released from all cell types, and allow exchange of lipids, proteins, and RNA (Maas et al., 2017, Raposo and Stahl, 2019). They can export material between donor and recipient cells and are thought to play a novel role in intercellular communication, tumor aggressiveness, and metastasis (Skog et al., 2008, Higginbotham et al., 2011, Demory Beckler et al., 2013). EVs are classified not only by size, but also by their biogenesis pathway (Colombo et al., 2014)(**Fig. 1**). Two major pathways for EV release have been described. The first occurs when intraluminal vesicles are formed by inward budding into late endosomes (multivesicular bodies;

MVBs) followed by release of those vesicles (exosomes) when MVBs fuse with the plasma membrane. Exosomes are a distinct subset of small EVs (sEVs) approximately 30-150nm in size that were originally discovered in the 1980s in studies of transferrin receptor trafficking in reticulocytes (Harding et al., 1983, Pan et al., 1985). Using electron microscopy, transferrin receptors were found to associate with small vesicles that were released when endosomes fuse with the plasma membrane. Johnstone and colleagues first used the term “exosome” to describe the small vesicles that form within MVBs that are released by exocytosis (Johnstone et al., 1987). The other major pathway of EV release occurs by direct budding of the plasma membrane causing secretion of a heterogeneous mixture of mostly large EVs (greater than 150nm)(Kowal et al., 2016, Raposo and Stoorvogel, 2013). As purification techniques evolve, so has vesicular nomenclature (Thery et al., 2018). Distinct EV subclasses are being characterized based on size (small EVs, large EVs, and non-vesicular content), cargo content, and biogenesis pathway (Jeppesen et al., 2019, Kowal et al., 2016). The EV field is constantly evolving, therefore the International Society of Extracellular Vesicles continues to update its processes for studying and characterizing EVs (Thery et al., 2018).

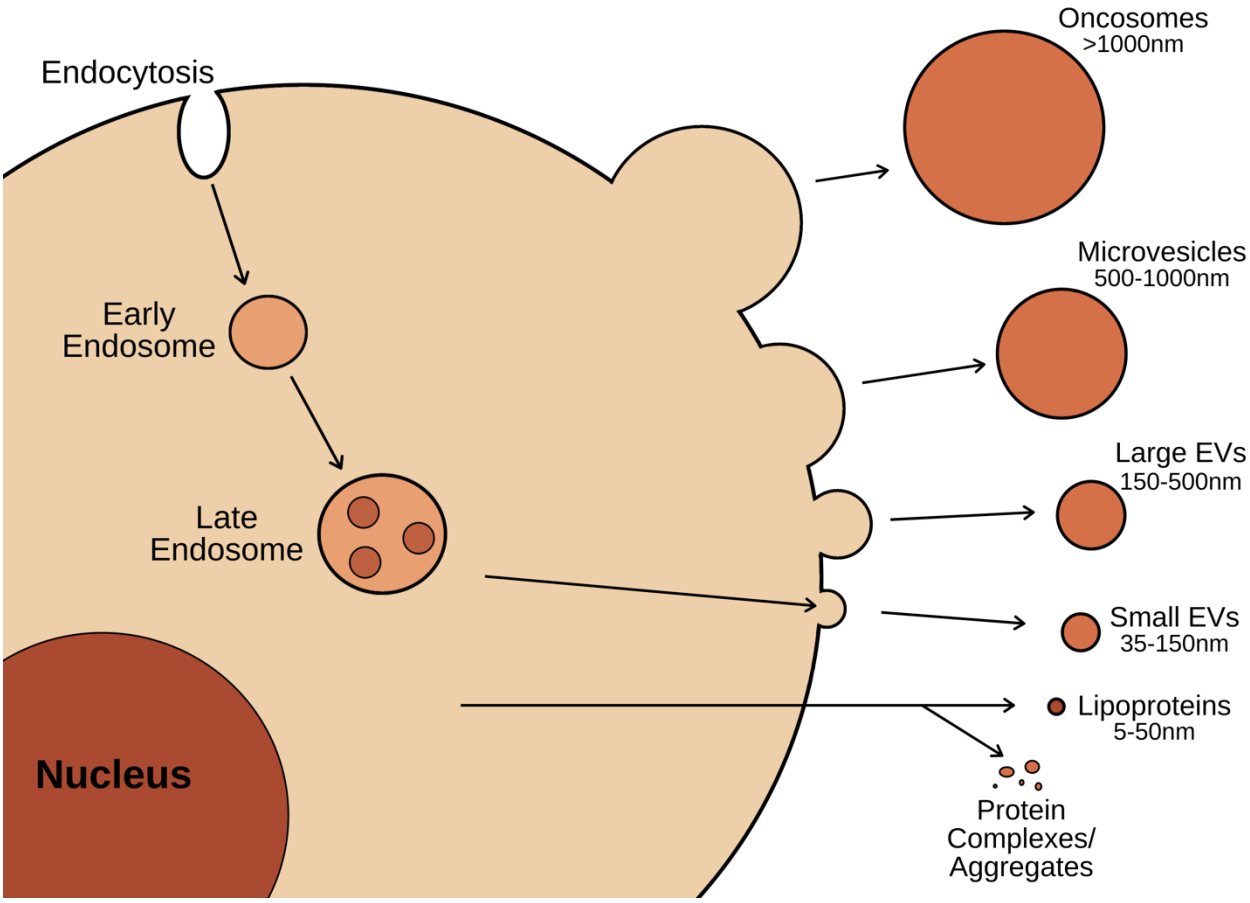

Fig. 1. EV biogenesis and secretion. Extracellular vesicles (EVs) are released from cells by two major pathways. Direct budding of the plasma membrane secretes oncosomes, microvesicles, and a heterogenous mix of large EVs into the extracellular space. Fusion of late endosomes (multivesicular bodies) release small EVs, traditionally referred to as exosomes. Extracellular RNA can also be released from cells associated with lipoproteins and protein-RNA complexes.

Depending on the biogenesis pathway, different mechanisms regulate the contents and release of EVs. MVBs are formed as part of the endocytic pathway (Gould and Lippincott-Schwartz, 2009). Internalization of the plasma membrane via phagocytosis or clathrin-mediated endocytosis forms early endosomes. Early endosomes mature and progress to MVBs, while inward budding of the membrane

forms intraluminal vesicles (ILVs) inside. MVBs were previously thought to just fuse with the lysosome for degradation (Futter et al., 1996); however, certain MVBs can fuse with the plasma membrane and release their contents (Raposo et al., 1996, Jaiswal et al., 2002). The primary pathway for ILV formation (and thus exosome formation) is via endosomal sorting complexes required for transport (ESCRT) machinery (Schmidt and Teis, 2012). Proteomic studies have detected a number of ESCRT proteins in secreted vesicles (Thery et al., 2001), and ESCRT complexes have been proposed to regulate exosome secretion (Hoshino et al., 2013, Colombo et al., 2013). Although ESCRT machinery seems to be the main driver of exosome secretion, ESCRT-independent mechanisms have been identified and seem to rely on specific lipids, like ceramide, at the surface of MVBs that are responsible for secretion (Matsuo et al., 2004). A heterogenous mixture of large EVs, like microvesicles (MVs), form from direct budding of the plasma membrane. MVs can be formed through contraction of cytoskeletal proteins and the redistribution of phospholipids at the plasma membrane. Actin polymerization is needed for initial MV budding. Flippases and floppases can form asymmetric microdomains, and phosphatidylserine redistribution leads to membrane curvature and budding of the plasma membrane (Bevers et al., 1999, Hugel et al., 2005, D'Souza-Schorey and Schorey, 2018). However, some overlap between biogenesis pathways exist, for example TSG101, an ESCRT-I subunit, has been linked to both MV and exosome biogenesis (Colombo et al., 2013). Therefore, understanding the diversity and heterogeneity of EVs and their biogenesis is becoming increasingly more important.

The orientation of EVs is similar to cells, such that extracellular receptors and ligands are positioned on the outside, and cytoplasmic proteins and RNAs are on the inside. This gives EVs the ability to protect their internal cargo and potentially deliver it to specific cells through ligand-receptor binding or by other mechanisms that could include direct transfer by gap junctions, fusion of EVs with the plasma membrane, uptake of EVs by some form of endocytosis, release of ligands from or on the surface of EVs stimulating receptors on the cell surface, or connection of cells through nanotubes or microtubes (Maas et al., 2017).

EV-mediated Cell-Cell Communication in the Tumor Microenvironment

Studies have shown that cancer cells secrete significantly more EVs than normal cells (D'Souza-Schorey and Clancy, 2012), thereby making them attractive vehicles to transport cargo both locally and at distant sites. This could prove advantageous to cancer cells by contributing to overall cancer progression and drug resistance (Melo et al., 2014, Boelens et al., 2014). A key to this success is the involvement of the tumor microenvironment. The tumor microenvironment consists of a heterogenous mixture of cancer cells, normal cells, vasculature, extracellular factors, and extracellular matrix proteins. The seed and soil hypothesis by Stephen Paget in 1889, posits that the "seed" (cancer cells) needs the proper "soil" (tumor microenvironment) to grow (Paget, 1889). This theory was derived in part based on work by Langenbeck, who concluded that "every single cancer cell must be considered a living organism, alive and capable of development" (Paget, 1889). Thus, for cancer cells to grow and develop, not only does

the tumor microenvironment play a role, but also the pre-metastatic niche provides the proper soil for tumor spread.

Recently, EVs have been proposed to serve as a unique form of cell-cell communication, both locally within the tumor microenvironment and at distant metastatic sites. They can affect cell-cell communication within the tumor microenvironment and also play a role in metastasis through pre-metastatic niche formation (Peinado et al., 2017). The pre-metastatic niche facilitates future arrival of metastatic cells in a seed and soil manner. The development of metastasis-promoting mutations, and a suitable environment for metastasis, are key factors necessary for the formation of the pre-metastatic niche (Wortzel et al., 2019). The decision regarding where metastasis will occur is not random, but rather a precise, predetermined process regulated by primary tumor-secreted factors (Kaplan et al., 2005). In breast cancer, pre-metastatic niches can be formed in the brain by EV transfer of tumor derived *miR-122* (Fong et al., 2015). Similarly, *miR-23b* can be secreted from bladder cancer cells to support metastatic progression (Ostenfeld et al., 2014). Cell-cell communication is vital for metastasis, and crosstalk between primary tumor cells and the microenvironment of distant organs via EVs may be a key contributor to the formation and sustainment of the pre-metastatic niche (**Fig. 2**) (Wortzel et al., 2019). Metastatic melanoma EVs were proposed to promote pre-metastatic niche formation by educating and reprogramming bone marrow-derived cells towards a pro-vasculogenic phenotype (Peinado et al., 2012). When EV secretion in tumor cells was reduced by knockdown of Rab27a, pre-metastatic niche formation and metastasis was impaired (Peinado et al., 2012).

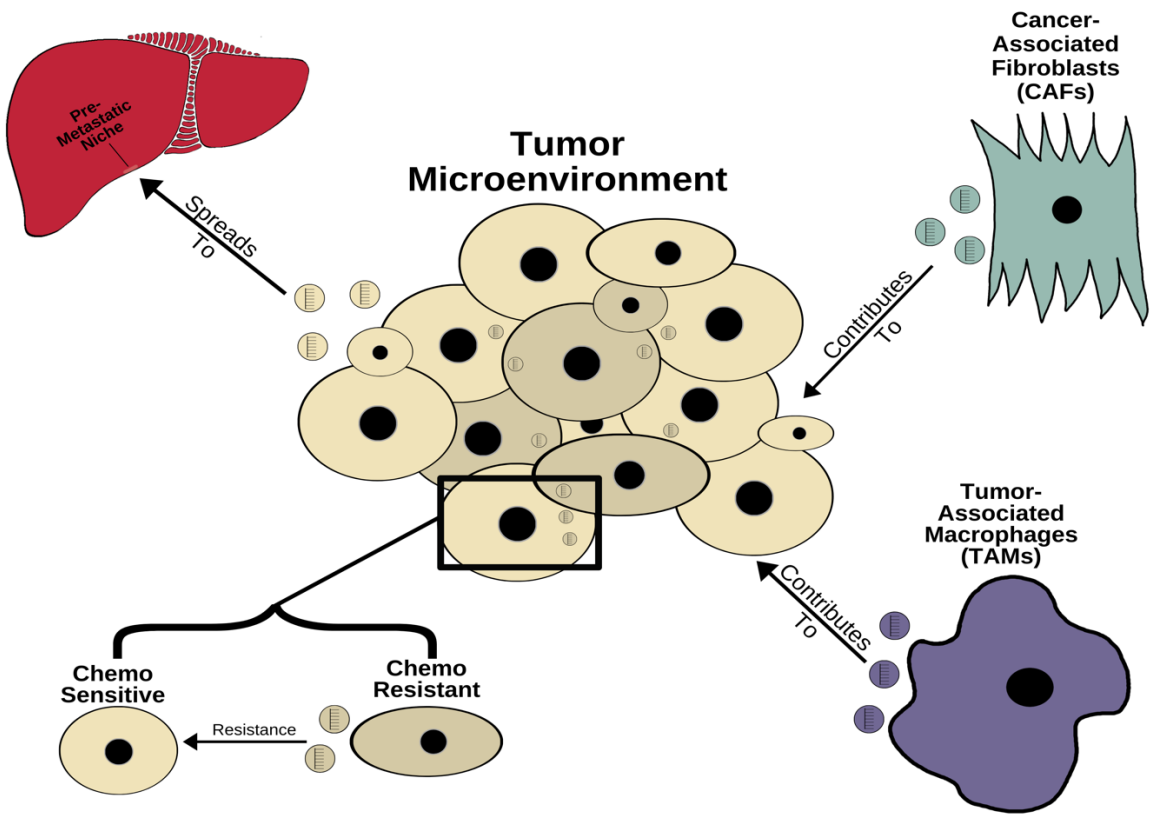

Fig. 2. Crosstalk between cells and the tumor microenvironment via EVs. Cell-cell communication via EVs can contribute to the spread of chemoresistance and the formation of the pre-metastatic niche. CAFs and TAMs secrete EVs that can influence the tumor microenvironment. Chemoresistant cells can transfer resistance to chemosensitive cells via EVs, which can then spread to and contribute to pre-metastatic niche formation.

Bidirectional communication between cells in the tumor microenvironment via EVs can play a key role in cancer initiation, development, and progression (Hu et al., 2020). Enhanced secretion of EVs from cancer cells, along with the changes in EV cargo has contributed to increased tumorigenesis. Cancer associated fibroblasts (CAFs) are a key component in tumor development, and interplay between these cells and tumor cells within the tumor microenvironment contributes to tumor progression

(Fozzatti and Cheng, 2020). The bidirectional communication between cells and extracellular matrix (ECM) components can shape tissues through cell-matrix interactions and remodeling of the ECM (Winkler et al., 2020). Immune cells, like tumor associated macrophages (TAMs), play critical roles in ECM remodeling and promoting tumor angiogenesis by serving as important sources for ECM remodeling proteases (Winkler et al., 2020). Overall, this communication allows tumors to take advantage of their surroundings and create an environment that supports tumor growth and metastasis.

EVs and Chemotherapy Resistance

Resistance to chemotherapy is a common problem that complicates therapeutic approaches to cancer treatment. Both *de novo* and acquired mutations within tumors can lead to the selection of cells that escape treatment and decrease survival times. Current research seeks to understand the mechanisms of resistance to identify key genes whose mutation can confer drug resistance. While combinations of chemotherapeutic agents that target multiple gene products can sometimes overcome mutational forms of resistance, non-mutational forms of resistance can be more difficult to treat. Understanding the mechanisms underlying epigenetic or non-mutational forms of resistance is needed to identify additional drug targets that will allow versatile treatment strategies. EVs are gaining an increasingly important role in drug resistance, and therapeutic approaches that can inhibit the ability of EV-mediated drug resistance would be a powerful ally in cancer treatment.

One way drug resistance can be transferred is via EVs (Lu et al., 2017, Qu et al., 2016, Zhang et al., 2018a, Lei et al., 2018, Santos and Almeida, 2020, Au Yeung et al., 2016). Drug resistance is a complex process with a plethora of known mechanisms, some of which include alterations in drug metabolism, mutation of drug targets, DNA damage repair, or enhanced drug efflux (Alsop et al., 2012, Cardona et al., 2017, Nientiedt et al., 2017, Sakai et al., 2008, Fletcher et al., 2016). Cetuximab (CTX) is a monoclonal antibody against the epidermal growth factor receptor (EGFR) that is used to treat colorectal cancer (CRC) and head and neck squamous cell carcinoma (HNSCC)(Brand et al., 2011, Montagut et al., 2012, Arena et al., 2015, Bardelli and Siena, 2010). Development of CTX resistance occurs frequently and poses a significant problem for treatment (**Fig. 3**). Commonly, CTX resistance is due to mutation in EGFR or downstream signaling pathways (Brand et al., 2011). However, Coffey and colleagues found that cellular levels of MIR100HG, along with *miR-100* and *miR-125b*, are elevated in CTX resistant CRC and head and neck cancer cell lines leading to activation of Wnt signaling (Lu et al., 2017). Similarly, *miR-143* and *miR-145* are downregulated in colon cancer but overexpression of these miRNAs can lead to increased sensitivity to CTX (Gomes et al., 2016). Also, *miR-302a* expression is decreased in CRC cells and tissues leading to decreased overall survival (Sun et al., 2019). In normal cells, *miR-302a* inhibits metastasis and maintains CTX susceptibility by targeting NFIB and CD44 (Sun et al., 2019). Lastly, decreased expression of *miR-31* enhances CTX susceptibility; patients with low expression of *miR-31* responded better to CTX compared to Bevacizumab (another antibody to treat CRC) (Laurent-Puig et al.,

2019). We have recently discovered that *miR-100* and *miR-125b* are enriched in EVs and can spread CTX resistance (unpublished).

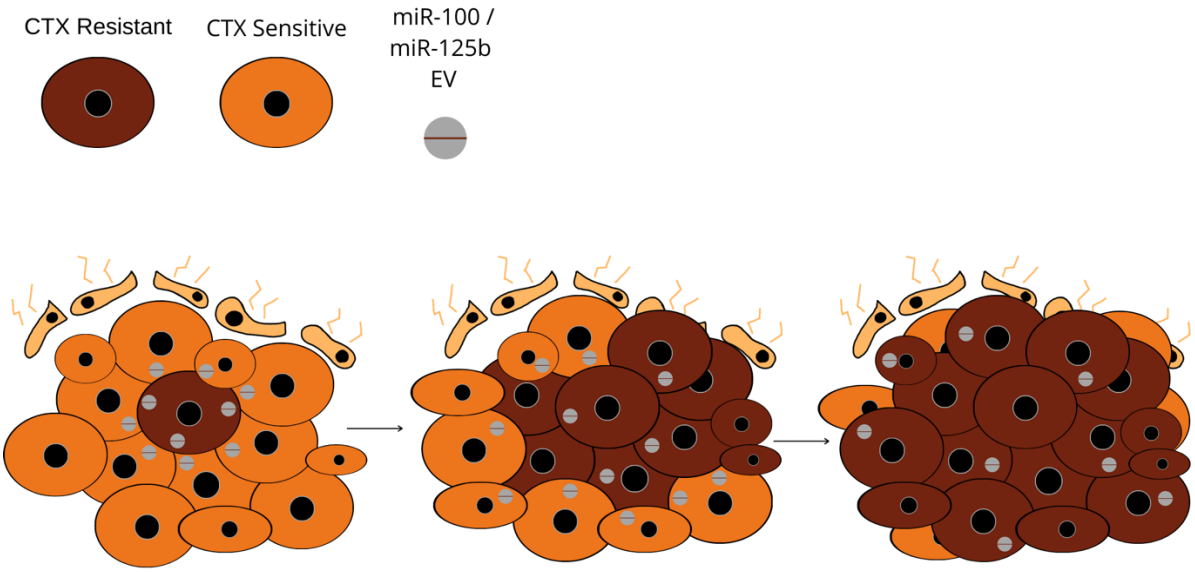

Fig. 3. Development of cetuximab resistance. CTX resistant cells can transfer resistance to CTX sensitive cells via EVs containing *miR-100* and *miR-125b*.

Sunitinib is a small molecule, multitarget receptor tyrosine kinase (RTK) inhibitor used to treat renal cell carcinoma (RCC). Resistance to Sunitinib poses a major challenge to patients with RCC. Qu et al. (2016) first identified lncARSR (lncRNA Activated in RCC with Sunitinib Resistance) and found that its overexpression correlated with poor Sunitinib response (Qu et al., 2016). Like *miR-100* and *miR-125b*, EV transfer of lncARSR from Sunitinib resistant cells can transfer resistance to recipient RCC cells. The mechanism behind resistance is due to lncARSR serving as a

competing endogenous RNA that competitively binds and sequesters *miR-34* and *miR-449* (Qu et al., 2016). A single nucleotide polymorphism (SNP) within lncARSR (rs7859384) was found to correlate with decreased risk of RCC, and may therefore act as a prognostic biomarker for RCC patients (Xing et al., 2019). In hepatocellular carcinoma (HCC), upregulation of lncARSR promoted doxorubicin resistance so that lncARSR might also serve as a prognostic biomarker for HCC (Li et al., 2017).

Like Sunitinib, Erlotinib and Gefitinib are small molecule RTK inhibitors that act as EGFR inhibitors in the treatment of non-small cell lung cancer (NSCLC). The lncRNA RP11-838N2.4 is upregulated in Erlotinib-resistant NSCLC cells and knocking down this RNA promotes Erlotinib-induced cytotoxicity (Zhang et al., 2018a). Treatment with exosomes containing RP11-838N2.4 causes transfer of Erlotinib resistance to sensitive cells (Zhang et al., 2018a). Similarly, lncRNA H19 is packaged into exosomes (mediated by hnRNPA2/B1) and can be transferred to spread Gefitinib resistance in NSCLC (Lei et al., 2018).

Cancer associated fibroblasts (CAFs) secrete EVs that can promote drug resistance through extracellular RNA (exRNA) (Santos and Almeida, 2020). EVs that originate from CAFs can induce chemotherapy resistance in several different cancer types. *miR-21* secreted from CAFs has been proposed to promote Paclitaxel resistance in ovarian cancer (Santos and Almeida, 2020, Au Yeung et al., 2016). In pancreatic cancer, EVs released from CAFs contain *miR-106b* and *miR-146a*, that are thought to increase proliferation, in addition to inducing resistance to Gemcitabine, a nucleoside

analog that blocks DNA replication (Fang et al., 2019, Richards et al., 2017). EVs from CAFs in head and neck cancer contain *miR-196a,* and transfer of *miR-196a* is thought to lead to Cisplatin resistance (Qin et al., 2019). In addition to drug resistance, CAF EVs containing *miR-16* and *miR-148a* are thought to increase proliferation and metastasis in breast cancer (Zhou et al., 2020).

Besides CAFs, tumor associated macrophages (TAMs) also play a key role in the spread of chemotherapy resistance in cancer. TAMs are macrophages that invade tumors and are the most prevalent immune cell within the tumor microenvironment (Santos and Almeida, 2020, Son et al., 2016). EVs secreted by TAMs containing *miR-365* have been shown to play a role in Gemcitabine resistance in pancreatic cancer cells (Binenbaum et al., 2018). Transfer of *miR-21* from TAMs led to Cisplatin resistance in gastric cancer cells, as well as suppression of apoptosis (Zheng et al., 2017). *miR-223* secreted from TAMs can also induce Cisplatin resistance in ovarian cancer cells (Zhu et al., 2019). Taken together, both CAFs and TAMs appear to release EVs that can induce the spread of chemotherapy resistance within the tumor microenvironment. The ability to block EV release or in other ways block the action of secreted miRNAs could be important for improvement of cancer treatment and therapy (Poggio et al., 2019, Chen et al., 2018, Haderk et al., 2017).

Tumor cells themselves can release EVs that have the potential to alter gene expression patterns in adjacent normal cells and also increase the spread of drug resistance within the tumor microenvironment. One of the targets of *miR-100* is mTOR

and transfer of *miR-100* from KRAS mutant CRC cells to wild type KRAS cells can alter mTOR expression in recipient cells (Cha et al., 2015). *miR-200b* is upregulated in colorectal cancer and promotes the suppression of p27 expression to promote cell proliferation (Zhang et al., 2018c). In non-small cell lung cancer, Gefitinib resistance can spread via EV transfer of *miR-214* (Zhang et al., 2018b, Guo et al., 2020). Through TEM and nanoparticle trafficking, Wei et al. (2014) noted that resistant breast cancer cells were able to transfer resistance to non-resistant cells by transfer of *miR-221* and *miR-222* (Wei et al., 2014). EV transfer of *miR-30a*, *miR-100* and *miR-222* also contributes to chemotherapy resistance in breast cancer (Chen et al., 2014c). Jaiswal et al. (2012) reported that EVs secreted from multidrug resistant cells can transfer miRNAs from drug-resistant to drug-sensitive cells leading to altered gene expression in recipient cells (Jaiswal et al., 2012). EVs from breast cancer cell lines were also proposed to be capable of transferring specific miRNAs (*miR-100, miR-222, and miR-30a*) from drug-resistant cells to drug-sensitive cells following co-culture with EVs (Chen et al., 2014c). Also, *miR-1246, miR-23a, miR-16, and let-7a* were four of the 20 most abundant miRNAs found in EVs secreted from drug-resistant cells in a breast cancer model, and incubation of these EVs could transfer docetaxel resistance to recipient cells (Chen et al., 2014b).

Extracellular Vesicle Cargo

Given the above studies that showed how EVs play a role in cell-cell communication and transfer of drug resistance, a key next step is to identify the essential cargo components that contribute to phenotypic transfer. EV cargo includes

varying amounts of lipids, proteins, and RNA molecules. The cargo present within EVs has been widely assessed and found to be cell-, disease-, and context-specific. Datasets have pointed to large numbers of proteins and RNAs secreted into vesicles (Kalra et al., 2012). Distinct classes of EVs likely contain a unique composition of their respective cargo due to differences in biogenesis pathway (Raposo and Stoorvogel, 2013).

EV Protein Cargo

Protein cargo is an important component in EVs, and proteomic profiles can vary depending on how vesicles are purified. Original studies on protein composition in dendritic cell exosomes found that specific sets of protein families were enriched in these vesicles, and that these sEVs were clearly different from apoptotic vesicles (Thery et al., 2001, Thery et al., 1999). EVs are extremely abundant in plasma membrane, cytoskeletal, cytosolic, vesicular trafficking, and heat shock proteins, while containing minimal amounts of nuclear, Golgi, and endoplasmic reticulum proteins (Thery, 2011). Recent findings have reassessed the composition of EVs, and sought to standardize proteins used for detection (Jeppesen et al., 2019). Currently, the main proteins used as EV markers include: tetraspanins (particularly CD63, CD81, and CD9), and ESCRT and accessory proteins (like Alix, Flotillin, TSG101, and HSP70) (Thery et al., 2018). Tetraspanins are arguably the most used EV marker. They are a highly conserved family of membrane proteins enriched on the surface of EVs and involved in the sorting of various cargo to EVs (van Niel et al., 2015, Buschow et al., 2009, Chairoungdua et al., 2010). Interestingly, EVs also contain receptor ligands and cell receptors,

supporting a mechanism in cell-cell communication that involves receptor signaling (Demory Beckler et al., 2013, Higginbotham et al., 2011, Skog et al., 2008, Singh and Coffey, 2014). Depending on cell type, EVs display cell-type specific proteins that account for their fate and function (van Niel et al., 2018).

EV RNA Cargo

Extracellular RNA (exRNA) encompasses RNA molecules found outside the cell, usually packaged in EVs, lipoproteins, or protein complexes (Sadik et al., 2018). In 2007, Lotvall and colleagues reported that mouse mast cells secrete functional mRNAs that can be taken up by recipient cells (Valadi et al., 2007). Since then, a large number of different RNAs have been detected in the extracellular space including miRNAs, mRNAs, fragmented tRNAs, fragmented rRNAs, circRNAs, lncRNAs, and many other small ncRNAs (Valadi et al., 2007, Cha et al., 2015, Hinger et al., 2018, Crescitelli et al., 2013, Dou et al., 2016). miRNAs have been discovered in almost every body fluid including serum, urine, and breast milk, usually packaged in EVs (Freedman et al., 2016). Virtually all known classes of RNA can be detected at varying levels of abundance in EVs, but those levels often do not reflect cellular abundance suggesting either differential stability or selective export (**Fig. 4**).

Quantitative analysis of miRNA content in EVs has suggested that only a small fraction of EVs actually carry miRNAs raising questions as to how effective gene expression can change in recipient cells (Chevillet et al., 2014). Also, many of the RNAs that can be detected in EVs are fragments of larger RNAs, which could indicate

that the majority of secreted RNAs are simply being discarded as trash by cells (Turchinovich et al., 2016). However, many papers have indicated that RNA transfer is indeed possible and that exRNAs can have functional effects on recipient cells (Cha et al., 2015, Valadi et al., 2007, Hinger et al., 2018, Dou et al., 2016). Research is ongoing to fully understand the quantitative effects that EVs can have on gene expression in recipient cells.

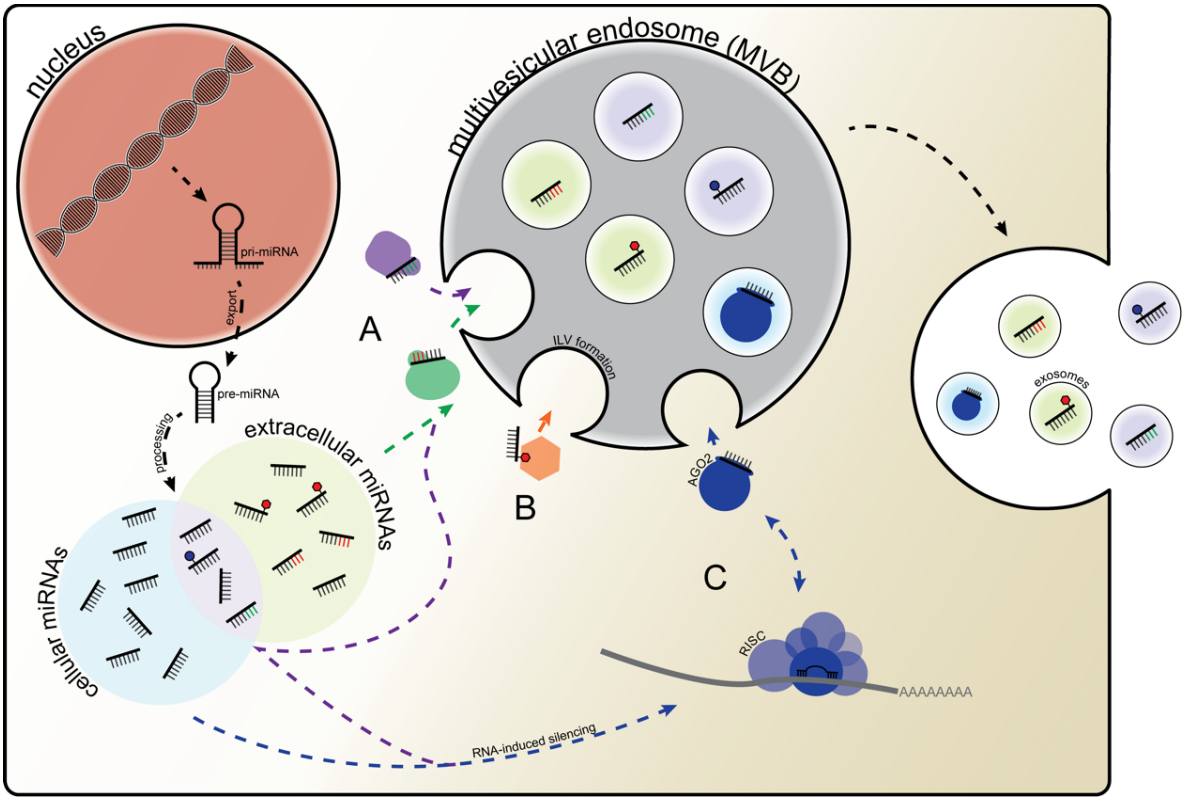

Fig. 4. Selective export of miRNAs. Cellular RNA levels do not always reflect RNA levels in EVs suggesting selective export. Possible mechanisms regulating selective miRNA export include sequence-specific export signals (A), specific RNA base modifications (B), or preferential loading of miRNAs associated with RISC on the surface of MVBs (C) (McKenzie et al., 2016, Gibbings et al., 2009).

EV miRNAs

MicroRNAs (miRNAs) are the best characterized and most well studied group of exRNA. A surprising finding from the human genome sequencing project is that only about 2-3% of the genome encodes proteins. While it was previously thought that the remainder of the genome consisted of lots of "junk" DNA, it is now clear that the majority of the human genome is transcribed into RNA in cell- and developmental-specific patterns (Hangauer et al., 2013). The majority of noncoding RNA transcripts remain uncharacterized with the exception of miRNAs and a small subset of long noncoding RNAs (lncRNAs). miRNAs are 22 nucleotides long and post-transcriptionally regulate gene expression by binding to 3'UTR elements in target mRNAs (Krol et al., 2010, Bartel, 2018, Gebert and MacRae, 2019). Primary and precursor miRNA transcripts are processed by Drosha and Dicer, respectively, in order to form mature miRNAs (Kim, 2005). During processing, miRNAs associate with one or more members of the Argonaute family in RNA Induced Silencing Complexes (RISC)(Filipowicz, 2005). The mechanism for gene silencing involves binding of miRNAs to partially complementary sequences in mRNA targets causing deadenylation, decapping, and degradation of transcripts (Giraldez et al., 2006, Guo et al., 2010). If binding is perfect, mRNA degradation occurs due to cleavage by Ago2 within the RISC. miRNAs play important roles in a number of processes including development, regeneration, cancer and metastasis (Alvarez-Garcia and Miska, 2005). They have also been shown to associate with various extracellular complexes including EVs (Cha et al., 2015, Valadi et al., 2007), Ago2 complexes (Arroyo et al., 2011), and high density lipoproteins (HDLs) (Vickers et al., 2011).

EV lncRNAs

lncRNAs are classified as transcripts >200 nucleotides that lack open reading frames greater than 100 amino acids (Rinn and Chang, 2012, Kopp and Mendell, 2018). It is estimated that there may be over 100,000 lncRNAs in the human genome with most completely uncharacterized (Zhao et al., 2016). For those that have been characterized, the evidence indicates that lncRNAs are involved in numerous cellular and biological processes including chromatin dynamics and gene regulation (Kopp and Mendell, 2018). lncRNAs are expressed in all cells, with misregulation linked to tumorigenesis and metastasis (Bhan et al., 2017, Fang and Fullwood, 2016). lncRNAs can influence gene expression or regulate chromatin either in *cis* or in *trans* by multiple potential mechanisms: 1) regulation of chromatin accessibility due to transcription of the lncRNA, 2) direct mediation of sequence-specific effects by the lncRNA, 3) function as a scaffold to link proteins together, or 4) serve as a guide targeting proteins or protein complexes to specific locations, including DNA. Some lncRNAs act as host genes such that the lncRNA itself might not have a function but instead, smaller RNAs, including miRNAs, are processed from the larger lncRNA (Rodriguez et al., 2004). As more and more lncRNAs are characterized, they have been proposed to play important roles in cellular communication, metastasis, and tumor cell progression (Schmitt and Chang, 2016). It is also possible that small open reading frames within lncRNAs can be translated (Chen et al., 2020).

miR-100, miR-125b, and Cancer

Two of the more well studied miRNAs whose expression patterns have been extensively analyzed in cancer cells, and that are also enriched in EVs from cancer cells, are *miR-100 and miR-125b* (Cha et al., 2015, Hinger et al., 2018, Emmrich et al., 2014, Luo et al., 2017). These miRNAs are encoded within intron 3 of the highly conserved lncRNA MIR100HG (Emmrich et al., 2014). A second *miR-125b* locus is encoded within intron 6 of the lncRNA LINC00478 (Emmrich et al., 2014).

miR-100 and *miR-125b* can regulate multiple signaling cascades including the Wnt/β-catenin pathway and multiple pathways downstream of transforming growth factor-beta (TGF-β) (Lu et al., 2017, Jiang et al., 2016, Ottaviani et al., 2018). Lu and colleagues found that *miR-100* and *miR-125b* activate Wnt signaling by targeting and repressing five negative regulators of Wnt signaling in colorectal cancer cells (Lu et al., 2017). In contrast, *miR-100* was reported to inhibit the migration and invasion of breast cancer cells by targeting the receptor FZD-8, leading to inhibition of Wnt/β-catenin signaling (Jiang et al., 2016). In adrenocortical carcinoma, Wnt signaling, along with IGF2 and TP53 pathways, are dysregulated leading to downregulated expression of *miR-100* and *miR-125b* (Cherradi, 2016, Patterson et al., 2011). Ottaviani et al. (2018) determined that *miR-100* and *miR-125b* regulate multiple pathways downstream of TGF-β (Ottaviani et al., 2018). TGF-β induces expression of *miR-100* and *miR-125b* and inactivation of these miRNAs affects TGF-β-mediated responses in pancreatic ductal adenocarcinoma. In contrast, *miR-100* and *miR-125b*, in conjunction with *miR-99a* and *let-7a*, are highly expressed in hematopoietic stem cells and an aggressive

form of leukemia, and function to block TGF-β signaling by repressing SMADs while also elevating Wnt signaling by inhibiting the destruction complex (Emmrich et al., 2014).

In breast cancer, expression of *miR-125b* has been postulated to have both negative and positive effects on prognosis and outcomes. Luo et al. (2017) reported that *miR-125b* is significantly increased in breast cancer tissues compared to noncancerous tissues, and that increased expression of *miR-125b* correlates with poor prognosis (Luo et al., 2017). However, Hu et al. (2018) and Feliciano et al. (2013) reported that *miR-125b* acts as a tumor suppressor as it is significantly downregulated in breast cancer tumors and cell lines compared to non-tumor tissues and control cell lines (Hu et al., 2018, Feliciano et al., 2013). Similar to *miR-125b*, expression of *miR-100* has also been reported to have opposite effects depending on cancer cell types. Jiang et al. (2016) reported that *miR-100* inhibited breast cancer cells ability to migrate and invade, while Wang et al. (2015) observed that overexpression of *miR-100* in macrophages led to enhanced invasion and chemotherapy resistance (Jiang et al., 2016, Wang et al., 2015). In contrast, silencing of *miR-100* in SK-BR-3 breast cancer cells induced cell cycle arrest and apoptosis, leading to the suppression of tumor cell growth *in vitro* and *in vivo* (Gong et al., 2015).

For colorectal cancer (CRC), *miR-100 and miR-125b* have been studied extensively. In wildtype KRAS CRC cells, *miR-100* levels are increased compared to mutant KRAS CRC cells (Cha et al., 2015). However, when compared to BRAF-mutant

CRC cells, mutant KRAS CRC cells showed increased expression of *miR-100* (Lundberg et al., 2018). Chen et al. (2014) proposed that *miR-100* is a good biomarker for prognosis of CRC, with expression levels dramatically lower in CRC tissues compared to normal tissues and with lower expression levels correlating with decreased overall survival (Chen et al., 2014a). For metastasis, downregulation of *miR-100 and miR-125b* was reported to be closely associated with lymph node metastasis in early CRC (Fujino et al., 2017). In contrast, high expression levels of *miR-125b* were reported to be associated with poor prognosis and tumor invasiveness (Nishida et al., 2011).

Overall, both positive and negative roles in a variety of cancers have been proposed for the cellular levels of *miR-100* and *miR-125b*. Studies have started to look at the potential of these miRNAs as biomarkers in the extracellular space as well as prognostic biomarkers for cancer (Liu et al., 2017, Fan et al., 2018, Yamada et al., 2015). Ongoing research will continue to shed light on the multifaceted nature of miRNAs.

Regulation of EV Cargo Loading

Although EV cargo includes protein components, a focus of this dissertation is how specific RNAs are exported into EVs. As described above, EVs contain a diverse population of RNAs, but the mechanism controlling their loading and function in EVs remains largely unknown. Varying levels of RNA molecules between cellular and EV samples have led to a desire to understand what accounts for these differences. Some

of the differences could be due to differential stability, but a specific regulatory mechanism might also drive selective export of specific RNAs. Mechanisms regulating cargo content have been proposed in cell- and disease-specific contexts and many studies have shown that distinct subsets of miRNAs are secreted from cells (Simons and Raposo, 2009, Shifrin et al., 2013, Maas et al., 2017, Cha et al., 2015, McKenzie et al., 2016, Shurtleff et al., 2016, Shurtleff et al., 2017, Villarroya-Beltri et al., 2013, Squadrito et al., 2014, Santangelo et al., 2016). However, to date, there is no universal mechanism that can account for selective miRNA export across a variety of model systems. Proposed mechanisms regulating export and differential enrichment of miRNAs in EVs thus far include RNA sequence motifs and specific RNA binding proteins, however, a combination of the two or something else entirely may be the key for a unifying mechanism of selective miRNA export.

One proposed mechanism for selective export is an RNA sequence motif where a small motif could serve as the signal for export of miRNAs to EVs. There are a number of different motifs that have been identified thus far. Villarroya-Beltri and colleagues used an unbiased search for specific sequence motifs that were overrepresented in exosomal miRNAs (Villarroya-Beltri et al., 2013). In human primary T cells they identified the EXO motif (GGAG) that occurred in the 3' half of miRNAs in 75% of cases tested (Villarroya-Beltri et al., 2013). Another EXO motif (CCCU) was also identified, but it does not occur at a characteristic position (Villarroya-Beltri et al., 2013). A different sequence motif, hEXO, was identified in targeting miRNAs to EVs in hepatocellular carcinoma cells. The presence of GGCU, the core sequence of the

hEXO motif, was found to greatly enhance miRNA loading into hepatocyte exosomes (Santangelo et al., 2016). Cis-acting sequences, or zipcodes, have also been identified using bioinformatic approaches. A combination of three sequences (ACCAGCCU, CAGUGAGC, and UAAUCCCA) was found significantly enriched in secreted exosomal RNAs (Batagov et al., 2011). Another zipcode sequence, CUGCC, was enriched in mRNAs from human glioblastoma multiforme microvesicles and shown to enhance their export to these vesicles (Bolukbasi et al., 2012).

The likelihood is that specific RNA binding proteins bind the above motifs to drive miRNA export. Heterogeneous nuclear ribonucleoprotein A2/B1 (hnRNPA2/B1) specifically binds exosomal miRNAs containing the EXO motif (Villarroya-Beltri et al., 2013). Sumoylation of hnRNPA2/B1 apparently controls its binding to miRNAs in T cells (Villarroya-Beltri et al., 2013). Synaptotagmin-binding cytoplasmic RNA-interacting protein (SYNCRIP) was identified as a component of the hepatocyte exosomal (hEXO) miRNA sorting machinery (Santangelo et al., 2016). Knockdown of SYNCRIP was found to impair sorting of miRNAs containing hEXO motifs to exosomes (Santangelo et al., 2016). In HEK293T cells, Shurtleff and colleagues identified the RNA binding protein Y-box protein 1 (YBX1) as an important mediator of miRNA export (Shurtleff et al., 2016). Using a cell-free system they showed that YBX1 binds to *miR-223* and is required for its sorting to exosomes (Shurtleff et al., 2016).

Overall, the data support the view that RNA secretion into EVs is a selective process, but no single motif or RNA binding protein has been identified that could unify the various studies.

Regulation of EV Export by Rab13

Previously, we showed that EV cargo is regulated in a KRAS-dependent manner (Cha et al., 2015, Hinger et al., 2018, Dou et al., 2016, McKenzie et al., 2016). Specifically, differential enrichment of miRNAs and lncRNAs was observed when cellular and EV RNA profiles were compared between KRAS mutant and wildtype colorectal cancer cell lines (Cha et al., 2015, Hinger et al., 2018). Recently, we also found that Rab13 can act as both a cargo protein and regulator of sEV secretion (Hinger et al., 2020). Analysis of our data from the above papers identified some of the previously mentioned RNA sequence motifs and RNA binding proteins contributing to miRNA export, but many exported miRNAs did not contain these sequence elements and it was unclear if any one RNA binding protein was driving export. This led us to test the role of RNA base modifications in miRNA export. Secretion signals might include both an RNA motif and one or more modified nucleotides, either within the motif itself or directly adjacent to the motif (Wu et al., 2018a).

RNA Modifications as a Mechanism for Selective Export

As discussed above, numerous mechanisms and RNA binding proteins have been proposed to regulate EV RNA cargo, but none provide a unifying or universal mechanism. While it remains possible that all export is cell and context specific, it is

also possible that additional work will generate a common mechanism. In Chapter 2, this dissertation includes data that support a role for RNA base modifications as part of the regulatory machinery that regulates EV miRNA export. RNA modifications have been studied for well over 50 years. Modified nucleotides were first discovered in abundant cellular RNAs in 1960 (Cohn, 1960), with the first 10 modifications identified after the sequencing of biological RNA in 1965 (Holley et al., 1965). Currently there are over 130 modifications identified (Schaefer et al., 2017). RNA modifications are gaining increasing attention due to their dynamic role in regulating gene expression and RNA metabolism. Modifications are controlled by distinct writers, readers, and erasers of RNA modifications. Writers and erasers are responsible for adding and removing modifications, respectively, while readers bind to modifications and mediate a lot of the functions and mechanisms of writers and erasers (Zaccara et al., 2019, Roundtree et al., 2017, Barbieri and Kouzarides, 2020). The dynamic quality of addition, subtraction, and reading of RNA base modifications are thought to play important roles in regulating splicing, export, degradation, or translation of RNA (Zaccara et al., 2019, Roundtree et al., 2017).

Modifications are seen across a number of different RNA molecules including tRNAs, rRNAs, mRNAs, and ncRNAs. With approximately 13 modifications per molecule, tRNAs are the heaviest modified class of RNA in regards to number, density, and diversity (Pan, 2018). rRNAs are the next highest modified RNA, with modifications critical for its biogenesis (Sloan et al., 2017). Improved methodology, including next-generation sequencing and mass spectrometry, have helped increase the ease of

studying modifications, especially internal mRNA modifications. Common RNA modifications include pseudouridine, N^6-Methyladenosine (m^6A), N^1-Methyladenosine (m^1A), and 5-Methylcytosine (m^5C). Although pseudouridine is the most common modification in cellular RNA and extremely abundant in tRNA and rRNA (Cohn, 1960), the most common RNA modification in mRNA is m^6A (Adams and Cory, 1975, Desrosiers et al., 1974).

m^6A was discovered in the 1970s when a simple, unique modification (consisting primarily of N^6-Methyladenosine) very different from the complex modifications in tRNA and rRNA was identified (Adams and Cory, 1975, Desrosiers et al., 1974). It is now one of the most abundant and well-studied mRNA modifications. The m^6A modification is most commonly found in the 3' untranslated region (UTR) near stop codons, possessing the consensus sequence RRACH (where R=A or G, and H=A, C, or U) (Dominissini et al., 2012, Ke et al., 2015, Meyer et al., 2012). Like other modifications, it is governed by its writers, readers, and erasers. The m^6A writer is a methyltransferase complex consisting of core components methyltransferase-like protein 3 (Mettl3), Mettl14, and Wilms tumor 1 associated protein (WTAP), where Mettl3 serves as the catalytic subunit that methylates N^6-adenosine (Bokar et al., 1994, Bokar et al., 1997, Liu et al., 2014, Sibbritt et al., 2013). Two demethylases, alkylation repair homolog protein 5 (Alkbh5) and fat mass and obesity-associated protein (FTO), have been identified as m^6A erasers and are responsible for reversing m^6A marks (Zheng et al., 2013, Jia et al., 2011). Several readers of m^6A have been discovered including YTH domain-containing family proteins 1-3 (YTHDC1-3) and insulin growth factor 2 binding proteins 1-3

(IGF2BP1-3) (Huang et al., 2018, Li et al., 2014, Xu et al., 2014). Originally hnRNPA2/B1 was proposed as a reader (Alarcon et al., 2015a), but new data suggest instead that it binds to adjacent sequences and acts as an "m^6A switch," where m^6A promotes accessibility of hnRNPA2/B1 to certain binding sites (Wu et al., 2018a).

The role of m^6A has been extensively studied in mRNA, however its effects on miRNAs are not fully understood. Studies have found m^6A can regulate primary-miRNA (pri-miRNA) processing due to the methyltransferases Mettl3 and Nsun2 (Yuan et al., 2014, Alarcon et al., 2015b). Mettl3 was shown to methylate pri-miRNAs, and knock down of Mettl3 resulted in an accumulation of unprocessed pri-miRNAs and a global reduction of mature miRNAs (Alarcon et al., 2015b). Nsun2 was able to methylate primary and precursor miR-125b, therefore inhibiting the processing of pri-miR125b to pre-miR125b (Yuan et al., 2014). Little is known about the extent of m^6A modification on mature miRNAs and the role it could play in regards to their function, but the presence of this modification has been detected (Yuan et al., 2014, Berulava et al., 2015, Konno et al., 2019). A better understanding of how m^6A and other potential modifications may affect mature miRNAs is still needed.

Conclusions

EVs have emerged as key players in cell-cell communication, not only in normal cells and tissues, but also in diseases such as cancer. It is important to understand the impact and downstream effects these vesicles can have as signaling molecules carrying diverse lipids, proteins, and RNA cargo. Individual cell types are known to differ in their

EV RNA composition. Combined with differences in EV purification techniques and heterogeneity of secreted vesicles, it has been challenging to find common regulatory mechanisms controlling export. Although a number of different mechanisms have shown evidence of selective miRNA export, there is still not a universal mechanism controlling sorting. This begs the question: is there a universal sorting mechanism? Understanding the mechanisms controlling cargo loading into EVs will no doubt increase our overall knowledge of EVs as well as provide insight into EV biogenesis. This will enhance understanding of the roles of EVs as disease biomarkers, therapeutic targets, and potential drug delivery methods.

Chapter 2

Regulation of miRNA export into extracellular vesicles by m^{6}A modification[1]

Abstract

Understanding the functional role of RNA modifications and to what extent they might regulate mature miRNA function and their secretion into extracellular vesicles (EVs) is unknown. Analysis of RNA content across a variety of EVs has shown differential miRNA enrichment when compared to parental cell expression patterns. Whether this is due to differential stability, specific regulation of miRNA export, or other mechanisms, is unclear. Here, we tested whether RNA base modifications and recognition of those modifications might underlie differential miRNA export into EVs derived from KRAS mutant cell lines. We found that decreased levels of Mettl3, a writer of N^6-methyladenosine (m^{6}A) modification, altered extracellular transfer of miRNAs containing consensus sequences for m^{6}A. Further, EVs prepared from cells expressing shRNAs against Mettl3 were incapable of conferring colony growth in 3D to wild-type KRAS cells. Our data indicate that m^{6}A modification plays an important role in miRNA export to EVs.

[1]Jessica J. Abner, Margaret A. Clement, Scott A. Hinger, Ryan M. Allen, Xiao Liu, John Karijolich, Qi Liu, Kasey C. Vickers, and James G. Patton. (2021). "Regulation of miRNA export into extracellular vesicles by m^{6}A modification." *iScience* (In Review).

Introduction

Over 130 RNA modifications have been identified (Schaefer et al., 2017) and recent work has highlighted the importance of understanding the potential role that RNA epitranscriptomics might play in regulating RNA metabolism and gene expression (Nachtergaele and He, 2018, Roundtree et al., 2017, Deng et al., 2018, Zaccara et al., 2019, Jonkhout et al., 2017, Barbieri and Kouzarides, 2020, Holoch and Moazed, 2015). As with chromatin modifications, there are distinct writers, readers, and erasers of RNA modifications with the best characterized of these involved with N^6-methyladenosine (m^6A) (Roundtree et al., 2017, Zaccara et al., 2019, Panneerdoss et al., 2018). Discovered in the 1970s, m^6A is one of the most abundant RNA modifications in eukaryotes (Adams and Cory, 1975, Desrosiers et al., 1974). This modification is often found in the 3'-untranslated region (UTR) near stop codons, having the consensus sequence RRACH, where R=A or G, and H=A, C, or U (Dominissini et al., 2012, Ke et al., 2015, Meyer et al., 2012). While the exact extent of dynamic changes in m^6A modification remains to be fully understood, it seems clear that m^6A marks can drive RNA turnover (Ke et al., 2017, Zhao et al., 2017), and that m^6A modification of chromatin associated RNAs can regulate chromatin accessibility and transcription (Liu et al., 2020).

Previous studies have shown that Mettl3 and Alkbh5 serve as a writer and eraser of m^6A, respectively (Bokar et al., 1994, Zheng et al., 2013). Methyltransferase-like protein 3 (Mettl3) is an RNA methyltransferase that acts as the catalytic subunit of the complex that methylates N^6-adenosine (Bokar et al., 1994, Bokar et al., 1997, Sibbritt et

al., 2013). Alkylation repair homolog protein 5 (Alkbh5) is a demethylase that can reverse m^6A in mRNA (Zheng et al., 2013). It was originally proposed that hnRNPA2/B1 was a key reader of m^6A (Alarcon et al., 2015a), but new data suggests that m^6A enhances the binding of hnRNPA2/B1 to adjacent sequences (Wu et al., 2018a). Beyond hnRNPA2/B1, additional RNA binding proteins have been identified that can serve as readers of m^6A modifications, and that m^6A modifications can regulate the binding of adjacent RNA binding proteins (Liu et al., 2015).

The majority of work examining the role of m^6A modifications has been directed toward its effects on mRNA metabolism, including turnover, splicing, export, and translation (Nachtergaele and He, 2018). For miRNAs, m^6A modifications have been found to regulate pri-miRNA processing (Alarcon et al., 2015b, Yuan et al., 2014), but the extent of modifications and any potential roles they might play within mature, processed miRNAs remains less clear (Berulava et al., 2015, Konno et al., 2019, Yuan et al., 2014). miRNAs are well characterized, small, non-coding RNAs that post-transcriptionally regulate gene expression (Bartel, 2018). Recently, miRNAs and a number of other mostly small RNAs have been detected in the extracellular space, usually packaged in extracellular vesicles (EVs), lipoproteins, or protein complexes (Valadi et al., 2007, Cha et al., 2015, Crescitelli et al., 2013, Dou et al., 2016, Hinger et al., 2018). EVs are nanosized particles secreted from every cell, that may play a novel role in cell-cell communication by transfer of RNA, lipid, and protein cargo (Maas et al., 2017, Tkach and Thery, 2016). Distinct mechanisms regulating cargo content have been proposed in cell- and disease-specific contexts (Simons and Raposo, 2009, Shifrin

et al., 2013, Maas et al., 2017). For miRNA export, numerous studies have shown that distinct subsets of miRNAs are secreted (Cha et al., 2015, Shurtleff et al., 2016, McKenzie et al., 2016, Wei et al., 2017, Villarroya-Beltri et al., 2013, Squadrito et al., 2014, Bolukbasi et al., 2012, Santangelo et al., 2016, Shurtleff et al., 2017), but it remains unclear how differential enrichment is achieved, whether by specific sorting mechanisms, differential stability, or other mechanisms. Specific RNA export sequences and RNA binding proteins have been proposed to play a role in selective miRNA sorting to EVs, but no unifying mechanism has been discovered (Shurtleff et al., 2016, Villarroya-Beltri et al., 2013, Squadrito et al., 2014, Statello et al., 2018, Bolukbasi et al., 2012, Batagov et al., 2011, Santangelo et al., 2016, Shurtleff et al., 2017, Kossinova et al., 2017).

Previously, we showed that EV cargo content is regulated in a KRAS dependent manner (Cha et al., 2015, Dou et al., 2016, Hinger et al., 2018, Demory Beckler et al., 2013). However, for secreted miRNAs, we were unable to identify a mechanism that could account for differential enrichment of specific miRNAs in EVs. Here, we sought to test whether RNA base modifications might underlie the mechanism of selective miRNA export to small EVs (sEVs) using KRAS mutant colorectal cancer cells. We found that Mettl3 knockdown causes a decrease in the secretion of specific RNAs that are enriched in consensus sequences for m^6A modification.

Results

miRNA Base Modifications and EV Secretion

We previously showed differential enrichment of specific miRNAs in EVs compared to their parental cells, and we also showed that specific miRNAs could be transferred between cells using Transwell cultures (Cha et al., 2015). However, we were not able to identify a unique RNA export sequence in our isogenic KRAS cell culture system (Shirasawa et al., 1993) and proteomic analyses identified differential enrichment of many RNA binding proteins, but none that stood out as universal regulators of miRNA export (Cha et al., 2015, Demory Beckler et al., 2013). Here, we decided to test whether RNA base modifications might play a role in miRNA export by recognition of specific marks or by regulating the binding of adjacent RNA binding proteins (or both). We initially identified numerous RNA base modifications (including m^6A) in EVs from mutant KRAS (DKO-1) cells using mass spectrometry and although some of those modifications were differentially enriched in EVs comparing mutant versus wild type KRAS (DKs-8) cells, their presence was not that surprising given that EVs contain fragments of highly modified tRNAs and rRNAs. To better assess whether mature miRNAs might be modified, we gel purified 22-23nt RNAs from DKO-1 EVs, and performed two-dimensional thin layer chromatography (2D TLC) analysis of modified nucleosides (**Fig. S1**). By radiolabeling RNase T2 products, significant levels of pseudouridine and m^6A were identified, in addition to at least five other potential modified nucleosides. Although it is possible that some of the size-selected RNA might have been derived from non-miRNA sources, our detection of methylated bases in EVs is consistent with reports that mature miRNAs contain m^6A (Berulava et al., 2015, Konno et al., 2019). Thus, we decided to test the effects of knockdown of a select group of writers, readers, and erasers of RNA modifications on miRNA export into EVs

(**Table S1**). Nanoparticle tracking analysis was used to quantify particle counts and vesicle size distribution and showed that none of the knockdown lines displayed overall defects in EV secretion (**Fig. S2**), setting the stage to determine whether miRNA export was differentially affected.

RNA methylation and miRNA export

To test whether any of the stable knockdown cell lines display altered miRNA transfer, we first used a previously described luciferase reporter and Transwell cultures to detect functional transfer of *miR-100* from donor KRAS mutant cells to recipient KRAS wild-type cells (Cha et al., 2015). Recipient DKs-8 cells were transfected with either a luciferase construct containing *miR-100* binding sites in the 3' UTR, or a control construct with a scrambled 3' UTR sequence not matching any known miRNA (**Fig. 5A**). Donor knockdown KRAS mutant cells were plated on top of Transwell membranes and luciferase levels were determined after 24 hours. We found that 6 of the cell lines showed significantly increased luciferase levels implying inhibition of *miR-100* export from donor cells (**Fig. 5B**). A common theme among all 6 of the knockdown lines is their role in RNA base methylation or recognition. Mettl3 is the catalytic subunit of the N^6-methyltransferase complex, the IGF2BP proteins are readers of m^6A, hnRNPA2/B1 is thought to be a reader of m^6A but may actually bind adjacent to m^6A, the Drosophila YBX-1 homolog recognizes 5-methylcytosine, and NSUN2 is a 5-methylcytosine transferase (Huang et al., 2018, Alarcon et al., 2015a, Wu et al., 2018a, Yuan et al., 2014, Shurtleff et al., 2016, Kossinova et al., 2017, Chellamuthu and Gray, 2020, Zou et al., 2020)(**Table S1**).

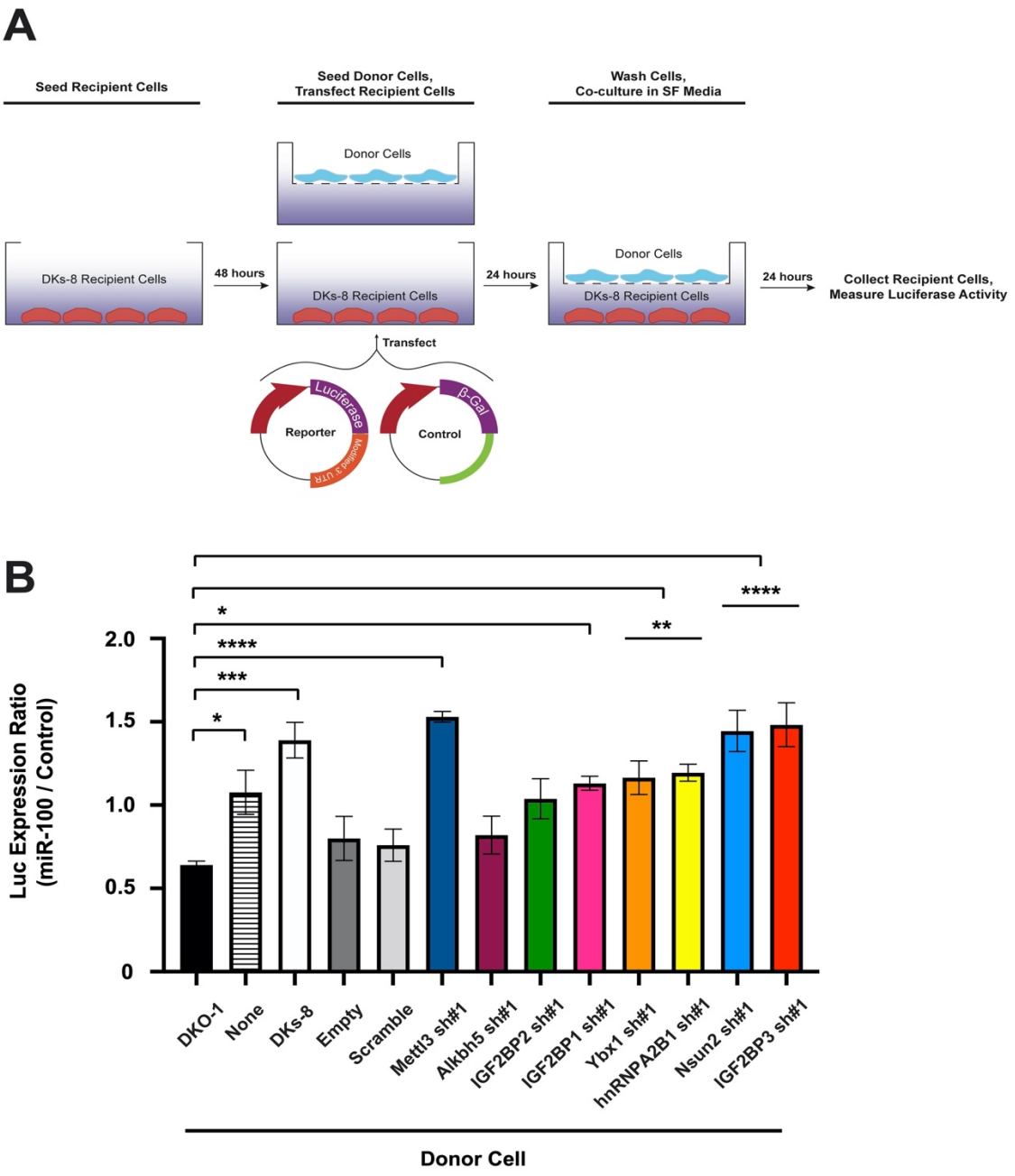

Figure 5. Reduced extracellular transfer of *miR-100* after knockdown of readers, writers and erasers of RNA modification. Stable shRNA knockdown cell lines were created using mutant KRAS (DKO-1) cells. Cell lines created include an empty shRNA vector, a scrambled control shRNA vector, and knockdown of 14 different proteins (see Table S1). **A**) Schematic of luciferase reporter assay. **B**) Luciferase reporter assay. DKs-8 recipient cells were seeded in the bottom of Transwell dishes and co-transfected with vectors expressing β-galactosidase and a luciferase reporter containing either a control 3'UTR or a modified 3'UTR with three perfect *miR-100* binding sites. Recipient cells were co-cultured with KRAS mutant donor cells for 24 hours before cell lysates were collected. Luciferase expression was quantified with decreased expression indicating increased transfer of *miR-100*. Significance was determined by one-way ANOVA. Data represent mean ± SE, n = 3. *p<0.05, **p<0.01, ***p=0.0002, ****p<0.0001.

Knockdown of Mettl3 alters levels and extracellular transfer of miR-100

Because 4 of the 6 knockdown lines involved m^6A modification and because we readily detected m^6A in 2D TLC analyses (**Fig. S1**), we decided to focus on the effects of decreased Mettl3 on miRNA secretion, complemented by similar analyses after knockdown of Alkbh5, an eraser of m^6A. The extent of knockdown for the two proteins was 60-70% across two independent shRNAs (**Fig. 6A**). We deliberately chose to use shRNA knockdowns because of the possibility of either lethality or widespread RNA metabolism changes after knockout. Nevertheless, because we detected significant changes in miRNA export without complete loss of Mettl3, we assayed the levels of *miR-100* in cells and EVs using RT/PCR (**Fig. 6B**), and used small RNAseq to globally analyze changes in cells and EVs (**Fig. 6C-F; Fig. 7**).

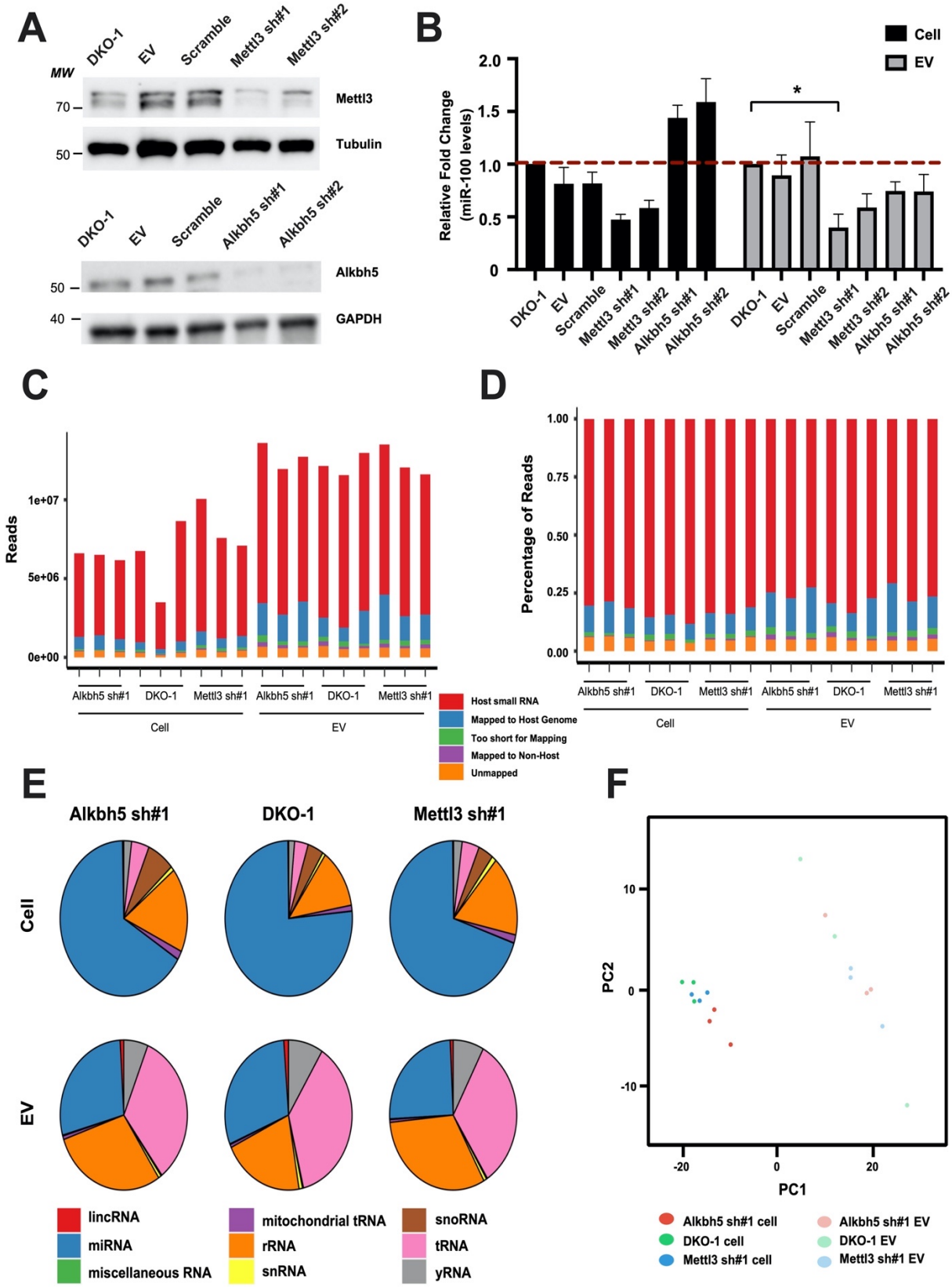
A
MW
DKO-1
EV
Scramble
Mettl3 sh#1
Mettl3 sh#2
70
Mettl3
Tubulin
50
Alkbh5 sh#1
Alkbh5 sh#2
Alkbh5
GAPDH
40
B
Cell
EV
Relative Fold Change (miR-100 levels)
2.0
1.5
1.0
0.5
0
*
C
Reads
1e+07
5e+06
0e+00
Alkbh5 sh#1
DKO-1
Mettl3 sh#1
Cell
EV
Host small RNA
Mapped to Host Genome
Too short for Mapping
Mapped to Non-Host
Unmapped
D
Percentage of Reads
1.00
0.75
0.50
0.25
0.00
E
Alkbh5 sh#1
DKO-1
Mettl3 sh#1
Cell
EV
lincRNA
miRNA
miscellaneous RNA
mitochondrial tRNA
rRNA
snRNA
snoRNA
tRNA
yRNA
F
PC2
PC1
10
0
-10
-20
20
Alkbh5 sh#1 cell
DKO-1 cell
Mettl3 sh#1 cell
Alkbh5 sh#1 EV
DKO-1 EV
Mettl3 sh#1 EV

Figure 6. Decreased levels of Mettl3 and Alkbh5 alters cellular and EV small RNA profiles. **A**) Western blots were performed on cell lysates from stable lines expressing an empty shRNA vector (Empty), a scrambled control shRNA vector, two independent shRNAs targeting Mettl3, and two independent shRNAs targeting Alkbh5. Representative immunoblots using antibodies against Mettl3, Alkbh5, Tubulin, and GAPDH. **B**) qRT/PCR analysis of *miR-100* levels in cellular (gray) and EV (black) samples. Significance was determined by one-way ANOVA. Data represent mean ± SE, n = 3, and *p<0.05. **C-E**) Small RNA sequencing was performed on DKO-1, Mettl3 knockdown, and Alkbh5 knockdown cells and EVs. The total number of reads in each library (**C**), the percentage of reads and their mapped positions (**D**), and (**E**) the small RNA read distribution in cellular and EV samples are as shown (color scheme as indicated). **F**) Principal component analysis comparing cellular (solid) and EV (opaque) RNA-seq data.

Analysis of *miR-100* levels by RT/PCR in Mettl3 and Alkbh5 knockdown cells and EVs showed contrasting differences (**Fig. 6B**). Cellular levels of *miR-100* decreased after knockdown of Mettl3, but opposite effects were observed after knockdown of Alkbh5. m^6A marks can either stabilize or destabilize mRNAs depending on their position and/or recognition by proteins such as IGF2BP1-3 (Huang et al., 2018, Mauer et al., 2017, Ke et al., 2017). One interpretation of the decreased cellular levels of *miR-100* after Mettl3 knockdown is that m^6A stabilizes miRNA half-life which is consistent with increased cellular levels after knockdown of Alkbh5 (**Fig. 6B**). For EVs, the trends we observed in cells were similar except the fold-changes after Alkbh5 knockdown were not as large. Also, the decrease in *miR-100* was significant for Mettl3 shRNA #1 compared to EVs from the parental DKO-1 cells.

Small RNA profiles after knockdown of Mettl3 and Alkbh5 are distinct between cells and EVs

To more broadly assess the effects of m^6A on miRNA export, we conducted RNAseq on libraries created from small RNAs purified from knockdown cells and EVs

and compared miRNA levels to parental DKO-1 cells and EVs. Total read numbers indicated sufficient coverage with over 5 million reads for almost every sample (**Fig. 6C**). Mapping of the reads indicated that over 75% of reads across all samples mapped to host small RNAs and that the overall read percentages were quite similar, whether from parental or knockdown cells or EVs (**Fig. 6D**). When quantifying read numbers across the main categories of small RNAs found in the respective libraries, the RNA profiles were similar, between both the parental and knockdown cells and between the parental and knockdown EVs (**Fig. 6E**). However, there was a clear difference in the read distribution comparing cellular to EV libraries. This is consistent with Principal Component (PC) analysis which showed distinct differences in RNA profiles comparing cells to EVs (**Fig. 6F**). The cellular profiles tended to cluster together whereas the EV profiles showed greater variation by PC analysis. Based on length distribution analyses, cellular and EV small RNA contents were distinct. Cellular small RNA profiles were largely composed of miRNAs; however, EV profiles contained miRNAs and slightly longer tRNA-derived reads (tDRs) and rRNA-derived reads (rDRs)(**Fig. S3A**). Differential expression analyses (DEseq2) of small RNA changes found that many miRNAs were significantly decreased in cells and EVs after knockdowns (**Fig. S3B**).

The pie charts in **Fig. 6F** demonstrate broad RNA profiles across the cellular and EV libraries. Individual comparisons across the different classes of small RNA reads allowed us to refine differences (**Fig. 7**). Because analysis of *miR-100* appeared to be more affected by knockdown of Mettl3 (**Fig. 5**), we decided to focus on Mettl3 knockdown but the individual comparisons for Alkbh5 knockdown are shown in **Fig. S4**.

When comparing parental (DKO-1) cells to Mettl3 knockdown cells, decreased expression of Mettl3 caused an equal or increased amount of small RNAs in all categories except miRNAs (**Fig. 7A**). However, the same was not observed for small EV RNAs where knockdown of Mettl3 caused either decreased or equivalent small RNAs in all categories except rRNA (**Fig. 7B**).

Mettl3 knockdown causes decreased enrichment of miRNAs containing m^{6}A sites in EVs

Even though miRNA expression profiles were decreased in Mettl3 knockdown cells, there was still a significant decrease in the enrichment of miRNAs in Mettl3 knockdown EVs (**Fig. 7B**). When we analyzed individual miRNAs that showed significantly decreased enrichment in EVs after Mettl3 knockdown, we found that 4 of the top 5 most downregulated miRNAs contained consensus sequences for m^{6}A (**Table 1**). This suggests that m^{6}A modification plays a positive role in miRNA export into EVs.

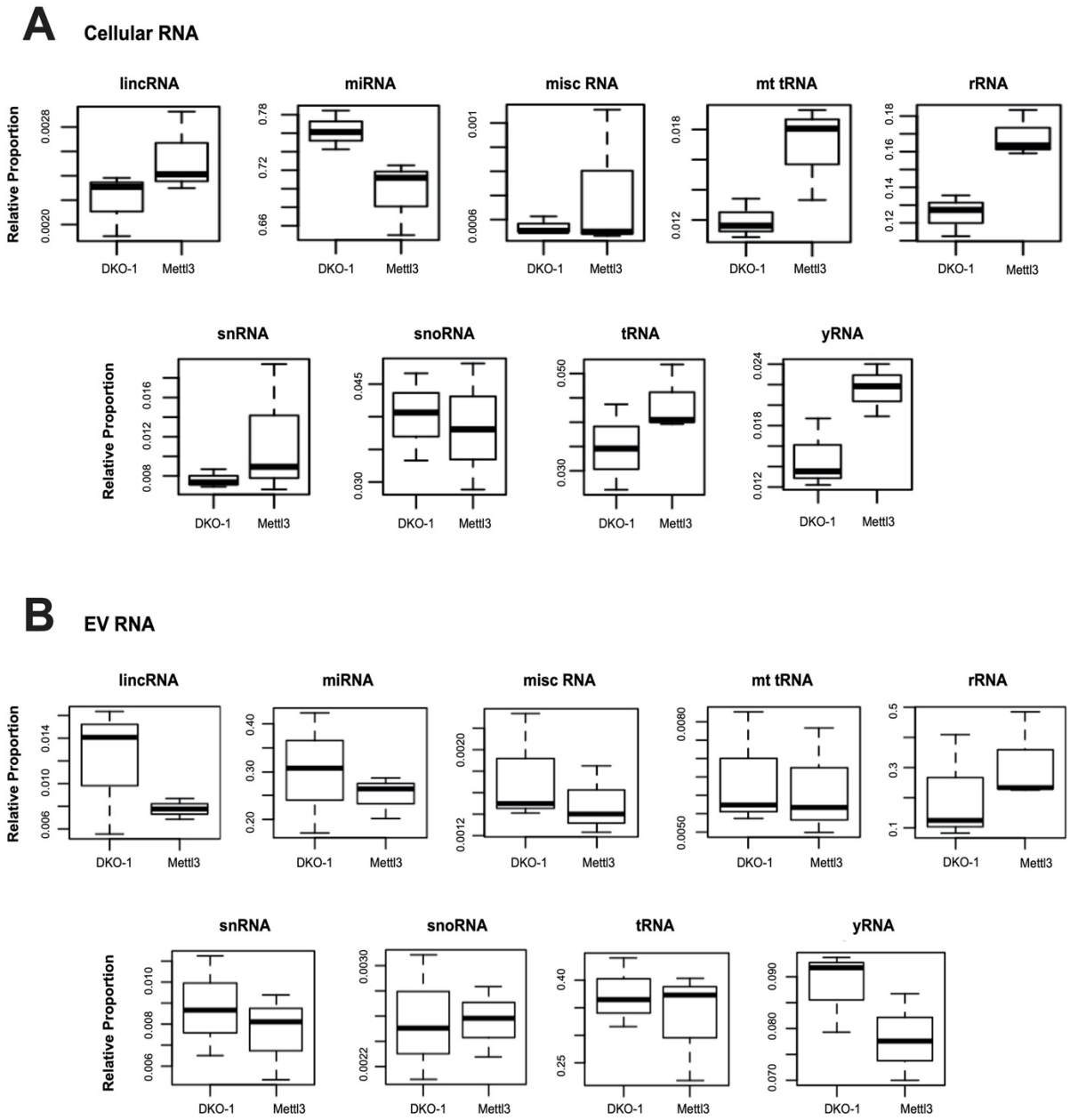

Figure 7. Relative proportion of RNA subgroups in DKO-1 and Mettl3 knockdown cellular and EV RNA samples. Small RNA sequencing results were analyzed to determine the relative proportion of mapped reads from the indicated small RNA subgroups present in cellular (**A**) and EV (**B**) RNA samples from the parental DKO-1 or Mettl3 knockdown cells.

Table 1. Downregulated miRNAs contain m^{6}A consensus sequences.

miRNA	Sequence	P-value	Adjusted P-value
miR-100-5p	AACCCGTAGATCCGAACTTGTG	1.09E-06	0.00074201
miR-99b-5p	CACCCGTAGAACCGACCTTGCG	1.07E-05	0.00314616
miR-193b-3p	AACTGGCCCTCAAAGTCCCGCT	1.39E-05	0.00314616
miR-365a-3p; miR-365b-3p	TAATGCCCCTAAAAATCCTTAT	6.37E-05	0.00990965
miR-125b-5p	TCCCTGAGACCCTAACTTGTGA	7.31E-05	0.00990965

Knockdown of Mettl3 reduces EV-mediated anchorage-independent growth

Small EVs from mutant KRAS cells can promote proliferation and anchorage-independent growth when exposed to wild-type KRAS cells (Demory Beckler et al., 2013, Higginbotham et al., 2011). Recently, we also reported that Rab13 sEVs can mediate effects on anchorage-independent growth via paracrine and autocrine signaling (Hinger et al., 2020). To test whether Mettl3 knockdown in DKO-1 cells would affect colony growth in soft agar assays, we purified sEVs from DKO-1 cells and Mettl3 knockdown cells. Analysis of the sEV preparations by western blots using antibodies against classical exosome markers showed that the sEVs from the parental and knockdown cells were similar, if not identical (**Fig. 8A**). Beyond the presence of protein markers of classical exosomes, the morphology of the sEVs was unaffected by knockdown of Mettl3, even when density-gradient purified EV were examined (**Fig. S5**).

To test the effects of Mettl3 knockdown on anchorage independent growth, we cultured wild-type KRAS (DKs-8) cells in soft agar in the presence or absence of sEVs from either DKO-1 or Mettl3 knockdown cells. Consistent with previous results (Demory Beckler et al., 2013, Higginbotham et al., 2011), an increase in colony formation was

observed when DKs-8 cells were treated with DKO-1 sEVs compared to untreated DKs-8 cells (**Fig. 8B**). In sharp contrast, when DKs-8 cells were treated with sEVs from Mettl3 knockdown cells, colony growth was largely abolished. Previously, we showed that cetuximab resistant cells derived from HCA-7 colorectal cancer cells can survive in 3D culture and express dramatically increased levels of *miR-100* and *miR-125b* (Lu et al., 2017). Since our RNAseq data after Mettl3 knockdown showed decreased levels of these miRNAs in sEVs, we tested whether exposure of cetuximab sensitive DKs-8 cells to sEVs from DKO-1 or Mettl3 knockdown cells could confer drug resistance. As shown, exposure to DKO-1 sEVs allowed colony growth in soft agar in the presence of cetuximab (**Fig. 8B**). In contrast, exposure to Mettl3 knockdown sEVs did not promote colony growth except for the occasional presence of rare clumps of cells/colonies with abnormal morphology. The overall conclusion is that the cargo contained within Mettl3 sEVs is not able to drive normal colony growth, consistent with at least in part, decreased levels of *miR-100* and *miR-125b*.

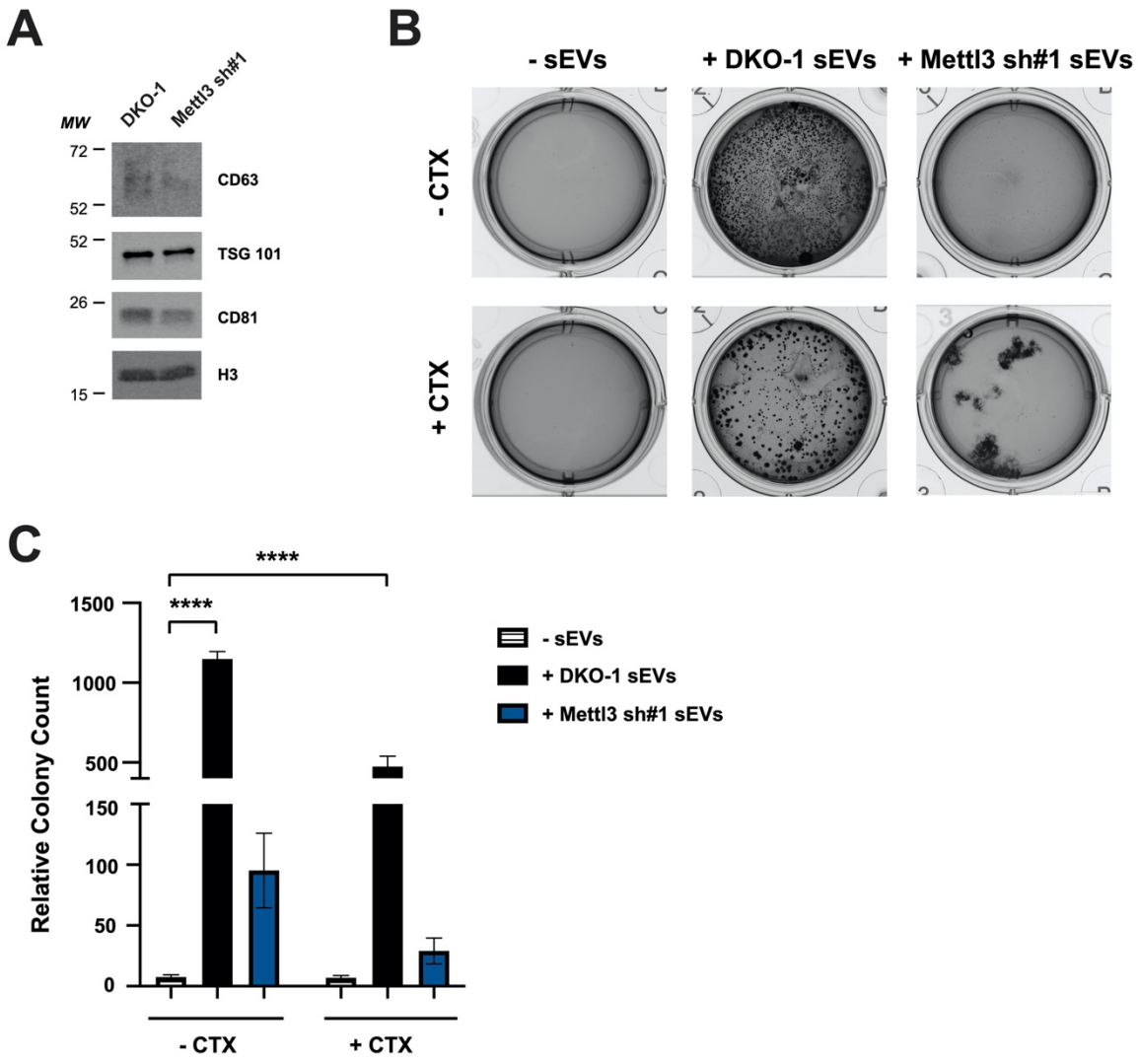

Figure 8. Knockdown of Mettl3 reduces EV-mediated anchorage-independent growth. **A**) Immunoblots of sEVs using antibodies against CD63, TSG101, CD81, and H3. **B,C**) DKs-8 cells were grown in soft agar for 2 weeks in the presence or absence of sEVs derived from with the parental DKO-1 cells or Mettl3 knockdown cells. Representative images (**B**) and quantification of colony counts (**C**) are shown. Significance was determined by one-way ANOVA. Data represent mean ± SE, n = 3, ****p<0.0001.

Discussion

In this study, we investigated whether RNA modifications play a role in sorting of miRNAs to sEVs in KRAS mutant colorectal cancer cells. Using luciferase reporter

assays, 6 of the stable shRNA-expressing cell lines showed decreased extracellular transfer of *miR-100* (**Fig. 5**). Of the 6 cell lines, 4 express shRNAs that target either m^{6}A addition (Mettl3) or m^{6}A recognition (IGF2BP1, IGP2BP3, and hnRNPA2/B1). hnRNPA2/B1 was originally proposed to be a reader of m^{6}A, but m^{6}A modification may actually regulate adjacent binding of hnRNPA2/B1 to RNA, and, more broadly, m^{6}A modification can alter RNA structure to regulate the binding of other RNA binding proteins (Alarcon et al., 2015a, Wu et al., 2018a, Liu et al., 2015). While the luciferase assays monitored export and transfer of *miR-100*, RNAseq analyses confirmed the effects of m^{6}A on miRNA export showing that after knockdown of Mettl3, 4 of the top 5 most downregulated miRNAs exported into sEVs contained consensus sequence motifs for m^{6}A addition. Notably, *miR-100* and *miR-125b* were among those 5 miRNAs, consistent with the fact that sEVs from Mettl3 knockdown cells were incapable of conferring resistance to cetuximab (Lu et al., 2017). Together, the data support the hypothesis that m^{6}A modification plays an important role in selective miRNA export into sEVs. That role could be due to differential stability afforded by m^{6}A marks or by altering the binding of proteins that promote export.

m^{6}A Modification, RNA Metabolism and Disease

m^{6}A modifications are abundant across many different types of RNA (Nachtergaele and He, 2018, Zaccara et al., 2019). Broadly, m^{6}A modification can alter RNA structures thereby regulating recognition by RNA binding proteins (Liu et al., 2015, Harcourt et al., 2017). Readers of m^{6}A have been proposed to affect the stability of mRNAs (Huang et al., 2018, Heck et al., 2020, Ke et al., 2017, Mauer et al., 2017,

Wang et al., 2014, Zhao et al., 2017), but might also serve as nucleation sites for the formation of condensates that might underlie non-membranous compartments or complexes such as P-bodies, stress granules, and nuclear speckles (Ries et al., 2019). The presence of readers, writers and erasers of m^6A suggest the potential for dynamic changes in gene expression at the RNA level (Zhou et al., 2015, Meyer and Jaffrey, 2014, Roundtree et al., 2017). Related to our work on colorectal cancer, dynamic changes in m^6A modification have been proposed to regulate cancer growth and progression and serve as potential anti-cancer drug targets (Boriack-Sjodin et al., 2018, Barbieri and Kouzarides, 2020, Panneerdoss et al., 2018, Deng et al., 2018).

m^6A Modifications and miRNA

Beyond the more well characterized effects of m^6A modification on mRNAs, there have been reports identifying m^6A modification on mature miRNA and others demonstrating how m^6A modifications control the processing of precursor miRNAs (Berulava et al., 2015, Konno et al., 2019, Alarcon et al., 2015b, Yuan et al., 2014). Our discovery of RNA modifications by 2D TLC analysis of size-selected RNA from sEVs is consistent with m^6A deposition on mature miRNAs, but our analyses also suggest the potential for additional modifications. With the caveat that some of the modifications we detected could be due to fragmented tRNAs or rRNAs within our sample, we detected the presence of pseudouridine, an unknown modification of adenosine, 4 modifications most likely derived from guanosine, and an uncharacterized modification of cytosine (**Fig S1**). tRNAs are abundantly modified, with approximately 13 modifications per molecule (Pan, 2018). rRNAs are the next highest modified class of RNA with

approximately 2% of its nucleosides modified (Sloan et al., 2017). As antibodies against specific marks become available, it will be important to identify and characterize the full range of base modifications that might alter miRNA function or export.

m^6A and miRNA Export

Numerous studies have demonstrated that comparison of miRNA profiles from cells and EVs show consistent differential enrichment of specific miRNAs within EVs (Cha et al., 2015, McKenzie et al., 2016, Skog et al., 2008, Valadi et al., 2007, Wei et al., 2017, Kosaka et al., 2010, Squadrito et al., 2014, Santangelo et al., 2016, Shurtleff et al., 2016). While such changes could be due to differential miRNA stability and/or some means of passive differential loading of miRNAs into EVs, it remains a key focus of current research to test potential mechanisms that specifically regulate miRNA export (Mateescu et al., 2017). RNA sequence motifs, roles for specific RNA binding proteins, and differential mRNA target expression have all been proposed to drive selective miRNA export but no universal mechanism has been identified (Shurtleff et al., 2016, Villarroya-Beltri et al., 2013, Squadrito et al., 2014, Statello et al., 2018, Bolukbasi et al., 2012, Batagov et al., 2011, Santangelo et al., 2016, Shurtleff et al., 2017, Kossinova et al., 2017). This might mean that all export control is context-specific, depending on the specific cell type or condition, or that we have thus far failed to recognize mechanistic similarities. For our colorectal cancer model, we detected KRAS-dependent differential miRNA enrichment, but were unable to identify a unique RNA sequence motif or RNA binding protein that could mediate selective export. This prompted us to test whether RNA base modifications or the combination of base modifications and recognition by

specific RNA binding proteins might drive deposition into sEVs. We show here that m^6A plays a role in miRNA export which raises the possibility that a combination of m^6A modification, either within or adjacent to RNA export motifs, and recognition by RNA binding proteins such as hnRNPA2/B1, YBX-1 and IGF2BP, could provide a common mechanism regulating miRNA export.

Cell-Cell Communication by EVs

EVs are now thought to represent a heretofore unappreciated form of cell-cell communication, both locally, for example within the tumor microenvironment and the immune synapse, and at a distance in the metastatic niche (Maas et al., 2017, Maia et al., 2018, Shurtleff et al., 2018, McAllister and Weinberg, 2014, Wortzel et al., 2019, Gutierrez-Vazquez et al., 2013). We previously showed that exposure of wild-type KRAS cells to sEVs from mutant KRAS cells could induce growth and proliferation in the wild-type cells (Demory Beckler et al., 2013, Higginbotham et al., 2011). In a model of cetuximab resistance, we showed that dramatic upregulation of cellular levels of *miR-100* and *miR-125b* caused activation of Wnt signaling and drug resistance (Lu et al., 2017). Here, we show that decreased levels of Mettl3 caused significantly less export of *miR-100* and *miR-125b* into sEVs. When we exposed cetuximab sensitive DKs-8 cells to those sEVs, we did not detect significant colony formation in 3D cultures. In contrast, sEVs from mutant KRAS DKO-1 cells dramatically stimulated colony growth in 3D. This argues that transfer of *miR-100* and *miR-125b* are in part responsible for transfer of cetuximab resistance although protein cargo likely also contributes.

Methods

Cell Culture

Isogenically matched KRAS colorectal cancer cell lines, DKO-1 and DKs-8, were used as previously described (Shirasawa et al., 1993). Cells were maintained in DMEM (Gibco) supplemented with 10% fetal bovine serum (FBS), 1% L-glutamine, 1% penicillin/streptomycin, and 1% non-essential amino acids. Cells were grown at 37°C in 5% CO_2.

Isolation of EVs

EVs were isolated as previously stated (Hinger et al., 2020). Briefly, cells were plated in 3-12 T175 flasks (Corning) for 48 hours until approximately 80% confluency. DKO-1 cells were seeded at $6.5x10^6$ cells per flask, and DKs-8 cells were seeded at $7.5x10^6$ cells per flask. Cells were washed three times with 1X Dulbecco's PBS (DPBS; Gibco), then grown in serum free media for 48 hours. Conditioned media (CM) was collected and subjected to three steps of differential centrifugation: 300xg for 10 mins at room temperature, 2000xg for 25 mins at 4°C, and 10,000xg for 30 mins at 4°C. For crude sEVs, CM was then centrifuged at 100,000xg for 17 hours at 4°C. Pellets were resuspended in 1X DPBS and washed twice at 100,000xg for 70 mins at 4°C. Pellets were resuspended in 50μl of 1X DPBS or 1X RIPA buffer. For gradient purified EVs, CM was concentrated using a Centricon Plus-70 concentrator (Millipore) to ~10 mL. Concentrated CM was centrifuged at 100,000xg for 17 hours at 4°C. The pellet was resuspended in cold 36% iodixanol solution (Optiprep). A discontinuous gradient of chilled 30-12% iodixanol solutions were layered on top of the 36% iodixanol solution

containing the sEVs, and centrifuged at 100,000xg for 17 hours at 4°C. Next, 12 fractions of 1 mL each were collected from top to bottom and mixed with 10 mL of 1X DPBS. Fractions were centrifuged at 100,000xg for 3 hours at 4°C, then resuspended in 25μl of 1X DPBS or 1X RIPA buffer.

Nanoparticle Tracking Analysis

Zetaview® Nanoparticle Tracking Video Microscope PMX-120 (Particle Matrix) and associated software were used to analyze particle sizes and numbers. The software was optimized and settings were held constant across all replicate samples. The typical concentration of vesicles ranged from 10^8 to 10^{11} particles/mL.

Transfection of shRNA Plasmids

Transfection of shRNA plasmids was carried out using Lipofectamine 2000 (ThermoFisher). DKO-1 cells were plated in 12-well plates (Corning) at a concentration of $1.0x10^5$ cells per well and allowed to adhere for 24 hours at 37°C. The following day, 0.5μg of DNA was incubated with 2μl of Lipofectamine 2000 at room temperature for 20 mins before being added dropwise to cells. Cells were incubated for 24 hours before antibiotic selection. Cells were treated with 1μg/mL of puromycin for approximately 2 weeks. Transfection was confirmed by visualization of GFP.

Western Blots

Cells were lysed and proteins were collected using 1X RIPA buffer (Millipore). Protein concentrations were determined using the Pierce BCA assay kit (Thermo Scientific).

Between 2-10μg of protein were loaded onto pre-cast gels (10% MINI-PROTEAN TGX™; Bio-Rad). Once separated, proteins were transferred onto PVDF membranes using the Trans-Blot Turbo Transfer System (Bio-Rad). Membranes were blocked in 5% milk in TBS-T for at least one hour. Membranes were then incubated with primary antibodies in 5% milk in TBS-T overnight at 4°C. The following day, membranes were washed 3 times with 1X TBS-T, then incubated with secondary antibodies in 5% milk in TBS-T for 45 minutes at room temperature. Membranes were washed 3 times with 1X TBS-T. To visualize bands, SuperSignal™ West Femto Maximum Sensitivity Substrate was used and blots were imaged on a ChemiDoc MP Imaging System (Bio-Rad). Primary antibodies include anti-Mettl3 (Bethyl Labs), anti-Alkbh5 (Sigma Aldrich), anti-GAPDH (Invitrogen), anti-α-Tubulin (Abcam), anti-CD63 (Abcam), anti-TSG 101 (Invitrogen), anti-CD81 (Santa Cruz), and anti-H3 (Abcam). All primary antibodies were used at a concentration of 1:1000, except for anti-H3, anti-GAPDH, and anti-Tubulin which were used at a concentration of 1:5000.

Luciferase Reporter Assay

DKs-8 recipient cells were seeded in 6-well plates (Corning) at a density of $2.5x10^5$ cells per well. After 48 hours, cells were co-transfected with 1.5μg of luciferase reporter plasmid and 1.5μg of β-gal plasmid DNA per well. Donor cells were plated on 0.4μm Transwell filters at a density of $2.5x10^5$ cells per well for 24 hours. Recipient and donor cells were washed with PBS three times and co-cultured in DMEM without FBS for 24 hours before recipient cells were harvested. Cell lysates were prepared in 1x reporter lysis buffer (Promega, E2510). Luciferase and β-galactosidase levels were determined

simultaneously from the lysates according to the manufacturer's protocol (Promega, E2510 and E2000, respectively). Luciferase expression was normalized to β-galactosidase expression to account for differences in transfection efficiency (Luc/β-gal). Luc/β-gal of target miRNA was normalized to control, and the ratio was plotted. All assays were performed on three biological replicates, each with three technical replicates.

RNA Purification

Total RNA from cells and EVs was isolated using TRIzol (Life Technologies). Pellets were resuspended in 60μl of RNAse-free water, then further purified with the miRNeasy kit (Qiagen).

qRT/PCR

Taqman small RNA assays (Life Technologies) were performed for U6 snRNA and *hsa-miR-100-5p* on cellular and EV samples. In short, 10ng of total RNA was used for each individual RT reaction; 1μl of the resultant cDNA was used in 10μl qPCR reactions. qRT/PCR reactions were performed in 384-well plates using a Bio-Rad CFX384 Real-Time System. All C(t) values were ≤ 40. Triplicate C(t) values were averaged and normalized to U6 snRNA. Fold changes were calculated using the ΔΔC(t) method, where $\Delta = C(t)_{miR\text{-}100} - C(t)_{U6\ snRNA}$, and $\Delta\Delta C(t) = C(t)_{EV} - C(t)_{cell}$, and $FC = 2^{-\Delta\Delta C(t)}$. Analysis was performed on three independent cell and EV RNA samples.

RNA Sequencing

High-throughput small RNA sequencing was performed on small RNA libraries generated using NextFlex small RNA library preparation kit v3 (PerkinElmer) with modified step F. Libraries were size-selected (136-200nt) using Pippin Prep (Sage) and quality was assessed by 2100 Bioanalyzer (Agilent). Libraries were sequenced (SE-75) using the NextSeq500 system (Illumina). Cutadapt (https://github.com/marcelm/cutadapt) was used to trim adapters. TIGER (https://github.com/shengqh/TIGER), was used to perform small RNA-seq analysis, including reads mapping, miRNA quantification and differential analysis (Allen et al., 2018). Specifically, Bowtie was used to map reads to human miRNAs using miRBase v22. It was also used to map reads to tRNA, rRNA, snRNA, snoRNA, lincRNA, yRNA, other miscellaneous sRNAs, and the human reference genome hg19. Principle component analysis was performed to assess the similarity between samples. DESeq2 was used to detect differential expression between Mettl3 knockdown and WT. Dirichlet-multinomial regression model was used to evaluate differences in small RNA composition between Mettl3 knockdown and DKO-1 while accounting for the proportions of all of the other small RNA populations.

Soft Agar Assay

Soft agar assays were carried out as previously described (Hinger et al., 2020, Borowicz et al., 2014). Briefly, warmed 1% noble agar (Sigma-Aldrich) was mixed with 2X DMEM media and 500μl of this mixture was plated as the bottom layer in each well of a 12-well dish until it solidified at room temperature. For the middle layer, 2,000 cells

(6,000 per triplicate) were resuspended in 500μl of standard DMEM media and incubated with or without 10μg of sEVs at 37°C for 2 hours. After incubation, cells were centrifuged for 5 mins at room temperature and resuspended in 1.5 mL of 0.3% Noble Agar/1X DMEM solution. This mixture was plated on top of the bottom layer and allowed to solidify at room temperature. Standard DMEM media (500μl per well) was added to each well, supplemented with or without sEVs. Cultures were incubated for 2 weeks at 37°C, with media changed every 4 days. Colonies were stained with nitroblue tetrazolium chloride solution (Sigma) overnight at 37°C, then counted the next day.

Transmission Electron Microscopy

Transmission electron microscopy (TEM) was performed as previously described (Hinger et al., 2020). EVs were absorbed onto blow discharged carbon-coated formvar grids (Electron microscopy sciences) for 5 mins at room temperature by floating the grids on 5μl of sample. After absorption of the vesicles, the grids were washed quickly in ddH_2O, blotted, stained in 2% uranyl acetate for 30 secs, and then dried on filter paper. TEM was performed using a Tecnai T12 microscope with an AMT CMOS camera. Negative staining was carried out in part through the use of the Vanderbilt Cell Imaging Shared Resource (supported by NIH grants CA68485, DK20593, DK58404, DK59637, and EY08126).

Two-Dimensional Thin Layer Chromatography (2D TLC)

EV RNA was separated on 12% polyacrylamide gels and bands corresponding to 22-23 nt RNAs were excised. Gels were minced and RNAs were eluted and then digested to

completion with 1 U of RNase T2 (Worthington) in 50 mM ammonium acetate, 0.05% SDS, and 1 mM EDTA. Mononucleosides were then 5′ ^{32}P-labeled using 10 units of T4 polynucleotide kinase (Fermentas) in the presence of 1 µL of [γ-32P] ATP (6000 Ci/mmol; Perkin-Elmer). After ethanol precipitation, the labeled RNA was resuspended in 10 µL of 50 mM sodium acetate (pH 5.5) and digested to 5'-monophosphonucleosides by RNase P1 (Sigma-Aldrich). Three microliters of the samples were applied to glass-backed PEI-cellulose plates (MerckMillipore) and developed in a solvent system composed of isobutyric acid:0.5 M NH4OH (5:3, v/v) in the first dimension and isopropanol:HCl:water (70:15:15, v/v/v) in the second dimension. TLC plates were visualized by autoradiography and nucleosides were identified by comparison with published reference maps (Grosjean et al., 2004).

Statistical Analysis

One-way ANOVA analyses were used to calculate significance using GraphPad Prism 7 software. The threshold for significance (alpha) was 0.05, and p-values are specified in each figure legend. All data are represented by a mean value ± standard error.

Data and Software Availability

Raw data for the RNA sequencing analysis have been deposited at Gene Expression Omnibus (GEO) [Accession number: GSE166643].

Author Contributions

Conceptualization, J.J.A. and J.G.P.; Methodology, J.J.A., S.A.H.; Investigation, J.J.A., M.A.C., S.A.H., R.M.A., and J.K.; Formal Analysis, X.L. and Q.L. Writing – Original Draft, J.J.A. and J.G.P.; Writing – Review & Editing, J.J.A., J.K., K.C.V., and J.G.P.; Resources, J.K. and K.C.V.; Supervision, J.G.P.; Funding Acquisition, J.G.P.

Acknowledgments

We would like to thank Drs. Jeffrey L. Franklin, Robert J. Coffey and Peter Dedon for initial analysis of EV base modifications by mass spectrometry. We also thank Dr. Evan Krystofiak of the Cell Imaging Shared Resource core for assistance with processing TEM images. This work was supported by a grant from the National Institute of Health and the National Cancer Institute (P01 CA229123) to Drs. Alissa M. Weaver, Robert J. Coffey and James G. Patton. We thank the Weaver, Patton, and Coffey labs for discussion, suggestions, and comments, especially Dr. Jeffrey L. Franklin.

Supplemental Materials

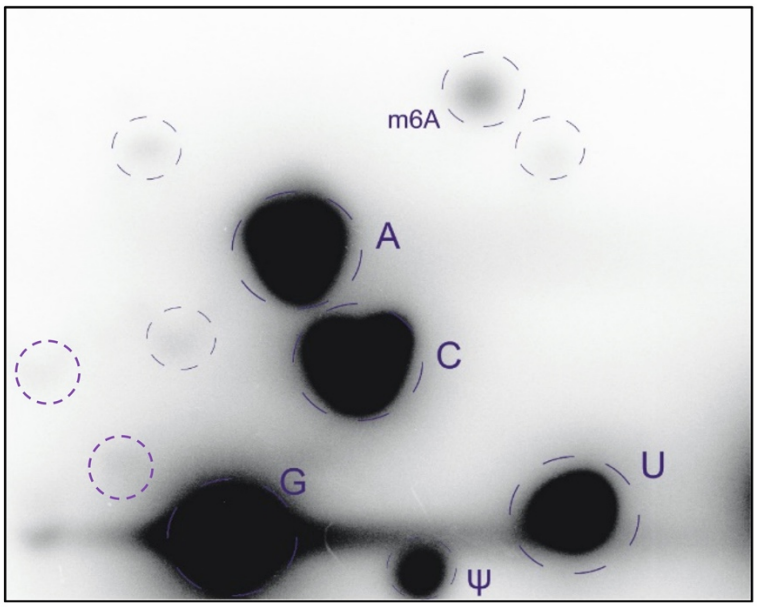

Figure S1. KRAS mutant sEVs contain m^6A. sEVs were isolated from DKO-1 cells, total small RNA was purified, separated on 12% polyacrylamide gels, and 22-23 nt RNAs were gel purified. After digestion with RNase T2 and ^{32}P labeling with T4 polynucleotide kinase, samples were subjected to 2D TLC, as described in the Methods. The resulting products were visualized by autoradiography and nucleosides were identified by comparison with published reference maps (Grosjean et al., 2004).

Table S1. Stable shRNA knockdown cell lines.

Protein	Function	References
Alkbh5	m^6A eraser	(Zheng et al., 2013)
hnRNPA2/B1	m^6A reader; Binds adjacent to m^6A	(Wu et al., 2018a, Alarcon et al., 2015a)
IGF2BP1	m^6A reader	(Huang et al., 2018)
IGF2BP2	m^6A reader	(Huang et al., 2018)
IGF2BP3	m^6A reader	(Huang et al., 2018)
Mettl3	m^6A writer	(Bokar et al., 1994)
nsMAse II	miRNA sorting to EVs	(Cha et al., 2015, Kosaka et al., 2010, Trajkovic et al., 2008)
Nsun2	m^5C writer	(Chellamuthu and Gray, 2020, Kossinova et al., 2017)
Nsun6	m^5C writer	(Haag et al., 2015)
PIAS1	Involved in sumoylation which facilitates sorting to EVs	(Kunadt et al., 2015)
TRM5	m^1G writer	(Christian et al., 2010)
UBC9	Involved in sumoylation which facilitates sorting to EVs	(Kunadt et al., 2015)
VAP-A	Vesicle transport	(Wyles et al., 2002, Santos et al., 2018)
Ybx1	Binds to m^5C; miRNA sorting to EVs	(Kossinova et al., 2017, Zou et al., 2020, Shurtleff et al., 2016)

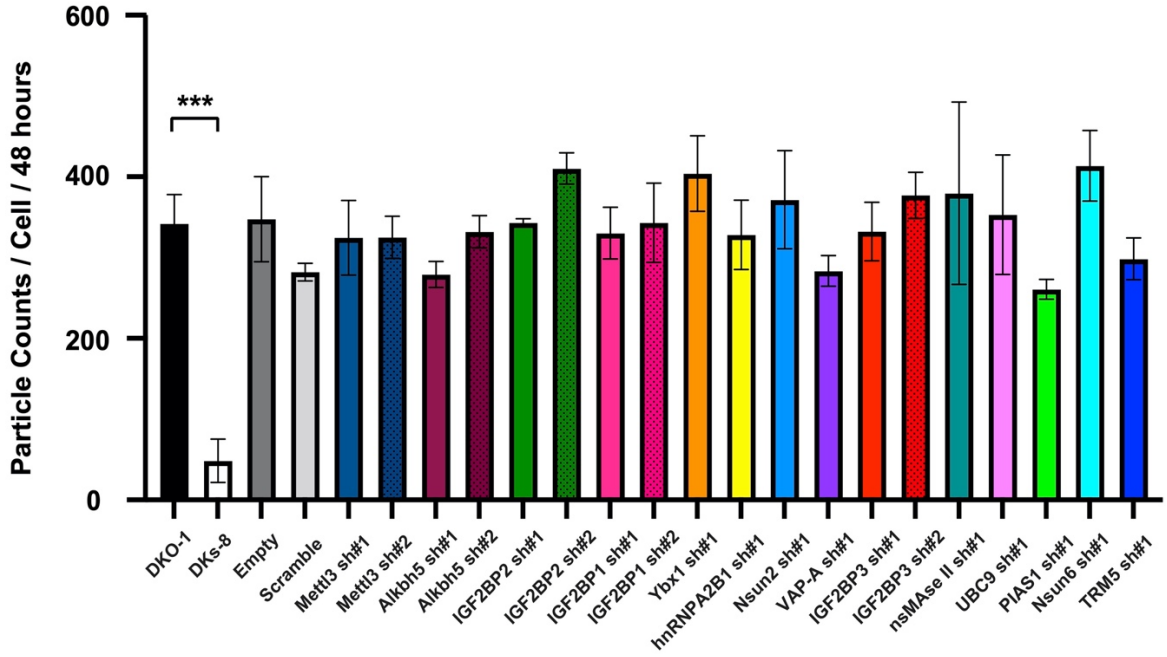

Figure S2. Effects of knockdown on EV secretion. Stable knockdown cells lines expressing shRNAs against the factors delineated in Table S1 were created starting with parental mutant KRAS (DKO-1) cells. Nanoparticle tracking analysis (NTA) was performed on mutant KRAS DKO-1 cells, wild type KRAS DKs-8 cells, and all stable knockdown cell lines. Significance was determined by one-way ANOVA. Data represent mean ± SE, n = 3, and ***p=0.0004.

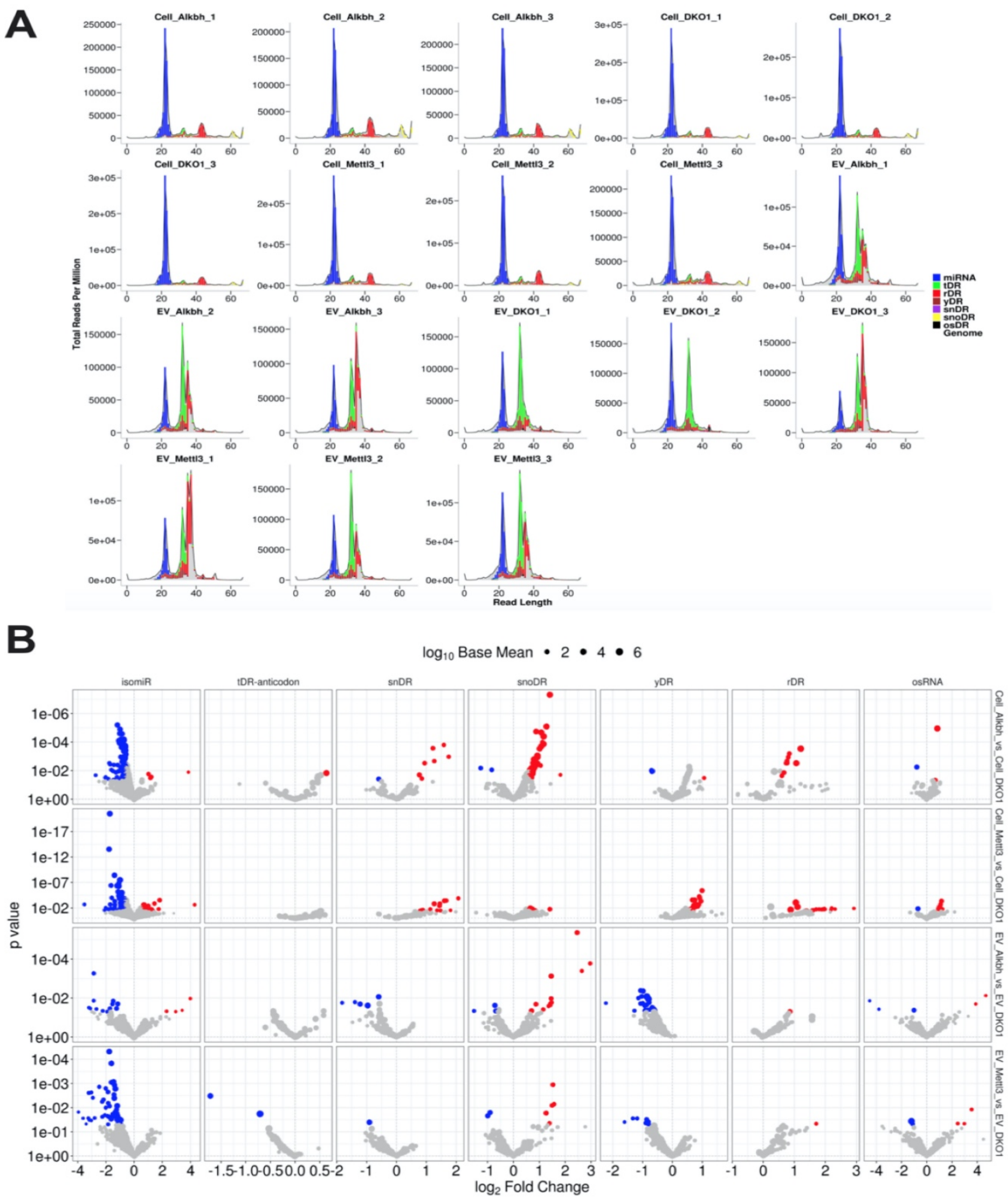

Figure S3. Differential expression and enrichment of small RNAs after knockdown. RNA sequencing was performed on libraries of cellular and EV small RNAs. **A**) Length distribution plots of cellular and EV small RNA classes. Read lengths of miRNAs (blue), tRNA-derived RNAs (tDRs; green), rRNA-derived RNAs (rDR; red), and other small RNA classes are as indicated. **B**) Volcano plots of significant differentially expressed small RNAs for cells and enriched EVs. Blue, significantly decreased; red, significantly increased.

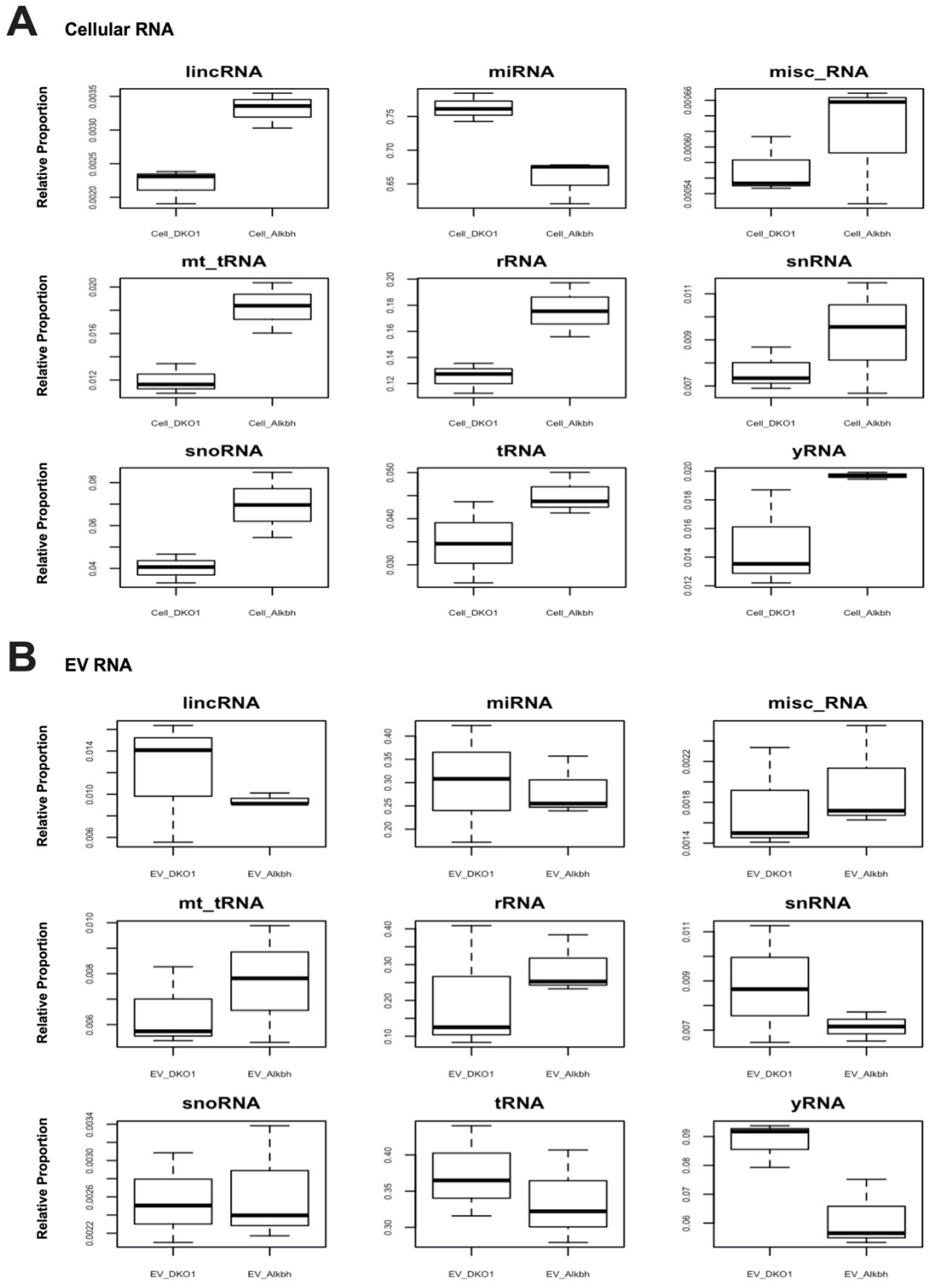

Figure S4. Relative proportion of RNA subclasses in DKO-1 and Alkbh5 samples. Small RNA sequencing results depict the relative proportion of mapped reads from different RNA subclasses in the parental DKO-1 or Alkbh5 knockdown cellular (**A**) and EV (**B**) RNA samples.

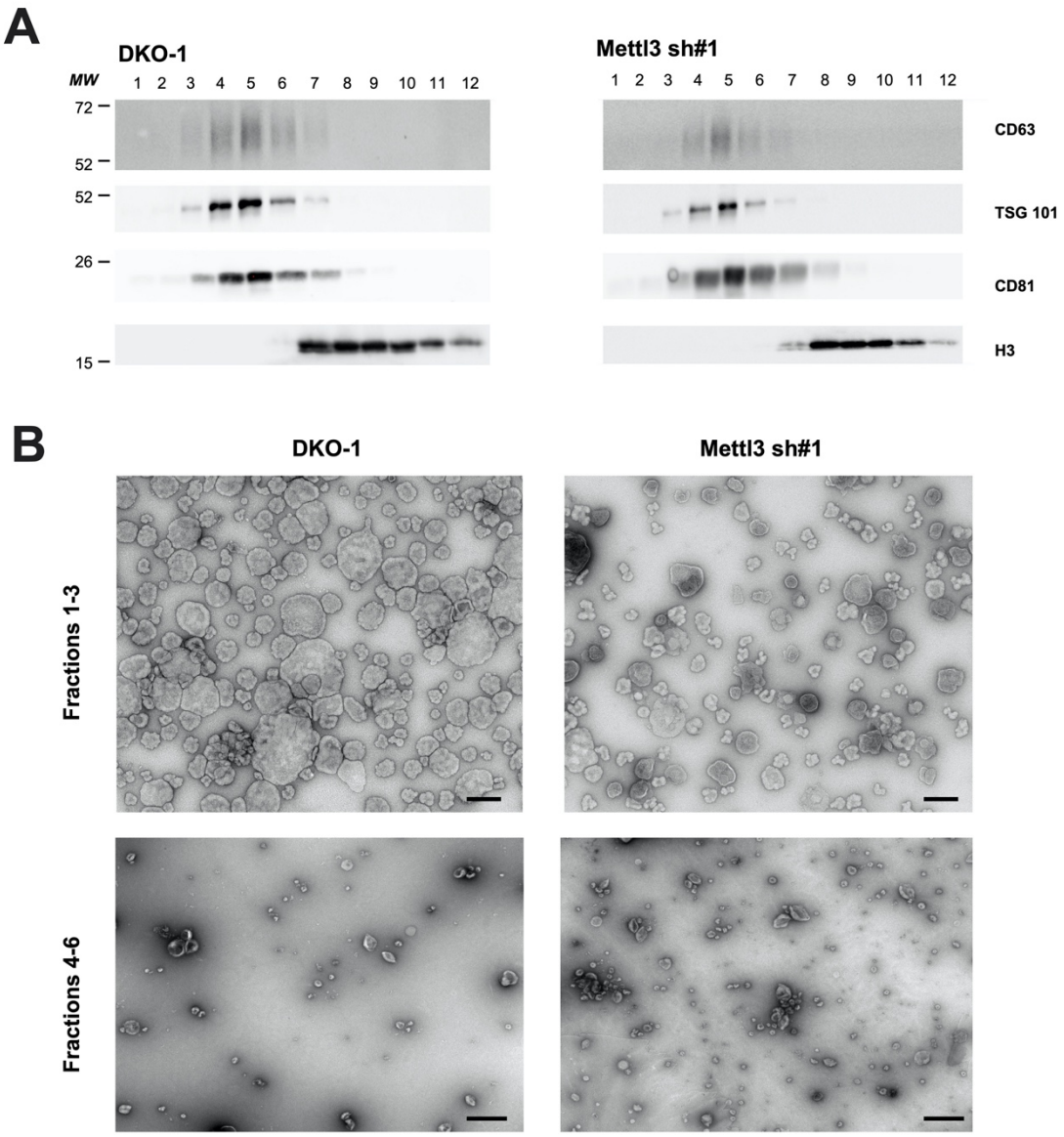

Figure S5. No effects on sEV protein markers and morphology after Mettl3 knockdown. **A**) sEVs were purified using differential ultracentrifugation followed by high resolution iodixanol gradients. Purified fractions were analyzed for known EV markers by western blots using antibodies against CD63, TSG101, CD81, and H3. **B**) Transmission electron microscopy (TEM) of DKO-1 and Mettl3 knockdown sEVs in fractions 1-3 and fractions 4-6. Scale bar, 200nm and 400nm, respectively.

Chapter 3

Discussion

EVs and their associated cargo have continued to gain interest and attention as an underappreciated form of cell-cell communication. Over the last decade, the field has grown exponentially and ongoing work continues to test the extent to which transfer of EV cargo can alter gene expression patterns in recipient cells. While precise quantitation of phenotypic changes driven by EV transfer is underway, cell-cell communication via EVs has been implicated in a number of important biological processes including development, immune function, drug resistance, and cancer (Colombo et al., 2014, Kalluri, 2016, Han et al., 2019). The presence of EVs in various body fluids can serve as a proxy for donor cell status raising the possibility that detection of EV cargo can serve as disease biomarkers or as delivery vehicles for therapeutic purposes (Cortez et al., 2011, S et al., 2013, Li et al., 2017, Poggio et al., 2019, Chen et al., 2018, Yamada et al., 2015). However, in order to fully tap the potential of EVs as disease biomarkers or therapeutic targets, better characterization and understanding of biogenesis pathways, mechanisms of cargo loading, and mechanisms of uptake by recipient cells needs to occur.

Key Findings from this Dissertation

In Chapter 2, I discovered a role for RNA modifications in miRNA export to EVs in KRAS mutant colorectal cancer cells. Although RNA modifications, especially m^6A,

have been well studied, knowledge of their effects on cargo loading into EVs is limited. Here, I show that knockdown of Mettl3, an m^{6}A writer, can significantly decrease export of miRNAs that contain m^{6}A consensus sequence elements. I created stable shRNA-expressing cell lines against multiple factors hypothesized to be involved in miRNA sorting or else known to be required for RNA base modification. Six of the lines tested altered extracellular transfer of *miR-100,* with 4 of the 6 cell lines involving proteins implicated in m^{6}A modification. 2D TLC analysis revealed the presence of m^{6}A, pseudouridine, and at least 5 other unknown modifications in KRAS mutant EVs. Analysis of *miR-100* levels in cells and EVs by qRT/PCR led to decreased levels of the miRNA in Mettl3 knockdown cells and EVs compared to DKO-1. To identify global RNA changes, small RNAseq on cells and EVs from parental (DKO-1) and knockdown (Mettl3 and Alkbh5) cell lines was performed. RNA transcripts from various classes were identified in all samples tested, with small RNA profiles showing distinct patterns of enrichment when comparing cellular and EV levels after knockdown of Mettl3 and Alkbh5. The majority of small RNA reads from cellular profiles were primarily miRNAs, while EV profiles were composed of miRNAs, tRNA fragments, and rRNA fragments. Interestingly, when examining the RNAseq data to identify individual miRNAs that were significantly decreased in EVs after Mettl3 knockdown, 4 of the top 5 miRNAs contained the m^{6}A consensus sequence. Furthermore, Mettl3 knockdown EVs were not able to confer colony growth in 3D. Taken together, our data suggest an important role for m^{6}A in selective export and functional activity of EVs.

The findings in this dissertation also further support a role for EVs in cell-cell communication *in vivo* (Didiano et al., 2020)(**Appendix A**). An *in vivo* screen to identify sources of EVs that could induce a regenerative response in zebrafish retinas was performed. We found that 12 sources of EVs stimulated Müller glia (MG) proliferation as shown by a significant increase in Proliferating Cell Nuclear Antigen (PCNA)-positive cells across the inner and outer nuclear layers upon injection into wildtype retinas. C6 glioma EVs produced the highest and most consistent increase of PCNA+ cells. Further purification of C6 EVs found that exosomes were responsible for MG-derived proliferation. Proteomic analysis of C6 exosomes revealed an enrichment of classical exosome markers as well as proteins involved in endo- and exocytosis. Small RNAseq analysis of cells and sEVs found differential enrichment of miRNAs in EVs.

Overall, analysis on EVs, their cargo, and possible mechanisms regulating sorting contained in this dissertation have helped propel the field forward. EVs serve as a relatively new mechanism of cell-cell communication and the work here contributes to the growing body of literature supporting this role. I propose that RNA modifications constitute a new mechanism driving selective export of miRNAs. Further research and analysis are needed to determine the full realm of possibilities that RNA base modifications could have on EV biogenesis and EV cargo, but this work demonstrates that m^6A modification is important for miRNA export.

Mechanisms Regulating Selective Export

Various studies have shown that miRNAs are secreted from cells, and a number of different mechanisms regulating miRNA cargo content have been suggested to play a role in export (Simons and Raposo, 2009, Shifrin et al., 2013, Maas et al., 2017, Cha et al., 2015, McKenzie et al., 2016, Shurtleff et al., 2016, Shurtleff et al., 2017, Villarroya-Beltri et al., 2013, Squadrito et al., 2014, Santangelo et al., 2016). However, to date, these mechanisms often seem to be cell- and disease-specific, and a universal or unifying mechanism responsible for RNA export to EVs has yet to be determined. This suggests 1) there is no universal mechanism (all context-specific), 2) combinations of existing mechanisms are needed to control export, or 3) an undiscovered unifying mechanism remains to be determined. My data suggest that RNA base modifications could be part of a unifying mechanism, however, further work is needed to fully elucidate the links between existing mechanisms and a specific role for RNA base modifications.

Currently, a number of RNA binding proteins and RNA sequence motifs have been identified and proposed to mediate selective export of miRNAs to EVs. The RNA binding proteins SYNCRIP, YBX1, and hnRNPA2/B1 have all been suggested to control miRNA sorting in their respective systems (Santangelo et al., 2016, Shurtleff et al., 2016, Villarroya-Beltri et al., 2013). As for sequence motifs, the EXO motif ‘GGAG’ was found enriched in exosomal miRNAs from T cells (Villarroya-Beltri et al., 2013), while the hEXO motif ‘GGCU’ increased miRNA export to EVs in hepatocellular carcinoma cells (Santangelo et al., 2016). Purely bioinformatics approaches identified zipcode

sequences (ACCAGCCU, CAGUGAGC, UAAUCCCA, and CUGCC) enriched in RNAs found in exosomes and microvesicles (Batagov et al., 2011, Bolukbasi et al., 2012). My work suggests that m^{6}A may serve as a signal that can target miRNAs for export and serve as a binding partner for specific RNA binding proteins, the combination of which could drive export (**Chapter 2**).

To examine whether m^{6}A consensus sequences might overlap with proposed miRNA export sequence motifs, I compared previously identified motifs with the m^{6}A modification consensus sequence (**Table 2**). My analysis reveals some similarities and striking overlap between some of the sequence motifs. The m^{6}A consensus sequence and the hnRNPA2/B1 binding site possess the same sequence motif. The EXO motif shares a 3 base overlap with m^{6}A and hnRNPA2/B1 ('GGA'), as well as a 3 base overlap with the zipcode sequence CAGUGAGC ('GAG'). The EXO and hEXO motifs can have variations in their sequence, however, the first letter indicated in the table is the most common nucleotide. If you take into account the other variations, the EXO motif has a 4 base overlap with m^{6}A and hnRNPA2/B1 ('GGAC'), while the hEXO motif has a 3 base overlap with those sequences ('GGA'). In addition to overlap between the motifs, there is also some overlap of these motifs with *miR-100* and *miR-125b*, 2 of the top 5 miRNAs downregulated in Mettl3 knockdown EVs (**Chapter 2**). Both miRNAs contain m^{6}A sites with overlapping or adjacent hnRNPA2/B1 sites. The m^{6}A consensus sequence present in the proposed sequences are highlighted in red in **Table 3**. Interestingly, there is also a 3-4 base overlap between *miR-125b* and 3 of the proposed zipcode sequences (ACCAGCCU, CAGUGAGC, and UAAUCCCA). In addition, *miR-*

100 contains a 3-4 base overlap with 2 of the zipcode sequences (ACCAGCCU and UAAUCCCA). For all the reported zipcode sequences and consensus motifs, there are preferred bases but the precise composition varies. Thus, although the overlap between m^{6}A sequences, RNA binding motifs, *miR-100*, and *miR-125b* might be relatively small, they are consistent with a role for these proteins in miRNA export.

Table 2: Sequence motifs proposed to control miRNA export to EVs

Name (miRNA or motif)	Sequence
miR-100	AACCCGUAGAUCCGAACUUGUG
miR-125b	UCCCUGAGACCCUAACUUGUGA
m^{6}A	RRACH (where R=A or G, H=A, C, or U)
hEXO	G/U/A G/A/U C/A/G U/A
EXO	G/U G A/C/G G/C, C/U/G C C U/G/A
hnRNPA2B1	RGAC
Zipcode	ACCAGCCU, CAGUGAGC, UAAUCCCA, CUGCC

Table 3: Overlap of m^{6}A consensus site with sequence motifs proposed to control miRNA export to EVs

Name (miRNA or motif)	Sequence
miR-100	AACCCGUAGAUCCGAACUUGUG
miR-125b	UCCCUGAGACCCUAACUUGUGA
m^{6}A	RRACH (where R=A or G, H=A, C, or U)
hEXO	G/U/A G/A/U C/A/G U/A
EXO	G/U G A/C/G G/C, C/U/G C C U/G/A
hnRNPA2B1	RGAC
Zipcode	ACCAGCCU, CAGUGAGC, UAAUCCCA, CUGCC

Based on the above and my RNAseq data after knockdown of Mettl3, the data support a combination of m^{6}A RNA base modifications and binding by specific RNA

binding proteins for regulated miRNA export, especially for *miR-100* and *miR-125b*. The hnRNPA2/B1 RNA binding protein was initially thought to serve as a reader of m^6A, but may actually bind adjacent to m^6A (Alarcon et al., 2015a, Villarroya-Beltri et al., 2013). YBX1, another RNA binding protein, specifically binds to the zipcode sequences ACCAGCCU, CAGUGAGC, and UAAUCCCA that are enriched in exosomal mRNAs (Kossinova et al., 2017). With strong evidence in support of RNA binding proteins and RNA sequence motifs playing a role in miRNA export to EVs, one could argue that a combination of mechanisms involving m^6A (or other base modifications) with an RNA binding protein could drive miRNA export. More work is needed to precisely define the role that RNA base modifications have on mature miRNA function, but the work in this dissertation suggests a role for miRNA export.

While my data support a role for m^6A modifications and export, I have only demonstrated this effect in a KRAS mutant colorectal cancer cell line. To address the role of cell context, more work is needed to extend my findings to additional cell types. Performing total RNAseq on parental and knockdown cells and EVs from a wider variety of cells might also provide insight into whether m^6A modifications regulate the export of other RNAs into EVs. In addition, I have only focused on one subunit of the m^6A methylase complex so it remains possible that other components in the m^6A writer complex could also play a role. Chevillet and colleagues observed that EV-associated miRNAs make up less than approximately 2-5% of the total secreted RNA, and even some of the most abundant miRNAs in the extracellular space have less than 1 miRNA copy per EV (Chevillet et al., 2014). Focusing on other abundant RNA molecules in

EVs and whether those RNAs contain base modifications may help to shed light on mechanisms of control. Using novel approaches and technologies specific for detection of additional RNA modifications could also help determine the significance or enrichment of these modifications in EV RNA. To identify m^6A sites throughout the transcriptome, Meyer et al (2012) developed m^6A-specific methylated RNA immunoprecipitation next-generation sequencing (MeRIP-Seq) (Meyer et al., 2012). Applying this technique to our data to determine if there are differences with Mettl3 knockdown would strengthen the argument that RNA modifications, or specifically m^6A, contribute to specific RNA export. Also, considering there are well over 100 known RNA modifications (Schaefer et al., 2017), there may very well be roles for other RNA modifications in export to EVs. Our data indicate the presence of abundant pseudouridine modification as well as other unknown modifications in EVs (**Fig. S1**), and it will be interesting to determine any role these modifications might play in export.

Beyond speculation that RNA base modifications might regulate export, it should also be pointed out that differential enrichment in EVs could also be simply due to differential stability of RNA molecules within EVs. It is possible that certain RNases are present at higher concentrations in EVs, and therefore cause depletion of specific RNAs that might contain a specific sequence motif (Mateescu et al., 2017). It is also possible that the presence of RNA binding proteins inside EVs could preferentially stabilize certain RNAs making them resistant to RNases (Chai et al., 2016). m^6A has many functions, with the best-established being to cause mRNA instability (Sommer et al., 1978). Readers of RNA modifications are also known to affect stability, translation,

and/or localization of mRNA molecules (Zaccara et al., 2019). YTH domain-containing family protein 2 (YTHDC2) promotes mRNA decay (Wang et al., 2014), while the IGF2BPs enhance mRNA stability (Huang et al., 2018). If in fact a large number of the RNA molecules present in EVs contain m^6A marks, the tightly controlled regulation of this modification by writers, erasers, and readers could impact the overall stability of RNA in EVs.

Limitations of the Study

Here, we focused on Mettl3 and Alkbh5, a writer and eraser of m^6A, and how knockdown of these proteins could alter miRNA secretion. Although we saw 60-70% knockdown of each protein (**Fig. 6A**), the remaining amounts likely account for why the PC analysis was not able to distinguish between parental and knockdown cells or EVs (**Fig. 6F**). Even though we did not achieve complete loss of either protein, the luciferase transfer assays and RNAseq data still showed differential enrichment of specific miRNAs in sEVs. One of the reasons we specifically chose to knockdown rather than knockout gene expression among the candidates outlined in **Table S1** is due to the possibility that complete loss of these factors could have widespread detrimental effects on the resulting cells since so much of RNA metabolism would be affected. In mice, Mettl3 knockout is embryonic lethal (Geula et al., 2015), and recent *in vivo* studies have demonstrated that Mettl3 is essential for proper gametogenesis with more severe phenotypes occurring the earlier Mettl3 was lost (Lasman et al., 2020). Loss of Mettl3 in mesenchymal stem cells has also been shown to induce osteoporosis in mice, impair bone formation, and increase bone marrow adiposity (Wu et al., 2018b).

In colon cancer cell lines, Mettl3 knockout decreased cell proliferation and inhibited colony and spheroid formation (Xu et al., 2020). Thus, although loss of Mettl3 is possible, we chose to avoid potential growth defects although we recognize this as a limitation of the current approach.

Future Directions

In order to expand on the work in this dissertation and begin to identify whether or not a universal mechanism regulating RNA secretion to EVs exists, some key steps need to be taken. First, the role of m^6A modification in RNA export needs to be elucidated in other cell- and disease-types to ensure this mechanism of regulation is not content-specific. Using cell- and disease-types already shown to support selective miRNA export could expedite this process. For example, using the pancreatic cancer model where *miR-100* and *miR-125b* are upregulated and serve as important effectors of TGF-β (Ottaviani et al., 2018). In our 2D TLC analysis, other modifications were present in our mutant KRAS EVs. Identifying these modifications and whether or not they contribute to RNA secretion is another critical step in determining a unifying mechanism for export. Another key step includes determining if a combination of proposed mechanism could be playing a role. Knocking down Mettl3 and RNA binding proteins like YBX1 or hnRNPA2/B1, or a combination of other factors, and identifying whether or not it affects RNA export has the potential to show if multiple mechanism of regulation are important. Taking these crucial first steps in expanding our knowledge on mechanisms regulating RNA secretion to EVs could help unlock the key to a unifying or universal mechanism.

Appendix

Induction of a proliferative response in the zebrafish retina by injection of extracellular vesicles[2]

Abstract

Cell transplantation studies and gene therapy approaches to deliver genes of interest have been making exciting progress to restore vision by retinal repair, but targeted delivery and complete cellular integration remain challenging. An alternative approach is to induce endogenous Müller glia (MG) to regenerate lost neurons and photoreceptors, as occurs spontaneously in teleost fish and amphibians. Recently, it has been shown that cytoplasmic material can be transferred between transplanted donor cells and retinal recipient cells. One potential mechanism of material transfer is via extracellular vesicles (EVs). We conducted an *in vivo* screen and identified 12 sources of EVs that could induce proliferation after intravitreal injection into undamaged zebrafish eyes. EVs from C6 glioma cells were the most consistent at inducing MG-derived proliferating cells. Proteomic and RNAseq analyses of EVs capable of inducing MG-derived proliferation identified targets for future therapeutic approaches.

Keywords: Retina, Müller glia, Extracellular Vesicle, Regeneration

---

[2]Dominic Didiano*, Jessica J. Abner*, Scott A. Hinger*, Zachary Flickinger*, Matthew Kent, Margaret A. Clement, Sankarathi Balaiya, Qi Liu, Edward M. Levine, and James G. Patton. (2020). "Induction of a proliferative response in the zebrafish retina by injection of extracellular vesicles." *Experimental Eye Research*. 200:108254. doi: 10.1016/j.exer.2020.108254. *These authors contributed equally.

Introduction

In mammals and humans, the extent of spontaneous repair after retina injury or disease is either nonexistent or extremely limited (Karl and Reh, 2010). Rather than regenerate, damaged mammalian retinas commonly undergo reactive gliosis and scar formation (Bringmann et al., 2006). Numerous strategies are being tested to treat a variety of human retinal disorders, including gene therapy approaches and transplantation of stem cell-derived progenitor cells (MacLaren et al., 2006, Pearson et al., 2012, Stern et al., 2018, Roska and Sahel, 2018, Cehajic-Kapetanovic et al., 2015). An attractive alternative would be to induce endogenous regeneration from a resident pluripotent adult retinal stem cell (Müller glia; MG) (Ahmad et al., 2011). The adult zebrafish retina contains two classes of cells with regenerative capacity derived from MG. After retina damage in zebrafish, MG spontaneously dedifferentiate and then undergo asymmetric division for self-renewal and the production of a pool of proliferating progenitor cells that can regenerate all lost or damaged retinal cell types (Bernardos et al., 2007, Wan and Goldman, 2016). Therapeutic strategies designed to induce endogenous mammalian MG to regenerate lost retinal neurons and photoreceptors would be a powerful approach to restore vision.

Extracellular vesicles (EVs) are secreted nanoparticle sized, membrane bound vesicles containing lipid, protein, and RNA cargo (Tkach and Thery, 2016, Maas et al., 2017, van Niel et al., 2018, Thery et al., 2018). All cells secrete a diverse array of heterogeneous extracellular vesicles that can mediate cell-cell communication through the delivery of cargo and/or induction of recipient cell signaling cascades in numerous

biological contexts (Maia et al., 2018, Raposo and Stahl, 2019, Robbins and Morelli, 2014, McGough and Vincent, 2016). EVs are classified both by size and biogenesis pathway (Colombo et al., 2014). Larger microvesicles (greater than 150nm) and a heterogeneous mixture of other vesicles are released by direct budding from the plasma membrane (Booth et al., 2006, Kowal et al., 2016). Smaller vesicles of endosomal origin (exosomes) are secreted when multivesicular bodies (MVBs) fuse with the plasma membrane, thereby releasing their intraluminal contents (Kalluri, 2016). These different classes of vesicles utilize distinct mechanisms controlling cargo selection in cell- and disease-specific contexts (Maas et al., 2017, Shifrin et al., 2013, Simons and Raposo, 2009). As purification strategies have been refined, protein markers and other cargo content found within the different classes of vesicles are being reassessed (Jeppesen et al., 2019). Heterogeneous mixtures of EVs can be readily purified by differential ultracentrifugation, but high resolution density gradient fractionation is now increasingly being utilized to enable separation and purification of small EVs (sEVs), large EVs, and non-vesicular fractions (Kowal et al., 2016, Willms et al., 2018, Jeppesen et al., 2019).

Once in the extracellular space, EVs can act both locally and distant in an autocrine or paracrine fashion (Cha et al., 2015, Wortzel et al., 2019, Tkach and Thery, 2016, Gutierrez-Vazquez et al., 2013). The precise mechanisms mediating selective EV uptake remain largely unknown, but because of their ability to transfer cargo between cell types and across membrane barriers, EVs have emerged as potentially potent therapeutic agents (Murphy et al., 2019, Kalluri, 2016, Wiklander et al., 2019,

Farber and Katsman, 2016, Wassmer et al., 2017, Silva et al., 2015). Here, we report the results of a screen for sources of EVs capable of inducing proliferation that can mimic the early stages of retina regeneration. We were prompted to test EVs based on findings that injected donor stem cells can engage in material transfer, cytoplasmic exchange, or cytoplasmic fusion (Pearson et al., 2016, Singh et al., 2016, Santos-Ferreira et al., 2016). Previous experiments indicating that transplanted donor cells had integrated into the host retina might have been confounded by exchange of protein content rather than actual integration. Follow up work suggested that both integration and material transfer can occur (Waldron et al., 2018). However, combined with papers demonstrating EV release from multiple retinal cell types and their ability to induce changes in gene expression in immortalized MG (Katsman et al., 2012, Peng et al., 2018), retinal ganglion cells (Mead and Tomarev, 2017), and retinal progenitor cells (Zhou et al., 2018), we sought to systematically test sources of EVs that could induce a proliferative response after intravitreal injection in otherwise undamaged retinas. We identified 12 different cell lines that secrete small EVs capable of inducing proliferation in zebrafish. Small EVs from C6 glioma cells (Grobben et al., 2002) were readily taken up by cultured human MG and were the most consistent source of MG-derived proliferation after *in vivo* injection.

Methods

Zebrafish

Wild-type AB or Tg*(1016tuba1a:gfp)* (Fausett and Goldman, 2006) zebrafish, 5-7 months old, were used for all experiments. All zebrafish lines were maintained at

28.5°C on a 14/10-hour light/dark cycle. Following retinal injections, zebrafish were maintained at 30°C for 72 hours before analysis. All procedures were approved by the Vanderbilt University Institutional Animal Care and Use Committee (IACUC).

Isolation of EVs

EVs were isolated from culture media. For standard lines, EVs were isolated after final culture for 48 hours in the absence of serum; stem cell culture media lacks serum. For C6 cells, T175 flasks (Corning) were seeded between 6-7x10^6 cells per flask and grown in the presence of serum to 80% confluency (~48 hours), washed three times with 1x Dulbecco's PBS (DPBS; Gibco), and then grown for 48 hours in serum free media. Media was collected and subjected to differential centrifugation in three steps: 1000rpm for 10 minutes (room temperature), 2000xg for 25 minutes (4°C), and then 10,000xg for 30 minutes (4°C). These steps produce cell pellets, cell debris and large EVs, and microvesicles, respectively. P100 pellets (crude sEVs) were obtained by centrifuging conditioned media (CM) through the three steps above, followed by an additional 17 hr at 100,000xg (4°C). Pellets were suspended in 1xDPBS and washed by centrifugation at 100,000xg twice for 70 minutes each (4°C). Final sEV pellets were resuspended in 20µL 1xDPBS. This level of purity was used for the EV screen shown in Fig 2. For density gradient preparations, CM subject to the three steps above was concentrated using a 100K concentrator (MilliPore) to ~5mL and then layered onto 1mL 60% iodixanol cushions (Optiprep), and centrifuged at 100,000xg for 17 hours (4°C). The bottom 3mL were collected and then layered on top of an iodixanol discontinuous gradient consisting of 3 ml layers of 40%, 20% (CM layer), 10%, and 5% iodixanol.

After centrifugation at 100,000xg for 17 hours (4°C), 1mL fractions (12) were collected (top to bottom). Each fraction was diluted in 12mL 1xDPBS and then centrifuged at 100,000xg for 3 hours (4°C). Final pellets were resuspended in 10-30µL 1xDPBS.

Nanoparticle Tracking Analysis (NTA)

Particle sizes and numbers were analyzed using the Zetaview® Nanoparticle Tracking Video Microscope PMX-120 (Particle Matrix) and associated software. After optimization, settings were held constant across all replicate samples. Samples were diluted and particle counts and sizes were generated following the manufacturers protocols. The concentration of vesicles ranged from 10^8 to 10^{11} particles/mL. The average diameter of vesicles counted was ~100nm, corresponding to the size of small EVs.

EV Injections

EVs were injected into the vitreous of adult zebrafish eyes using an adapted protocol as previously described (Thummel et al., 2008). Briefly, a sapphire blade scalpel was used to make an incision in the cornea near the pupil after anesthetizing fish with 4% tricaine. A Hamilton syringe was inserted into the incision site and used to inject 0.5µl of solution into the vitreous. Fish were immediately placed into a recovery tank after injections.

Immunohistochemistry

Injected adult zebrafish eyes were removed and fixed overnight at 4.0°C in 4% PFA and 1X PBS at 72 hours post injection. Following fixation, eyes were washed in 1X PBS with 5% sucrose and cryo-protected in 30% sucrose in PBS for 4 hrs. at room temperature (RT), followed by a 2:1 mixture of OCT (Thermo Scientific) to 30% sucrose for 4 hrs. at RT and 1 hr. in straight OCT at RT before embedding in OCT. Eyes were cut into 15-20 micron sections using a Leica CM 1950, placed on Histobond slides (VWR), and dried on a slide warmer before immunostaining. Prior to immunohistochemistry (IHC), sections were subjected to antigen retrieval by incubation in 5mM sodium citrate, 0.05 % TWEEN 20, pH 6.0 for 10-20 mins. at 95°C. Slides were then rinsed with PBS and blocked in 3% donkey serum and 0.1% Triton X-100 for 2 hrs. at RT before primary antibodies were added. Slides were incubated with primary antibodies for 4 hrs. at RT or overnight at 4.0°C in 1% donkey serum and 0.05% TWEEN. The following primary antibodies were used at 1:500 dilution: mouse anti-PCNA (Sigma); rabbit anti-PCNA (Abcam); mouse anti-GFP (Invitrogen) and rabbit anti-GFP (Torrey Pines Biolabs). Following three 10 min. PBS washes, the following secondary antibodies were added for 4 hrs. at RT or overnight at 4.0°C in 1% donkey serum, 0.05% TWEEN at 1:500 dilution: donkey anti-mouse AF488, donkey anti-rabbit AF488, donkey anti-mouse Cy-3, donkey anti-rabbit Cy-3 (Jackson Immuno-Research). TO-PRO-3 was added with secondary antibodies at 1:1000 dilution (Thermo-Fisher Scientific). Following secondary antibody incubation, slides were washed three times with PBS for 10 mins. each before being air-dried and treated with Vectashield (Vector Labs) before being cover slipped.

Transwell Assays

C6 cells were cultured to ~80% confluency in T75 flasks (Corning). Cells were washed once in 1xPBS and then incubated with fresh media containing 4µL DiI per 7mL media at 37°C for 24 hrs. (DiIC18(3), Invitrogen). Cells were then trypsinized and seeded into Transwell chambers (0.4µm pore well, Costar) at $0.1x10^6$ cells per well, and then incubated for 24 hrs. to allow adherence. Concurrently, human Müller cells were collected after trypsinization (Gibco) and stained using PKH67 (PKH67 GFP, Sigma). Müller cells were plated on coverslips, submerged in media within a 12 well dish (Corning), and incubated for 24 hours to allow adherence. The following day, both donor and recipient cells were washed three times in 1xPBS, and then co-cultured in fresh media for 48 hours. Following incubation, recipient cells were washed twice in 1x PBS and then fixed in 4% PFA for 20 minutes at RT (Sigma). Coverslips were then mounted on slides using Vectashield with DAPI (Vector).

Morpholino Injections

0.5 µl of 3'-lissamine labeled morpholinos (MO) from Gene Tools at a stock concentration of 1.5mM were injected into the intravitreal space of adult zebrafish eyes. The fish were allowed to recover for 1 hour after which 0.5µl of C6 sEVs or PBS were injected into the intravitreal space of adult zebrafish eyes followed by electroporation with two pulses of 75V for 50ms using a Biorad Gene Pulser Xcell (Thummel et al., 2008, Ramachandran et al., 2010, Ramachandran et al., 2012). The following morpholinos were used:

Control MO: 5'-CCTCTTACCTCAGTTACAATTTATA-3'

ASCL1a MO1: 5'-ATCTTGGCGGTGATGTCCATTTCGC-3'

ASCL1a MO2: 5'-AAGGAGTGAGTCAAAGCACTAAAGT-3'

Imaging and Scoring of Retinal Sections

Antibody stained retinal sections were imaged using a META Zeiss LSM 510 Meta confocal microscope under a 40X objective. Images were processed using ImageJ 2.0. For scoring of all retina sections, $PCNA^{+}$ cells were counted across inner and outer nuclear layers in double blind experiments utilizing undergraduate researchers. Subsequent experiments utilized co-staining with antibodies against glutamine synthase or Tg(*1016tuba1a:gfp*)$^{+}$ or Tg*(GFAP:GFP)*^{mi2001} lines which allowed determination of the number of $PCNA^{+}$ cells that co-localized with these markers, primarily in the inner nuclear layer in addition to scoring of all $PCNA^{+}$ cells across the inner and outer nuclear layers. Cells were counted from 2-4 non-consecutive sections and averaged for each eye, as indicated in respective figure legends. A Zeiss Axio Observer Z1 was used with a 40X objective.

qRT/PCR

Whole retinas were dissected and immediately placed into TRIzol (Life Technologies) 72 hours post injection. qRT/PCR for Ascl1a was performed on total RNA isolated from dissected retinas in TRIzol according to the manufacturer's protocol. cDNA templates were reverse transcribed with the Accuscript High Fidelity 1st Strand cDNA Synthesis Kit (Agilent). qPCR was performed with primers for Ascl1a (5'-

TGAGCGTTCGTAAAAGGAAACT-3' and 5'-CGTGGTTTGCCGGTTTGTAT-3') and 18S rRNA (5'-TTACAGGGCCTCGAAAGAGA-3' and 5'-AAACGGCTACCACATCCAAG-3') and SsoAdvanced Universal SYBR Green Supermix (Bio-Rad). Relative expression values were calculated using the ΔΔCt method and 18S rRNA for normalization. Statistical analysis was performed on log transformed expression values using two-tailed t-tests.

Western Blots

Protein lysates were collected using 1x RIPA lysis buffer (Millipore) and concentrations were determined using the Pierce BCA assay kit (Thermo Scientific). Proteins (1μg) were separated on 12% MINI-PROTEAN TGX pre-cast gels (Bio-Rad) and transferred onto PVDF membranes using the Trans-Blot Turbo Transfer System (Bio-Rad). Membranes were blocked in 5% milk in TBS-T for 1 hour and then incubated with primary antibodies in 5% milk in TBS-T overnight at 4°C. Primary antibodies were used at the following concentrations: anti-TSG101 (Invitrogen) at 1:1000, anti-CD81 (Santa Cruz Biotechnology) at 1:1000, and anti-Histone H3 (Abcam) at 1:5000. The next day, blots were washed with 1X TBS-T 3 times, then incubated with secondary antibodies in 5% milk in TBS-T at room temperature for 45 minutes. The following secondary antibodies were used at a concentration of 1:10,000: anti-Mouse ECL (GE Healthcare) and anti-Rabbit IgG (Cell Signaling). Blots were washed with 1X TBS-T three times and then treated with SuperSignal™ West Fenmto Maximum Sensitivity Substrate (Thermo Scientific) to visualize bands.

Proteomics

Sample preparation for shotgun proteomic analysis of cellular and exosomal proteins was performed using S-traps (https://www.protifi.com/s-trap/) according to the manufacturer's instructions. The resulting peptides were analyzed by high resolution LC-MS/MS. Briefly, peptides were autosampled onto a 200 X 0.1 mm (Jupiter 3 micron, 300A), self-packed analytical column coupled directly to a Q-exactive plus mass spectrometer (ThermoFisher) using a nanoelectrospray source and resolved using an aqueous to organic gradient. Both the intact masses (MS) and fragmentation patterns (MS/MS) of the peptides were collected in a data dependent manner utilizing dynamic exclusion to maximize depth of proteome coverage. The resulting peptide MS/MS spectral data were searched against the rat protein database to which common contaminants and reversed versions of each protein were appended using Sequest (https://link.springer.com/article/10.1016%2F1044-0305%2894%2980016-2). The resulting identifications were filtered and collated together at the protein level using Scaffold (http://www.proteomesoftware.com/).

RNAseq

Total RNA from cells and EVs was isolated using TRIzol (Life Technologies). For EVs, TRIzol was incubated with 100μl or less of concentrated EVs for an extended 15 min. incubation period prior to chloroform extraction. RNA pellets were resuspended in 60μl of RNase-free water and then re-purified using miRNeasy (Qiagen). RNAseq libraries were prepared using 200 ng of RNA and the NEBNext® Small RNA Library Prep Set for Illumina® (NEB, Cat: E7330S). Size selection targeting 100–200

nucleotides was performed on small RNA libraries using the Pippin Prep instrument and 3% agarose dye free gel (Sage Science #CDF 3010). Libraries were sequenced using the NovaSeq 6000 with 150 bp paired end reads targeting 50M reads per samples. Reads were trimmed post sequencing to 50 bp SE. RTA (version 2.4.11; Illumina) was used for base calling. Cutadapt (https://github.com/marcelm/cutadapt) was used to trim adapters. TIGER (https://github.com/shengqh/TIGER), was used to perform read mapping, miRNA quantification and differential analysis. Specifically, Bowtie was used to map reads to the rat miRNAs in miRBase and the rat genome. DESeq2 was used to detect differential expression between exosome and cells. Genes with fold change greater than 2 and adjusted p-value less than 0.01 were considered differentially expressed.

Functional Enrichment Analysis

Gene ontology analyses were performed on proteomics data using WebGestalt (Liao et al., 2019). Only proteins enriched in EVs with a value greater than 2-fold were used. Proteins were compared using Over-Representation Analysis (ORA) set to the genome protein-coding reference set. All groups were significant with an FDR < 0.05. For RNAseq data, predicted targets for the top 10 miRNAs enriched in EVs were determined using MicroRNA Target Prediction Database (mirdb.org). Only the top 5 predicted targets with a target score > 80 were used.

Statistical Analysis

Student t-tests or One-way ANOVA analyses were used to calculate significance depending on how many conditions were simultaneously performed using GraphPad Prism 7 software. Multiple comparison tests with one-way ANOVA are specified in each figure legend. The threshold for significance (alpha) was 0.05. All data are represented by a mean value +/- standard error.

Antibodies Used

Name	**Company**	**Catalog Number**	**Concentration**
Rabbit anti-TSG101	Invitrogen	PA5-31260	1:1000
Mouse anti-CD81	Santa Cruz Biotechnology	Sc-166029	1:1000
Rabbit anti-Histone H3	Abcam	Ab1791	1:5000
Anti-mouse ECL	GE Healthcare	NA931	1:10000
Anti-Rabbit IgG	Cell Signaling	7074	1:10000
Mouse anti-PCNA	Sigma	P8825	1:500
Rabbit anti-PCNA	Abcam	Ab18197	1:500
Mouse anti-GFP	Invitrogen	MAS-15256	1:500
Rabbit anti-GFP	Torrey Pines Biolabs	TP401	1:500
Donkey anti-mouse AF488	Jackson ImmunoResearch	715-545-151	1:500
Donkey anti-rabbit AF488	Jackson ImmunoResearch	711-545-152	1:500
Donkey anti-mouse Cy3	Jackson ImmunoResearch	715-165-160	1:500
Donkey anti-rabbit Cy3	Jackson ImmunoResearch	711-165-152	1:500
TO-PRO-3	Thermo Fisher Scientific	T3605	1:500

Results

In vivo screen of EVs capable of inducing MG-derived proliferation in undamaged zebrafish retinas

We sought to perform a large-scale *in vivo* screen of EV preparations for their ability to stimulate MG proliferation in the retina of zebrafish, as marked by the expression of Proliferating Cell Nuclear Antigen (PCNA). As a first test of whether EVs could be taken up by MG, we used Transwell assays and were able to detect uptake of fluorescently labeled EVs by primary cultured human MG (Capozzi et al., 2014) (**A.S1**). For the *in vivo* screen, a heterogeneous mix of mostly small EVs (sEVs) were purified by ultracentrifugation from both cell culture media and dissected tissue samples with an emphasis on stem-cell derived EVs in the hope that such cells might be more translatable to future human use. sEV preparations were analyzed by particle analysis and then 0.5μl were intravitreally injected into the eyes of 5-15 six month-old AB zebrafish and compared to PBS vehicle control injections for each clutch of zebrafish tested. Fish were sacrificed 72 hours after injection, eyes dissected and fixed, cryo-protected, sectioned, and antibody stained for PCNA (Rajaram et al., 2014). For each eye, 2-4 nonconsecutive sections per retina (from ~60 sections) were scored for the average number of $PCNA^+$ cells across the inner and outer nuclear layers (INL and ONL), excluding the circumferential germinal zone or ciliary marginal zone, which is known to proliferate through adulthood (Stenkamp, 2007, Fischer et al., 2013). To ensure that any increases in $PCNA^+$ cells were not simply due to nonspecific injury from the injections themselves, we performed TUNEL staining to detect apoptotic cells at 48 and 72 hours after injection with PBS or with EVs from C6 glioma conditioned media

(**A.S2**). No significant differences in TUNEL staining were detected between PBS and EV injected retinas. Injection of PBS alone induced a slight increase in $PCNA^+$ cells compared to uninjected control retinas which typically show little to no $PCNA^+$ cells except for rare single $PCNA^+$ cells in the ONL which are only observed in 5-10% of sections and likely correspond to rod precursors (**A.S3**). All statistical analyses were performed by comparing the number of $PCNA^+$ cells in EV injected retinas to PBS control injections.

In total, we screened 59 independent sEV preparations from a variety of cultured stem cells, primary neuronal cultures, iPS cells undergoing a variety of differentiation conditions, cancer cell lines and from wild type zebrafish retinas or zebrafish retinas undergoing regeneration after being subjected to constant intense light damage (Vihtelic and Hyde, 2000)(**A.1, Table A.S1**). In addition to the controls above, we injected cell free media or large EVs, but did not detect increased $PCNA^+$ counts compared to PBS control injections (**A.S4**)**.** Injection of microvesicles resulted in a modest but significant increase in $PCNA^+$ cells ($p<0.05$), whereas injection of sEVs resulted in the most significant induction of $PCNA^+$ cells ($p<0.001$)(**A.S4**). Nanosight tracking analysis revealed that particle size distribution from the different sEV preparations was similar (40-100nm) and that all sEV preparations had relatively high numbers of particles (**Table A.S1**). Although the particle counts between different preparations sometimes differed by an order of magnitude, there was no correlation between particle counts and the induction of $PCNA^+$ cells at the numbers tested. However, serial dilution of C6 sEVs

led to a corresponding decrease in PCNA$^+$ cell numbers and heat or protease treatment also abolished activity (**A.S5**)

Twelve sEV preparations induced statistically significant increases in PCNA$^+$ counts across the INL and ONL of injected wild type retinas (**A.1B**). Subsequent co-staining of sections with antibodies against glutamine synthase (GS), a marker of MG (Rajaram et al., 2014), showed that only a subset of EV preparations induced proliferation of PCNA$^+$ cells in the INL that co-localize with MG (**A.S6**). Of the 7 lines secreting sEVs that induced the most significant increase in PCNA$^+$ cells ($p<0.001$)(**A.1B**), 4 were derived from human iPS cells differentiating over time into the dopaminergic (DA) lineage (Neely et al., 2017). These sEVs most commonly induced proliferation of cells in the ONL (**A.S6**). sEVs that predominantly induced proliferation of cells in the INL include those derived from DKO-1 mutant KRAS colorectal cancer cells (Shirasawa et al., 1993), primary cultures of rat hippocampal glia (astrocytes), and C6 rat glioma cells (Grobben et al., 2002)(**A.S6**). For this paper, we focused on induction of proliferating cells in the INL that co-localize with markers consistent with MG-derived proliferation.

C6 sEVs induce proliferation in MG-derived cells

sEVs from C6 glioma cells were the most consistent at inducing statistically significantly increased levels of PCNA$^+$ cells in the INL and the majority of those cells co-localized with GS (**A.S6**) and with GFP using Tg*(1016tuba1a:gfp*) zebrafish in which GFP expression marks dedifferentiated MG and proliferating progenitor cells (Fausett

and Goldman, 2006)(**A.2A, B**). To further test whether a canonical regenerative response was initiated, we co-injected C6 sEVs into the Tg*(1016tuba1a:gfp*) line in the presence or absence of antisense morpholinos targeting *ascl1a.* Ascl1a is a transcription factor that is required for MG-derived retinal regeneration in zebrafish (Fausett et al., 2008, Ramachandran et al., 2011, Rao et al., 2017). Compared to control MO injection, co-injection of two independent *ascl1a* MOs resulted in a complete suppression of sEV-induced proliferation (**A.2C-G**).

Decreased levels of proliferation after injection of morpholinos targeting *ascl1a* suggest that C6 sEVs can induce expression of Ascl1a. To test this, we isolated RNA after intravitreal injection of C6 sEVs and performed qRT/PCR with primers against *ascl1a*. As shown in Fig. 2H, we observed a significant increase in *ascl1a* levels after C6 sEV injection when compared to control PBS injections.

C6 exosomes induce MG-derived proliferation

As EV purification protocols are being refined and optimized, additional purification steps and new standards are being adopted regarding the use of protein markers for specific subclasses of EVs (Thery et al., 2018, Jeppesen et al., 2019). To more precisely define the identity of the C6 sEVs that are responsible for increased numbers of $PCNA^+$ cells after intravitreal injection, we purified sEVs using iodixanol density gradient fractionation (Li et al., 2018)(**A.3A**). This allowed for separation of the sEV preparations used in the initial screen into 12 fractions corresponding to dense, non-vesicular protein-rich fractions (marked by histone H3), small intermediate density

vesicular fractions that include classical exosomes (marked by TSG101 and CD81), and larger, lipid-rich, vesicles (**A.3B**).

For intravitreal injections of gradient purified particles, we combined fractions into pools based on vesicle marker profiles (**A.3B**). Pool 1 (P1) contained fractions 1-4, composed of large vesicles, Pool 2 (P2) contained fractions 5-8, composed of sEVs, and Pool 3 (P3) contained fractions 9-12, composed primarily of nonvesicular lipoproteins, ribonucleoproteins, and protein aggregates. After injection into wild type AB fish and co-staining for both GS and PCNA, the highest proliferative activity was found to reside in P2, where significantly higher $PCNA^+$ cells were observed in the INL compared to the other fractions and to the PBS control (**A.3C-G**). The $PCNA^+$ cells were observed adjacent to and/or closely associated with GS-stained MG processes. Neither P1 nor P3 induced a proliferative response above control PBS injections. When we injected P2 sEVs into the Tg*(1016tuba1a:gfp*) line we detected a significant increase in the number of GFP^+ cells (indicating dedifferentiated MG) that co-localized or were adjacent to PCNA+ cells, consistent with MG-derived progenitor cells (**A.3H-J**). We also injected P2 sEVs into Tg(*gfap:gfp)* fish which express GFP in MG (Bernardos and Raymond, 2006). Again, the resulting $PCNA^+$ cells co-localized with and adjacent to GFP^+ MG in the INL at 72 hr post injection (**A.S7**), consistent with the idea that the MG are dedifferentiating into a progenitor state.

Proteomic analysis of C6 P2 exosomes

To begin to characterize what factors might be responsible for inducing proliferation after intravitreal injection of C6-derived sEVs, we performed proteomic analysis of P2 and identified enriched proteins compared to C6 cellular levels. From total spectral counts, 1849 unique proteins were identified with 33% enriched in C6 cells, 16% enriched in P2 sEVs, and ~50% shared between both (**A.4A-C**). Most proteins known to be enriched in sEVs were found in P2 including traditional exosome markers β1-integrin, CD29, CD63, CD9, Syntenin-1, and Caveolin-1 (Thery et al., 2018). Some proteins were found at or below the limits of detection in the cellular proteome, but were readily identified in P2 sEVs, indicating either rapid secretion and/or degradation in cells. **A.4A** includes all proteins detected in either the cellular or sEV proteomes (or both), including those where the cellular levels were at or below the limits of detection. **A.4B** includes only those proteins where fold enrichment values could be calculated, i.e. cellular levels well above background. The volcano plot in **A.4C** is derived from those proteins included in **A.4B** and depicts individual proteins enriched in either C6 cells (red) or sEVs (blue) with corresponding p-values.

Bioinformatic analyses of the most enriched proteins in C6 sEVs identified several expected protein classes, including proteins involved in endo- and exocytosis and regulators of such trafficking including the Rab family of GTPases (**A.4 and Table A.S2, Table A.S3A-C**). The protein with the highest spectral counts enriched in P2 sEVs was lactadherin, also known as MFG-E8 or SED1 (Stubbs et al., 1990, Taylor et al., 1997, Ensslin and Shur, 2007). MFG-E8 is a secreted protein that contains EGF

and Factor VIII domains that was originally identified on milk fat globules and thought to mediate adhesion to integrin-expressing cells (Taylor et al., 1997). MFG-E8 binds to phosphatidylserine on the surface of membrane vesicles or apoptotic cells (Oshima et al., 2002, Hanayama et al., 2002), and has also been shown to accumulate on exosomes (Veron et al., 2005). It also plays a role in photoreceptor-RPE interactions (Nandrot et al., 2007).

RNAseq of C6 Exosomes

Besides protein cargo, EVs carry a variety of RNAs, the best characterized being miRNA (Skog et al., 2008, Cha et al., 2015, Valadi et al., 2007, Patton et al., 2015). We purified small RNAs from gradient purified C6 sEVs and performed RNAseq to identify differentially enriched miRNAs between C6 cells and EVs. Analysis of the data identified numerous miRNAs enriched in C6 exosomes (**A.5A**). Previously, miRNAs were identified in EVs from neural progenitor cells that were proposed to inhibit inflammatory signaling and prevent microglia activation (Bian et al., 2020). Interestingly, we detected little overlap in the two data sets which could be consistent with P2 sEVs activating a regenerative response as opposed to blocking an inflammatory response. The Reh lab identified two miRNAs (*miR-25 and miR-124*) whose overexpression can induce Ascl1 expression during conversion of mouse MG into neuronal/progenitor cell phenotypes (Wohl et al., 2019). *miR-25* was not enriched in C6 EVs compared to parental C6 cells whereas *miR-124* showed enrichment in EVs but was expressed at low to undetectable levels in C6 cells.

We used the MicroRNA Target Prediction Database to identify mRNA targets for the most enriched miRNAs in P2 sEVs (**A.5B**). Gene Ontology analyses of these predicted targets did not result in significant enrichment of any specific category or biological process. Full analysis of the differentially enriched EV miRNAs and identification and validation of their mRNA targets will require complementary mRNAseq experiments in cells exposed to C6 EVs.

Discussion

We conducted an *in vivo* screen to identify EV sources capable of eliciting MG-derived proliferation after intravitreal injection into zebrafish eyes. For potential future translational applications, we focused largely on EVs prepared from a variety of stem cells and induced pluripotent stem cells (iPSCs) subject to distinct differentiation cascades promoting mostly neuronal lineages. Interesting differences were observed between the sEV preparations in terms of the localization of proliferating cells in the zebrafish retina. iPSCs differentiating into mature dopaminergic neurons tended to induce $PCNA^+$ cells that were found mostly in the ONL. In contrast, sEVs from C6 glioma cells induced $PCNA^+$ cells in the INL which mostly co-localize with MG markers. It will be interesting to determine the exact origin and lineage of the different populations of $PCNA^+$ cells induced by specific EV preparations with a view to determine whether different sources of sEVs induce distinctly different responses. Proteomic analysis of breast cancer derived EVs revealed that the cell of origin can often be inferred based on EV cargo content (Wen et al., 2019). This raises the possibility that the glial origin of C6 cells might result in membrane and cargo content that preferentially drives uptake by

MG and whose identify could help in future EV targeting experiments, perhaps including MFG-E8.

While we focused mostly on EVs that induced increased numbers of PCNA+ cells derived from MG in the INL, some of the PCNA$^+$ cells are likely to be rod precursors (Otteson et al., 2002, Raymond et al., 2006), microglia (Mitchell et al., 2018, Mitchell et al., 2019, Conedera et al., 2019), or other cells that might be preferentially sensitive to damage induced by the injected EVs. Induction of PCNA expression could be part of a regenerative response, but could also be due to damage by delivery of specific EV cargo or lipid content. TUNEL staining (**A.S2**) argues against extensive non-specific damage due to C6 EV injections, but it remains possible that some EVs might induce damage and that some PCNA$^+$ cells could be a response to such damage.

In vivo screening for sEVs that induce retina regeneration

The rationale of the *in vivo* screen used here was driven by increasing interest in the roles of EVs in cell-cell communication, findings that transplanted stem cells in the retina engage in material transfer, and that immortalized MG can take up EVs (Pearson et al., 2016, Singh et al., 2016, Santos-Ferreira et al., 2016). A challenge for the screen was to efficiently isolate EVs from numerous sources grown in the absence of serum to avoid contamination of mostly bovine EVs. The majority of sEV preparations did not induce significant numbers of PCNA$^+$ cells, some even led to slightly decreased levels of PCNA compared to PBS. This could indicate that some EVs can suppress

proliferation, but the changes are such that the effects should be carefully interpreted since we observed variation from fish to fish and from preparation to preparation.

Compared to the levels of proliferation typically observed using a variety of retina damage models in zebrafish (Lenkowski and Raymond, 2014), injection of sEVs led to far fewer PCNA^{+} cells. The notion that a single injection of sEVs into an undamaged retina could replicate effects observed after more extensive damage was not unexpected. Even in fish, retina regeneration is a multi-step process; it may be that EVs, and possibly combinations of EVs from multiple sources, will need to be delivered over time to induce a complete regenerative response, especially for application to mammalian retina regeneration. While the initial screen focused on identification of PCNA+ cells, the use of additional transgenic lines and the appearance of clusters of PCNA^{+} cells along MG processes after C6 EV injection is consistent with a bona fide regenerative response, as is the reduction in PCNA levels after Ascl1 knockdown.

sEVs carry cargo capable of inducing MG-derived proliferation

Intravitreal injection of C6-derived sEVs could induce retina regeneration in multiple ways. One mechanism could be that the sEVs bind to MG and induce a signal transduction cascade that initiates proliferation without actually being internalized. A second mechanism could be that sEVs are endocytosed and activate endosomal receptors such as Toll-like receptors (Fabbri et al., 2013). We identified 138 proteins enriched in C6 sEVs and performed knockdown of the most abundant of these, MFG-E8. While MFG-E8 plays a role in photoreceptor-RPE interactions (Nandrot et al.,

2007), that role would seem to be unrelated to activation of MG, unless reduced levels of MFG-E8 lead to photoreceptor death. Future work will be devoted to examination of additional candidates, but it is surprising that we did not identify any of the best characterized proteins involved in retina regeneration.

Despite the caveats, our data raise the possibility that EVs could be used as a therapeutic agent to induce retina regeneration. Chen and colleagues demonstrated that delivery of multiple factors using AAV vectors in mice can generate rod photoreceptors in a MG-derived pathway (Yao et al., 2016, Yao et al., 2018). AAV2 vectors that are associated with exosomes are also capable of gene delivery in the murine retina (Wassmer et al., 2017). Beyond viral vectors, Reh and colleagues showed that genetic delivery of Ascl1 and a general histone deacetylase inhibitor could stimulate MG-derived regeneration in mice (Jorstad et al., 2017). Thus, retinal delivery of genes or other cargo shows great promise to promote endogenous retina regeneration. EVs provide an alternative method of delivery that bypasses concerns about viral vectors and could potentially overcome obstacles related to genetic delivery. As an initial attempt to determine whether our approach in zebrafish might extend to mice, we intravitreally injected a subset of the EVs from our large screen into mice and our findings from those experiments will be reported separately. Moving forward, it will be interesting to determine whether the efficiency of EV-mediated regeneration can be enhanced using EVs loaded with factors capable of inducing retina and expressing surface proteins that target uptake by MG. Indeed, one possibility is that MFG-E8 somehow plays a role in targeting MG for uptake. Should MFG-E8 or other proteins be

identified that can target EVs to MG, it could be especially attractive as a delivery vehicle because it has been found that proteins associated with, or on the surface of EVs, are more active when delivered to recipient cells than when delivered as recombinant or purified proteins (Higginbotham et al., 2011).

Acknowledgments

We would like to thank the labs of Drs. Vivian Gama, Ethan Lippmann, Aaron Bowman, Diana Neely, Alissa Weaver, Ron Emeson, and John Penn from Vanderbilt and Dr. David Gamm from the University of Wisconsin, Madison for cell lines or culture media for EV isolation. The (*Tg(1016tuba1a:GFP)*) transgenic zebrafish line was provided by Dr. Daniel Goldman from the University of Michigan, and the Tg*(GFAP:GFP)*^{mi2001} line was provided by Dr. Pam Raymond from the University of Michigan. We would like to thank Dr. Bryan Mills in the Vanderbilt Cell Imaging Shared Resource for assistance with image analysis, and Qiang Guan for zebrafish maintenance and husbandry.

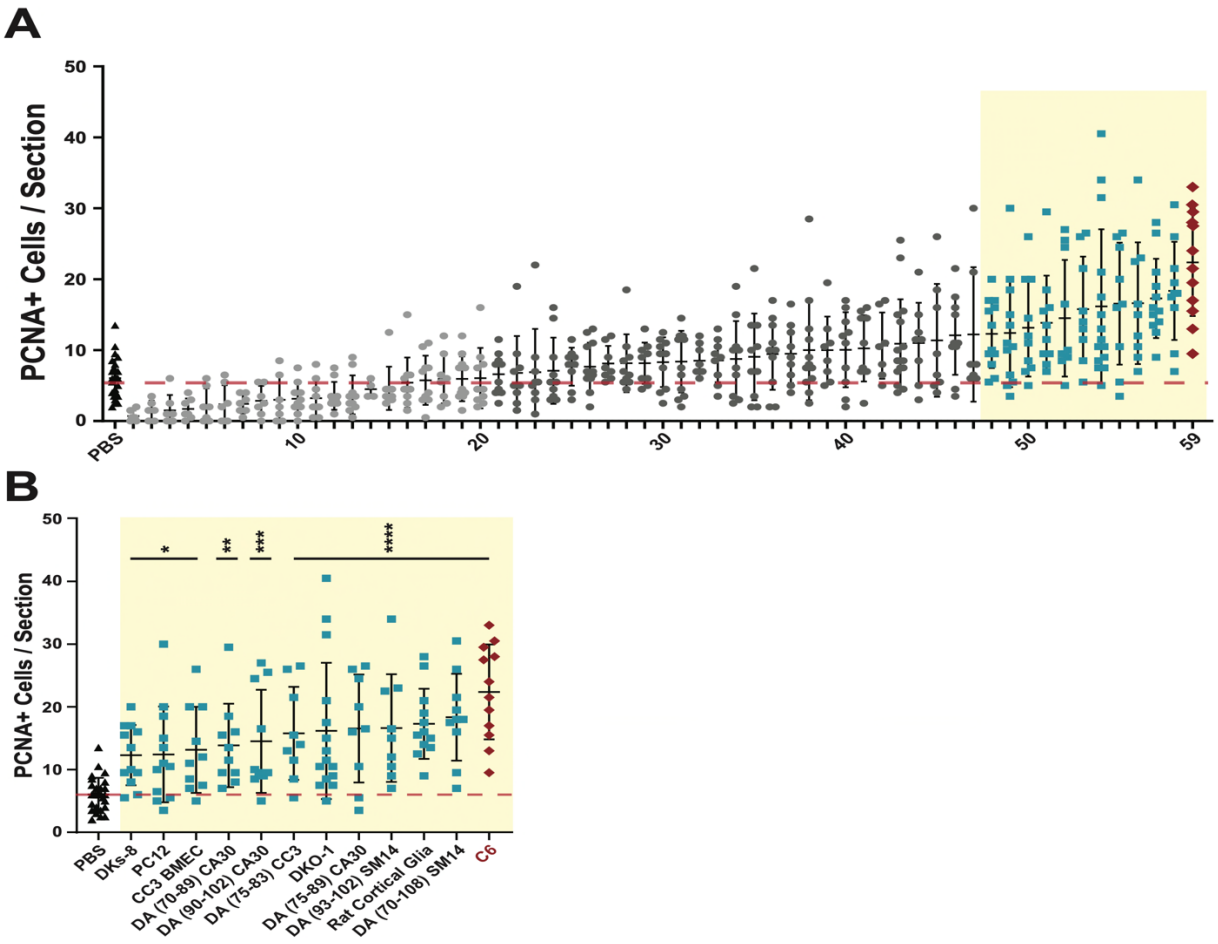

A.1. *In vivo* screen to identify EV sources capable of inducing increased numbers of PCNA$^+$ cells. EVs were isolated from conditioned media or dissociated tissues and intravitreally injected into undamaged wild type AB zebrafish eyes. After 72 hours, retinas were dissected, sectioned, and immunostained with antibodies against Proliferating Cell Nuclear Antigen (PCNA). **A)** 59 independent EV preparations were tested and PCNA$^+$ cells were counted across the inner nuclear layer (INL) and outer nuclear layer (ONL) and compared to control PBS injections. Each data point represents PCNA$^+$ cells from a single retina and consists of average counts from 2-4 nonconsecutive sections from the same eye. Light gray EV samples (1-20) led to PCNA counts less than or equal to PBS control background levels (red dotted line). Dark gray EV samples (21-47) induced non-significant PCNA counts slightly greater than background. Light blue EV samples (48-58) induced significant (p-values <0.05) PCNA counts greater than control PBS injections. C6 EVs (red diamonds) induced the most significant PCNA$^+$ counts compared to PBS controls. One-way ANOVA with Dunnett multiple comparison tests (to PBS injection) were used to determine significance. The identify of each EV preparation can be found in Table A.S1. **B)** Enlargement of EV preparations from (**A**) that produced significant increases in PCNA counts compared to PBS controls with the indicated source of EVs shown along the X axis. *p-value <0.05, **p-value = 0.0034, ***p-value = 0.0008, ****p-value <0.0001.

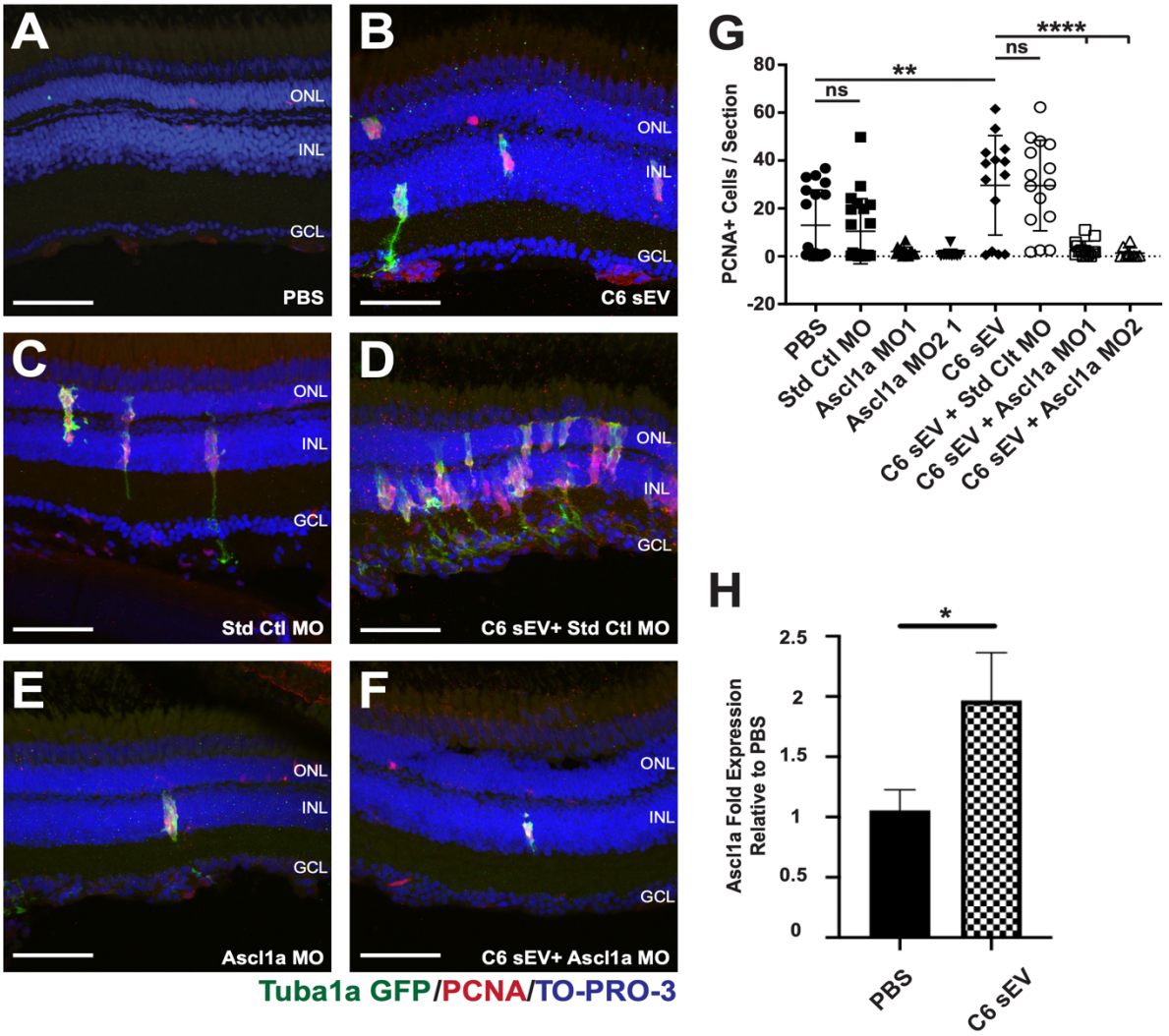

A.2. Knockdown of Ascl1a blocks C6 EV induced proliferation. A-B) PBS or C6 sEVs were injected into Tg*(1016tuba1a:gfp)* transgenic zebrafish eyes. Retinas were collected 72 hours after injection and immunostained with antibodies against PCNA to label proliferating cells and GFP to label dedifferentiated MG, respectively. Nuclei were stained with TO-PRO-3. **C-F**) Representative images of retinas from Tg*(1016tuba1a:gfp)* transgenic fish immunostained as in A and B. **C)** Control morpholinos were injected and electroporated into Tg*(1016tuba1a:gfp)* transgenic zebrafish retinas. **D**) Control morpholinos were injected and electroporated into Tg*(1016tuba1a:gfp)* transgenic zebrafish retinas in the presence of C6 sEVs. **E**) Morpholinos against *ascl1a* were injected and electroporated into Tg*(1016tuba1a:gfp)* transgenic zebrafish retinas. **F**) Morpholinos against *ascl1a* were injected and electroporated into Tg*(1016tuba1a:gfp)* transgenic zebrafish retinas in the presence of C6 sEVs. **G)** Quantification of PCNA^{+} cells across INL and ONL. Significance was calculated using one-way ANOVA with Holm-Sidak multiple comparison test, where **p-value=0.0083 ****p-value<0.0001. **H**) Zebrafish eyes were injected with PBS or C6 EVs. Retinas were isolated after 72 hours and pooled into groups of 3 for RNA purification. Data represent the mean +/- SEM with an N=5. Ascl1a expression was significantly higher among C6 EV injected conditions compared to PBS, where *p=0.036 using a two-tailed t-test. Scale bar, 50 μm.

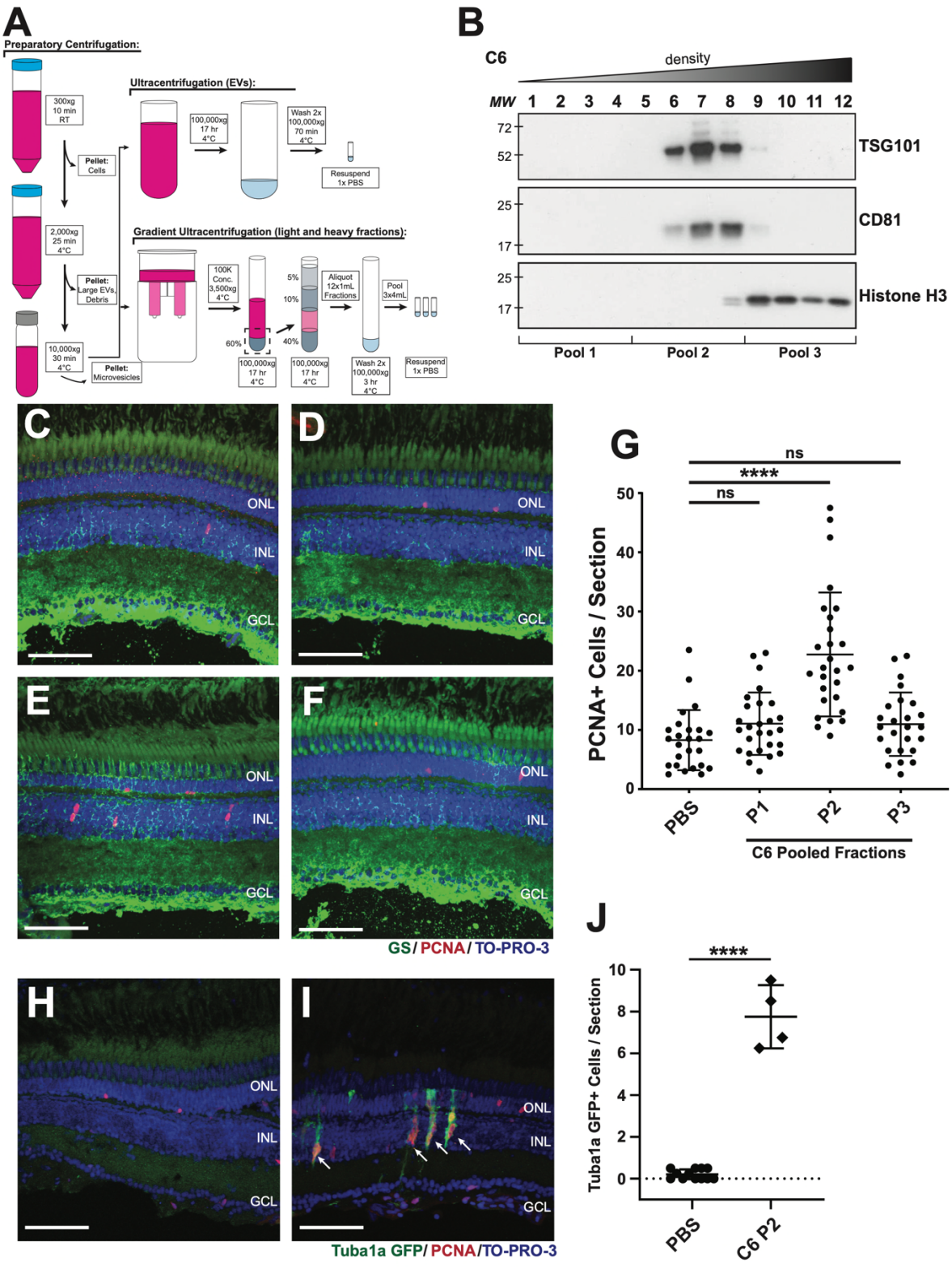

A.3. Gradient Purified C6 sEVs induce proliferation. A) Differential ultracentrifugation steps during sEV purification. **B)** Representative western blots of C6 density gradient fractions using

antibodies against CD81, TSG101, or histone H3. **C-F)** After iodixanol gradient ultracentrifugation, fractions were combined into three pools (four fractions per pool; P1, P2, P3). Intravitreal injections into wild type AB fish were performed with either PBS, P1, P2, or P3. Retinas were collected 72 hours after injection and representative images are shown after immunostaining with antibodies against PCNA and glutamine synthase (GS). **G)** Quantification of $PCNA^+$ cells after injection as in C-F, averaged across 2-4 non-consecutive retinal sections per eye, across INL and ONL. Significance was calculated using one-way ANOVA with Tukey multiple comparison test, where ****p-value<0.0001. **H, I**) Representative images of retinas from Tg*(1016tuba1a:gfp)* fish injected with either PBS (H) or C6 P2 sEVs (I). Sections were stained with antibodies against GFP and PCNA. **J**) Quantitation of GFP+ cells from experiments in H, I. Significance was calculated using ANOVA, where ****p-value<0.0001. Scale bar, 50 μm.

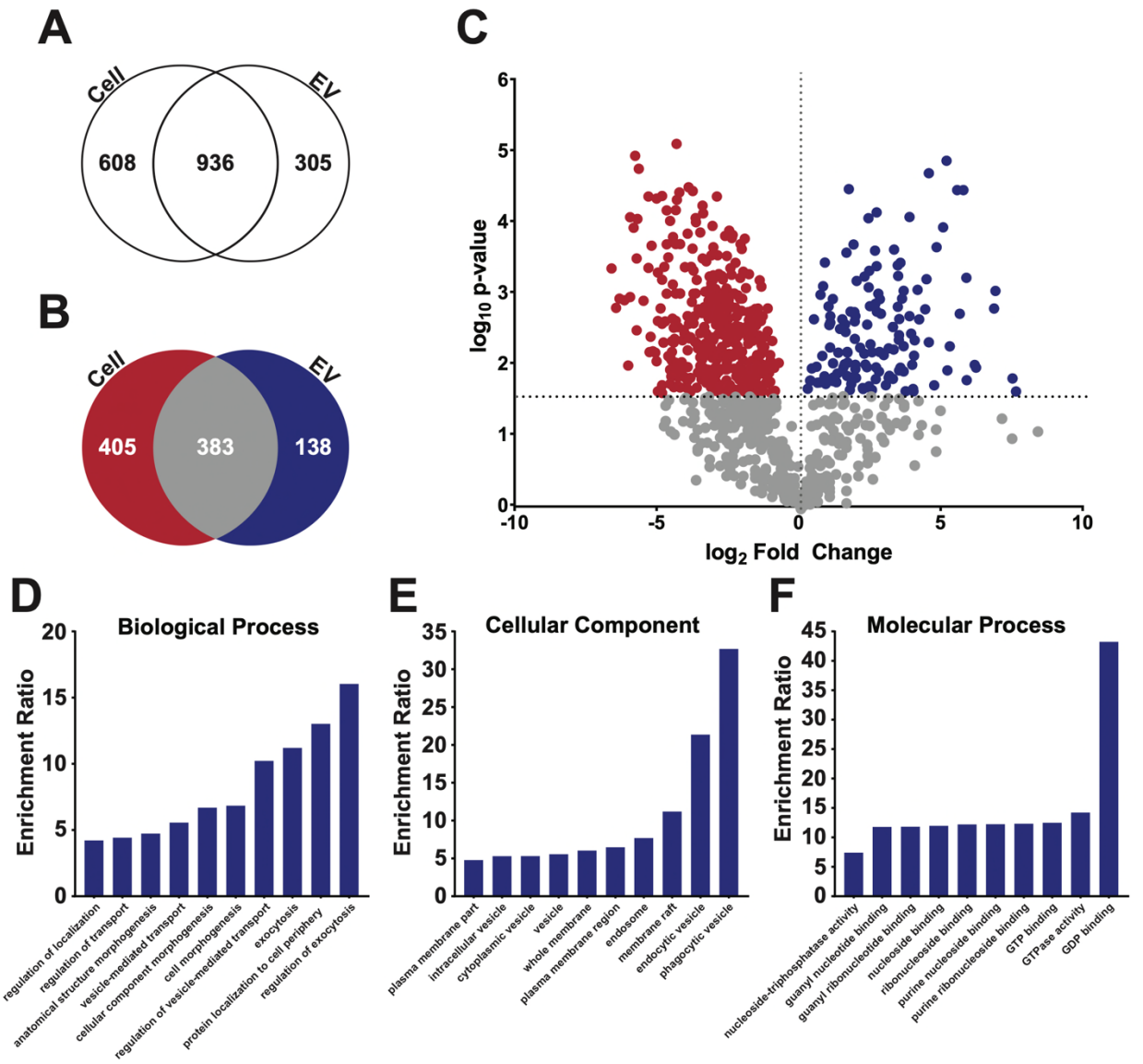

A.4. Proteomics analysis for C6 cells and EVs. **A)** Gradient purified sEVs from C6 fractions were subjected to mass spectroscopy and protein levels compared between sEVs and parent C6 cellular levels. Venn diagram showing total detectable spectral counts found in cells, EVs, or both. **B)** Venn diagram showing enrichment of proteins in cells, EVs or both after excluding proteins with little to no detectable cellular levels. **C)** Volcano plot of proteomic analysis plotting p-value versus the fold change between cells (red) and EVs (blue) after excluding proteins with little to no detectable cellular levels. Red and blue dots indicate individual proteins enriched in either cells (red) or sEVs (blue) above a p-value threshold of $p<0.02696$ using the Benjamini-Hochberg test. **D-F**) Gene Ontology analyses of proteins in P2 sEVs showed enrichment in categories as shown.

A

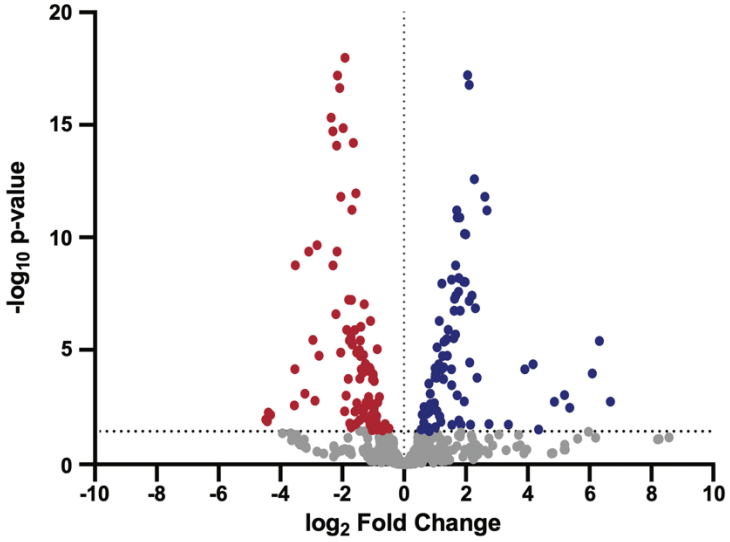

B

Enriched miRNAs	Predicted Targets
rno-miR-505-5p	Ptdss, Gdi2, Fgfr1op, Pip4k2b, Ispd
rno-miR-139-5p	Kat6a, Kmt5b, Xpo4, Gdf10, Slc23a2
rno-miR-664-2-5p	St6galnac6, Rere, Srd5a2, Arhgap35, Arhgef15
rno-miR-34b-3p	Itpr2, Med7, Wdr48, Nckap1, LOC688765
rno-miR-23a-5p	Ppef1, Dazl, Ablim3, Spryd7, Mtmr4
rno-miR-93-3p	Wdr26, Glcci1, Lyplal1, LOC298139, Car7
rno-miR-150-5p	Calcr, Gtpbp3, Sp1, Mgme1, Cbll1
rno-miR-125b-1-3p	LOC684871, Spock3, Ptpro
rno-miR-125a-3p	Mx1, Trpm3, Jakmip2, Mex3c, Akap2
rno-let-7d-3p	Pof1b, Parp2, Mex3c, Kcnd3, Rsu1

A.5. RNAseq analysis for C6 cells and sEVs. Small RNAs were isolated and purified from C6 cells and from gradient sEVs and subjected to RNA sequencing to identify differentially enriched miRNAs. **A**) The volcano plot shows p-values versus fold change levels between cells (red) and sEVs (blue). Dots represent individual miRNAs. **B**) Predicted mRNA targets for the most enriched miRNAs were determined using the MicroRNA Target Prediction Database.

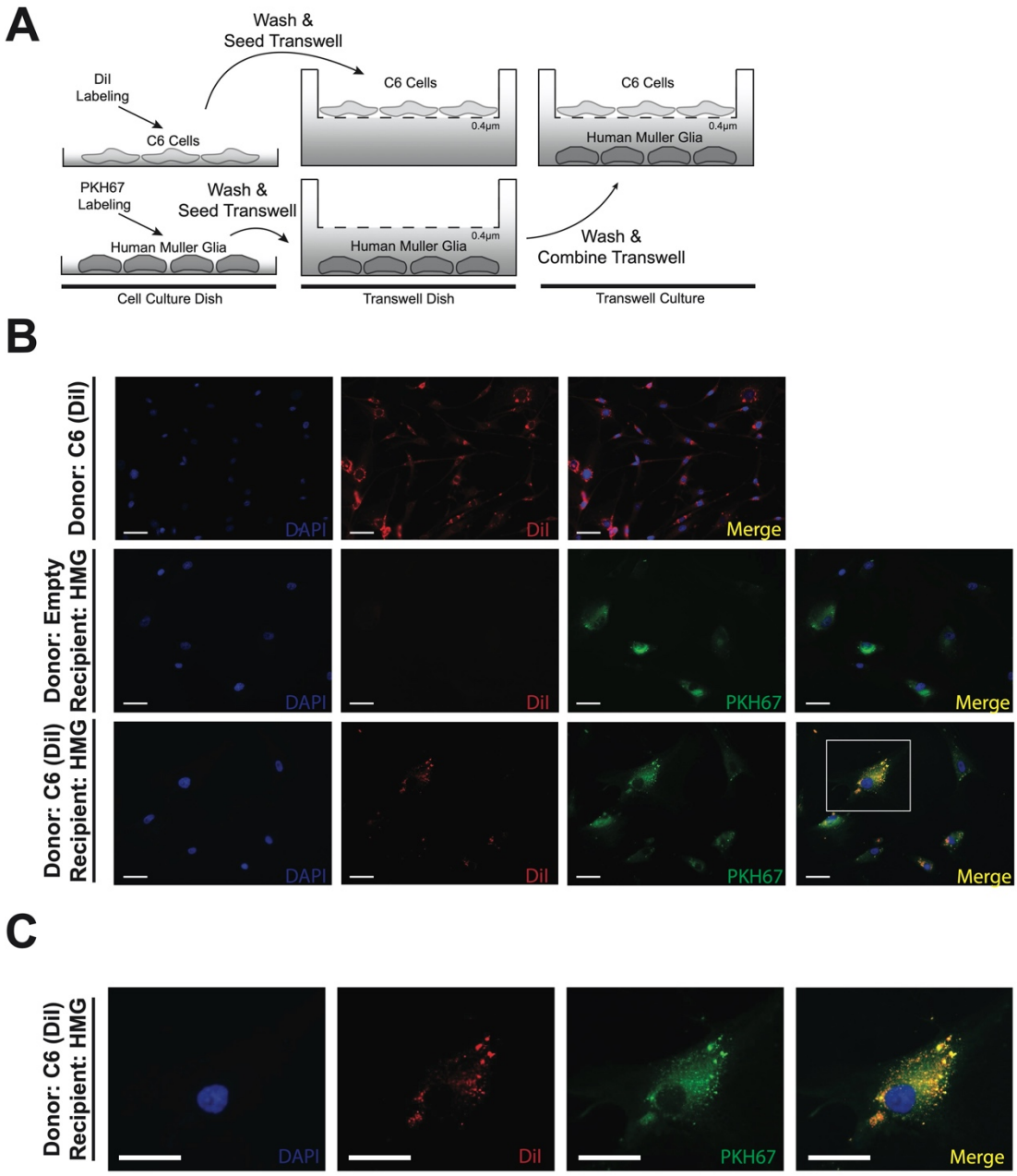

A.S1. Transfer of EVs between donor and recipient cells. A) Schematic of Transwell assay. C6 cells were DiI-labeled, washed, and seeded as donor cells on top of a 0.4uM polyester Transwell membrane. Primary human Müller glia (HMGs; (Capozzi et al., 2014, Madamanchi et al., 2014)) were PKH67-labeled, washed, and seeded as recipient cells in the bottom of the Transwell culture dish. After 24 hours, cells were washed and co-cultured in serum-free media for 48 hours. **B)** Representative confocal images of donor and recipient cells. When C6 donor cells were co-cultured with HMG recipient cells, co-localization (yellow) was visualized, indicating uptake of C6-derived EVs by HMCs. **C)** Enlarged images of cells depicted in B. Scale bar, 50 μm.

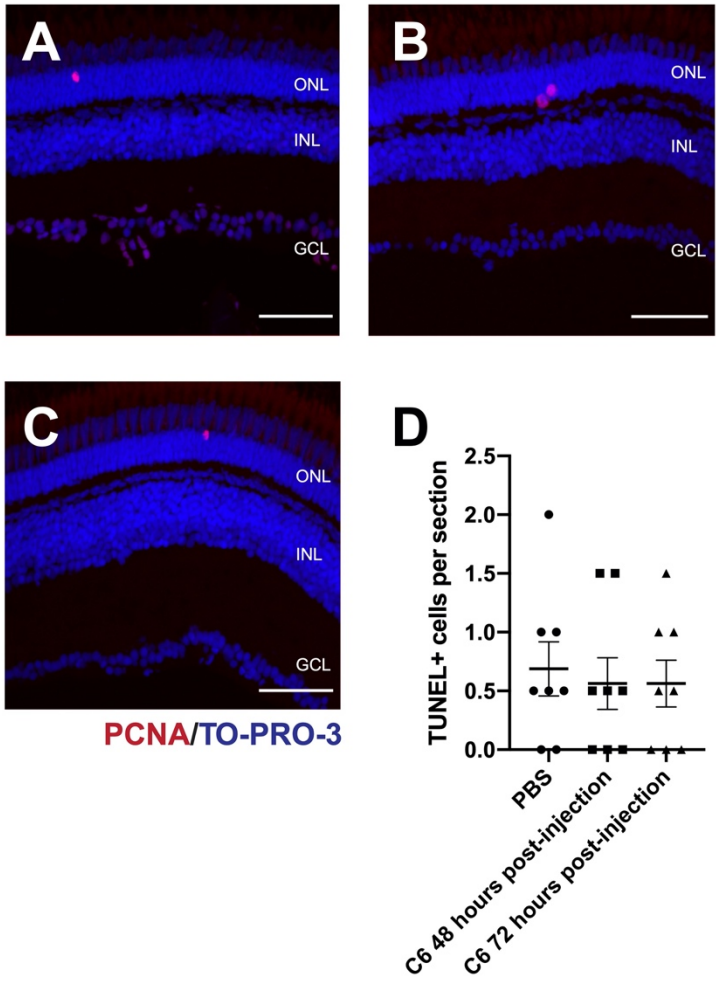

A.S2. TUNEL Staining to Detect Apoptosis after EV injection. *AB* wild type zebrafish were injected with either PBS or C6 sEVs. After recovery for either 48 hours or 72 hours, TUNEL staining was performed. Red-PNCA; Blue–TOPRO-3. Scale bar, 50 μm. ONL–outer nuclear layer; INL–inner nuclear layer; GCL–ganglion cell layer. (**A**) PBS injection (**B**) C6 sEV injections analyzed 48 hours post-injection. (**C**) C6 sEVs injection analyzed at 72 hours post-injection. (**D**) Scatterplot of TUNEL staining analysis. Each data point is from a separate eye and is an average of 2-4 non-consecutive sections, counting all TUNEL^{+} cells across all retinal layers. One-way ANOVA with Tukey multiple comparison tests were used for quantitation. Error bars are mean ±SEM; n=8.

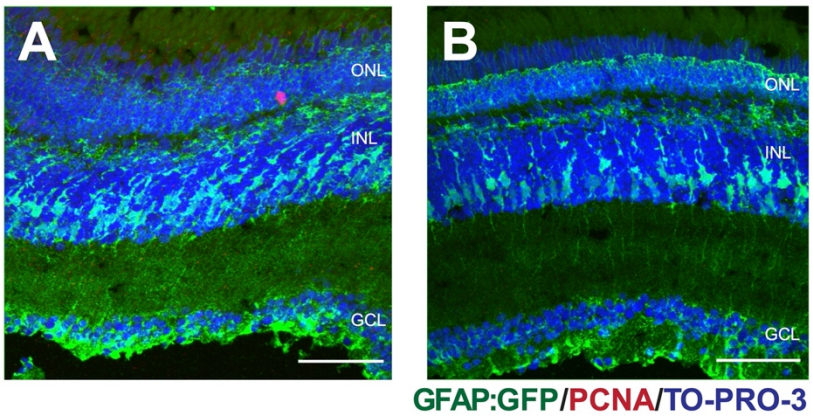

A.S3. Uninjected Retina. Z-stack of an uninjected retina from a *Tg(GFAP:GFP)*^{mi2001} transgenic zebrafish. Representative sections are shown with **(A)** showing a single PCNA^{+} cell in the ONL, most likely a rod precursor cell. Most sections had no detectable PCNA+ cells across all retinal layers **(B)**. Green–GFAP:GFP; red–PCNA; blue–TOPRO-3. Scale bar, 50 μm. ONL–outer nuclear layer, INL–inner nuclear layer, GCL–ganglion cell layer.

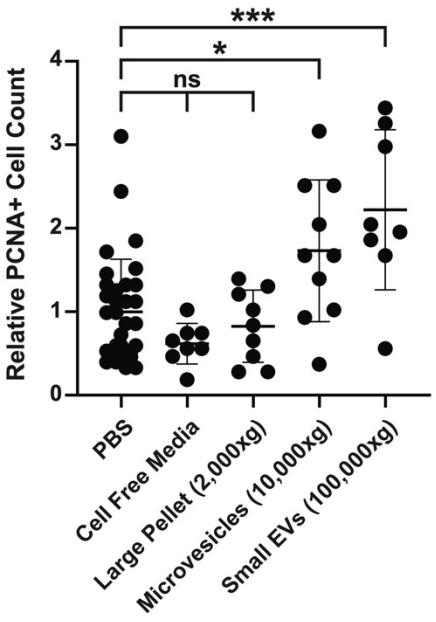

A.S4. Induction of proliferation by C6 EVs. The various stages of EV purification from C6 cell media were tested for their ability to induce proliferation as determined by $PCNA^{+}$ cell counts. The indicated fractions (see Fig. 4) or control PBS were injected into wild type zebrafish eyes. After 72 hours, retinas were dissected, sectioned, and immunostained with antibodies against PCNA. Each data point represents the average $PCNA^{+}$ counts from 2-4 nonconsecutive retinal sections per eye, across the INL and ONL. Significance was calculated by one-way ANOVA, where *p-value=0.0257 and ***p-value=0.0001.

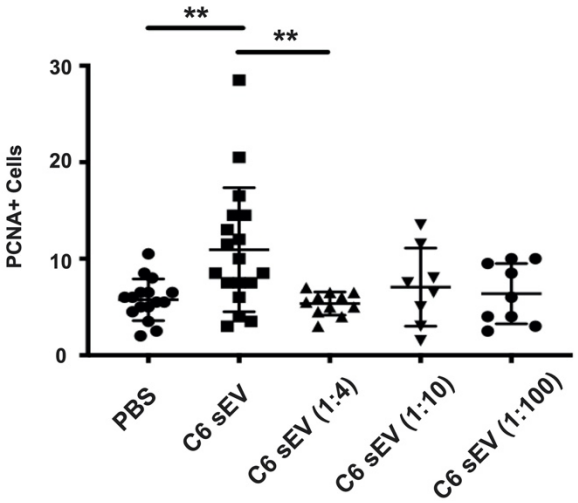

A.S5. Dilution of EVs. C6 EVs were diluted to test whether the induction of PCNA+ cells was dose dependent.

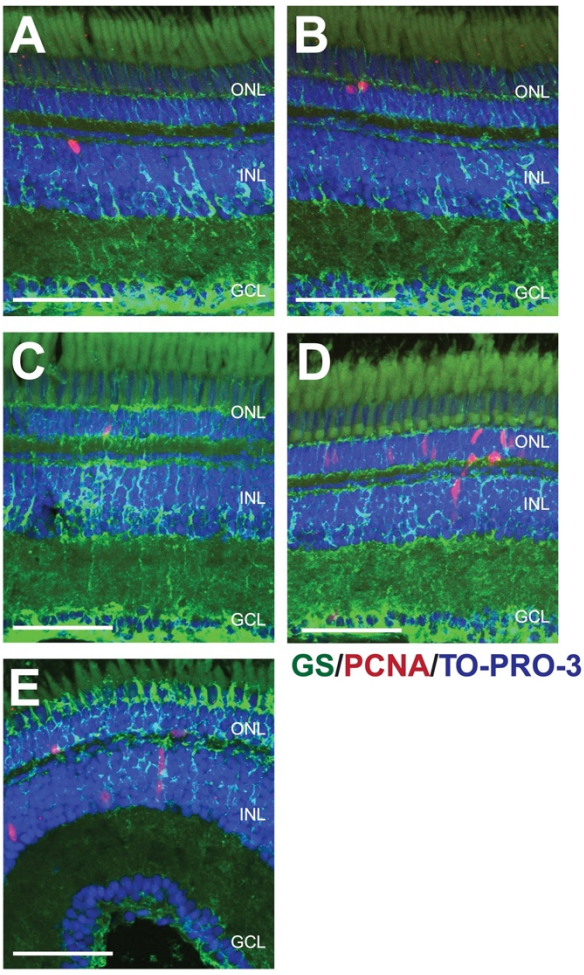

A.S6. Glutamine Synthase Co-Localization. Representative images of PBS control injected eyes (**A**), injection of EVs from IPS-derived cortical glutamatergic neurons at day 2-3 of differentiation (#16 from Fig. 2 and Table S1) (**B**), injection of EVs from iPS-derived cortical glutamatergic neurons at day 4-6 of differentiation (#30 from Fig. 2 and Table S1), **(C),** injection of EVs from CA30 mesencephalic dopaminergic neurons (#53 from Fig. 2 and Table S1) (**D**) and injection of EVs from C6 glioma cells (#59 from Fig. 2 and Table S1) (**E**) in AB wildtype zebrafish. Immunostaining was performed with antibodies against PCNA to label proliferating cells, co-stained with glutamine synthase (GS) which labels MG. Nuclei were stained with ToPRO-3. Scale bar, 50 μm.

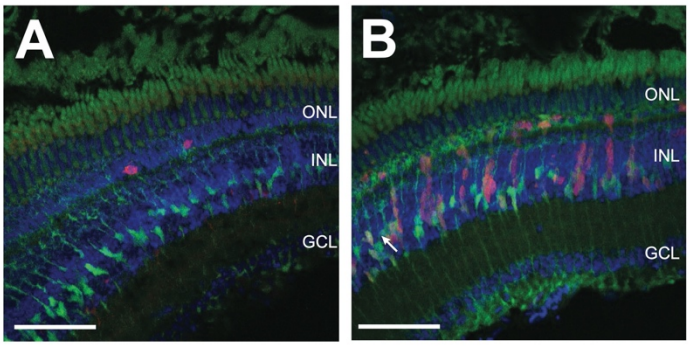

A.S7. Proliferating cells are derived from MG. Tg*(GFAP:GFP)*^{mi2001} transgenic zebrafish retinas were injected with either PBS **(A)** or C6 P2 sEVs **(B)**. After 72 hours, retinas were dissected, sectioned, and immunostained with antibodies against PCNA and GFP. Scale bar, 50 μm.

Table A.S1. Sources of EVs for *in vivo* screen.

Cell Line	Reference	Sample #	Significance
PBS		Ctl	n/a
CTX TSC Day 8-10	Neely et al. Tox. Sci. 159: 366	1	ns
hES H1	Rasmussen et al. Stem Cell Rep 10: 684	2	ns
FP Control Day1-2	Kumar et al. Sci Rep 4: 6801	3	ns
FP Park2 Day1-2	Kumar et al. Sci Rep 4: 6801	4	ns
FP Park2 Day 8-9	Kumar et al. Sci Rep 4: 6801	5	ns
KP3	Ikeda at al. Jpn J Cancer Res 81: 987	6	ns
CC3 CTX	Neely et al. Tox. Sci. 159: 366	7	ns
CTX Control Day 8-10	Neely et al. Tox. Sci. 159: 366	8	ns
FP Control Day 8-9	Kumar et al. Sci Rep 4: 6801	9	ns
CC3 CTX	Neely et al. Tox. Sci. 159: 366	10	ns
CC5 CTX	Neely et al. Tox. Sci. 159: 366	11	ns
CTXT2-9	Neely et al. Tox. Sci. 159: 366	12	ns
CTXT2-3	Neely et al. Tox. Sci. 159: 366	13	ns
sthdhq7	Kumar et al. Sci Rep 4: 6801	14	ns
sthdhIIII	Kumar et al. Sci Rep 4: 6801	15	ns
SHSY-5Y	ATCC CRL-2266	16	ns
TSC CTX	Kumar et al. Sci Rep 4: 6801	17	ns
hES H9	Rasmussen et al. Stem Cell Rep 10: 684	18	ns
CTXCC3 (92-103)	Neely et al. Tox. Sci. 159: 366	19	ns
ZF LD	Kara et al. Cell Reports 28: 2037	20	ns
HKe3	Shirasawa et al. 1993	21	ns
C2C12	CRL-1772	22	ns
BMDMsc	ATCC PCS-500-012	23	ns
CTX CA11	Neely et al. Tox. Sci. 159: 366	24	ns
CTX CD12	Neely et al. Tox. Sci. 159: 366	25	ns
DIV9-CN	Patel and Weaver, submitted	26	ns
Gama lab Day 4-6	Rasmussen et al. Stem Cell Rep 10: 684	27	ns
NSCP3	Kumar et al. Sci Rep 4: 6801	28	ns
Neuro2a	ATCC CCL-131	29	ns
RPE	Singh et al. Invest Ophth 54: 6767	30	ns
Flp-In-293	ATCC CRL 1573	31	ns
Gama lab Day 1-3	Rasmussen et al. Stem Cell Rep 10: 684	32	ns
CC3BMEC day1/2	Lippman et al. Fluids and Barriers 2013 10: 2	33	ns
ZF WT	Kara et al. Cell Reports 28: 2037	34	ns
FP Control Day 2-3	Kumar et al. Sci Rep 4: 6801	35	ns
FP Park2 Day 2-3	Kumar et al. Sci Rep 4: 6801	36	ns

CC3BMEC day3	Lippman et al. Fluids and Barriers 2013 10: 2	37	ns
HCT116	Lu et al. Nat Med 23: 1331	38	ns
Gama lab Day 7-9	Rasmussen et al. Stem Cell Rep 10: 684	39	ns
CC5 ipsc	Neely et al. Tox. Sci. 159: 366	40	ns
HuMSC	ATCC PCS-500-012	41	ns
CC3BMEC day6	Lippman et al. Fluids and Barriers 2013 10: 2	42	ns
Primary Human MG	Capozzi et al. 2014	43	ns
D1TNC1	Kumar et al. Sci Rep 4: 6801	44	ns
FP Park2 Day 7-8	Kumar et al. Sci Rep 4: 6801	45	ns
FP Control Day 7-8	Kumar et al. Sci Rep 4: 6801	46	ns
CC3BMEC day6	Lippman et al. Fluids and Barriers 2013 10: 2	47	ns
DKS8	Cha et al. eLife 2015 4e07197	48	*
PC12	ATCC CRL-1721	49	*
CC3BMEC day4	Lippman et al. Fluids and Barriers 2013 10: 2	50	*
DA (70-89) CA30	Neely et al. Tox. Sci. 159: 366	51	**
DA (90-102) CA30	Neely et al. Tox. Sci. 159: 366	52	***
DA (75-83) cc3	Neely et al. Tox. Sci. 159: 366	53	****
DKO1	Cha et al. eLife 2015 4e07197	54	****
DA (75-89) CA30	Neely et al. Tox. Sci. 159: 366	55	****
DA (93-102) SM14	Neely et al. Tox. Sci. 159: 366	56	****
Glia	Patel and Weaver, submitted	57	****
DA (70-108)SM14	Neely et al. Tox. Sci. 159: 366	58	****
C6	Grobben et al. 2002	59	****

Table A.S1. The identity of the cell sources for the EVs tested in Fig. 2 are shown as well as Nanosight Tracking (NTA) data for each preparation. All preparations had vesicles from 40-100nm in diameter. $PCNA^+$ cell counts for each preparation and statistics are as shown. One-way ANOVA with multiple comparisons (to PBS injection) was used to determine significance. *p-value <0.05, **p-value = 0.0034, ***p-value = 0.0008, ****p-value <0.0001.

Table A.S2. Most Enriched sEV Proteins

Gene Name	Protein	Fold Change (x)	log10 p-value (y)	Accession	Avg cell spectral counts	Avg EV spectral counts
Mfge8	Lactadherin	5.802392	4.4359875	sp|P70490|MFGM_RAT	17.33333333	967.33
Pdcd6ip	Programmed cell death 6-interacting protein	4.776104	1.682898	sp|Q9QZA2|PDC6I_RAT	8.333333333	228.33
Trim47	E3 ubiquitin protein ligase	7.6582117	1.5974426	tr|D3ZA22|D3ZA22_RAT	0.333333333	67.33
Tenm3	Teneurin transmembrane protein 3	5.2403145	1.8944564	tr|F1LV44|F1LV44_RAT	1.666666667	63
	Unknown	7.5313816	1.7808622	tr|D4AB52|D4AB52_RAT	0.333333333	61.67
Capn5	Calpain-5	6.199672	1.9716586	tr|G3V7U6|G3V7U6_RAT	0.666666667	49
Itga7	Integrin alpha 7	6.9307375	3.014809	sp|Q63258|ITA7_RAT	0.333333333	40.67
Gpc4	Glypican-4	5.9188633	1.7551898	tr|Q642B0|Q642B0_RAT	0.666666667	40.33
Htra1	Serine protease	6.8826427	2.7663803	sp|Q9QZK5|HTRA1_RAT	0.333333333	39.33
Plxnb2	Plexin B2	5.5849624	4.4366894	tr|D3ZQ57|D3ZQ57_RAT	0.666666667	32
Yes1	Tyrosine-protein kinase Yes	4.5849624	4.6742134	sp|F1LM93|YES_RAT	1.333333333	32
	Unknown	6.2479277	1.9335443	tr|F1LN24|F1LN24_RAT	0.333333333	25.33
Flot1	Flotillin-1	4.1898246	3.0292556	sp|Q9Z1E1|FLOT1_RAT	1.333333333	24.33
Alcam	CD166 antigen	4.5025005	3.1788697	sp|O35112|CD166_RAT	1	22.67
	Unknown	4.066089	2.100596	tr|F1LN51|F1LN51_RAT	1.333333333	22.33
Rap2c	Ras Associated Protein 2c	5.9068904	3.1990178	tr|D3ZK56|D3ZK56_RAT	0.333333333	20
Slc1a5	Amino acid transporter	4.2479277	2.6128428	tr|Q9Z1J7|Q9Z1J7_RAT	1	19
Ist1	IST1 homolog	5.6724253	2.692056	sp|Q568Z6|IST1_RAT	0.333333333	17
Col6a1	Collagen type VI alpha 1 chain	5.321928	2.2322626	tr|D3ZUL3|D3ZUL3_RAT	0.333333333	13.33
	unknown	5.209453	4.849454	tr|F1M0K5|F1M0K5_RAT	0.333333333	12.33
Myadm	Myeloid-assosciated differentiation marker	5.087463	3.911142	sp|Q6VBQ5|MYADM_RAT	0.333333333	11.33
Rras	Ras-related protein R-Ras	4.857981	3.6307838	sp|D3Z8L7|RRAS_RAT	0.333333333	9.67
Serpine2	Glia-derived nexin	4.5849624	2.2898607	tr|G3V7Z4|G3V7Z4_RAT	0.333333333	8
Slc7a1	High affinity cationic amino acid transporter 1	4.4594316	2.7553244	sp|P30823|CTR1_RAT	0.333333333	7.33
	unknown	4.087463	2.317613	tr|E9PTC0|E9PTC0_RAT	0.333333333	5.67

Table A.S2. Proteins that were the most enriched in sEVs from P2 pooled fractions are shown. Both the fold change and the average number of spectral counts are shown with the table ordered based on average spectral counts in sEVs.

Table A.S3A. GO Analysis Biological Process

Regulation of exocytosis			
User ID	Gene Symbol	Gene Name	Entrez Gene ID
P04897	Gnai2	G protein subunit alpha i2	81664
P35280	Rab8a	RAB8A, member RAS oncogene family	117103
P61765	Stxbp1	syntaxin binding protein 1	25558
P62836	Rap1a	RAP1A, member of RAS oncogene family	295347
P63322	Rala	RAS like proto-oncogene A	81757
Q62636	Rap1b	RAP1B, member of RAS oncogene family	171337
Q99P74	Rab27b	RAB27B, member RAS oncogene family	84590
Protein localization to cell periphery			
User ID	Gene Symbol	Gene Name	Entrez Gene ID
P35280	Rab8a	RAB8A, member RAS oncogene family	117103
P61765	Stxbp1	syntaxin binding protein 1	25558
P62836	Rap1a	RAP1A, member of RAS oncogene family	295347
P63025	Vamp3	vesicle-associated membrane protein 3	29528
Q4V8H8	Ehd2	EH-domain containing 2	361512
Q63377	Atp1b3	ATPase Na+/K+ transporting subunit beta 3	25390
Q9JJ19	Slc9a3r1	SLC9A3 regulator 1	59114
Q9Z1E1	Flot1	flotillin 1	64665
Exocytosis			
User ID	Gene Symbol	Gene Name	Entrez Gene ID
P04897	Gnai2	G protein subunit alpha i2	81664
P35280	Rab8a	RAB8A, member RAS oncogene family	117103
P61765	Stxbp1	syntaxin binding protein 1	25558
P62836	Rap1a	RAP1A, member of RAS oncogene family	295347
P63025	Vamp3	vesicle-associated membrane protein 3	29528
P63322	Rala	RAS like proto-oncogene A	81757
Q62636	Rap1b	RAP1B, member of RAS oncogene family	171337
Q99P74	Rab27b	RAB27B, member RAS oncogene family	84590
Regulation of vesicle-mediated transport			
User ID	Gene Symbol	Gene Name	Entrez Gene ID
P04897	Gnai2	G protein subunit alpha i2	81664
P35280	Rab8a	RAB8A, member RAS oncogene family	117103
P61765	Stxbp1	syntaxin binding protein 1	25558

P62836	Rap1a	RAP1A, member of RAS oncogene family	295347
P63322	Rala	RAS like proto-oncogene A	81757
P97829	Cd47	Cd47 molecule	29364
Q4V8H8	Ehd2	EH-domain containing 2	361512
Q62636	Rap1b	RAP1B, member of RAS oncogene family	171337
Q99P74	Rab27b	RAB27B, member RAS oncogene family	84590
Q9Z1E1	Flot1	flotillin 1	64665

Cell morphogenesis

User ID	Gene Symbol	Gene Name	Entrez Gene ID
D4A208	Srgap2	SLIT-ROBO Rho GTPase activating protein 2	360840
F1LYQ8	Farp1	FERM, ARH/RhoGEF and pleckstrin domain protein 1	306183
O35112	Alcam	activated leukocyte cell adhesion molecule	79559
P18614	Itga1	integrin subunit alpha 1	25118
P35280	Rab8a	RAB8A, member RAS oncogene family	117103
P61765	Stxbp1	syntaxin binding protein 1	25558
P62747	Rhob	ras homolog family member B	**64373**
P63025	Vamp3	vesicle-associated membrane protein 3	29528
Q568Z6	Ist1	IST1, ESCRT-III associated factor	307833
Q63258	Itga7	integrin subunit alpha 7	81008
Q9JJ19	Slc9a3r1	SLC9A3 regulator 1	59114
Q9Z1E1	Flot1	flotillin 1	64665

Cellular component morphogenesis

User ID	Gene Symbol	Gene Name	Entrez Gene ID
D4A208	Srgap2	SLIT-ROBO Rho GTPase activating protein 2	360840
F1LYQ8	Farp1	FERM, ARH/RhoGEF and pleckstrin domain protein 1	306183
O35112	Alcam	activated leukocyte cell adhesion molecule	79559
P18614	Itga1	integrin subunit alpha 1	25118
P35280	Rab8a	RAB8A, member RAS oncogene family	117103
P40241	Cd9	CD9 molecule	24936
P61765	Stxbp1	syntaxin binding protein 1	25558
P62747	Rhob	ras homolog family member B	64373
P63025	Vamp3	vesicle-associated membrane protein 3	29528
Q568Z6	Ist1	IST1, ESCRT-III associated factor	307833
Q63258	Itga7	integrin subunit alpha 7	81008
Q9JJ19	Slc9a3r1	SLC9A3 regulator 1	59114
Q9Z1E1	Flot1	flotillin 1	64665

Vesicle-mediated transport

User ID	Gene Symbol	Gene Name	Entrez Gene ID
G3V7W1	Pdcd6	programmed cell death 6	308061
P04897	Gnai2	G protein subunit alpha i2	81664
P0C0A1	Vps25	vacuolar protein sorting 25 homolog	681059
P35280	Rab8a	RAB8A, member RAS oncogene family	117103
P40241	Cd9	CD9 molecule	24936
P61765	Stxbp1	syntaxin binding protein 1	25558
P62747	Rhob	ras homolog family member B	64373
P62836	Rap1a	RAP1A, member of RAS oncogene family	295347
P63025	Vamp3	vesicle-associated membrane protein 3	29528
P63322	Rala	RAS like proto-oncogene A	81757
P97829	Cd47	Cd47 molecule	29364
Q4V8H8	Ehd2	EH-domain containing 2	361512
Q62636	Rap1b	RAP1B, member of RAS oncogene family	171337
Q99P74	Rab27b	RAB27B, member RAS oncogene family	84590
Q9Z1E1	Flot1	flotillin 1	64665

Anatomical structure morphogenesis

User ID	Gene Symbol	Gene Name	Entrez Gene ID
D3Z8L7	Rras	RAS related	361568
D4A208	Srgap2	SLIT-ROBO Rho GTPase activating protein 2	360840
F1LYQ8	Farp1	FERM, ARH/RhoGEF and pleckstrin domain protein 1	306183
G3V7W1	Pdcd6	programmed cell death 6	308061
O35112	Alcam	activated leukocyte cell adhesion molecule	79559
P18614	Itga1	integrin subunit alpha 1	25118
P35280	Rab8a	RAB8A, member RAS oncogene family	117103
P40241	Cd9	CD9 molecule	24936
P61765	Stxbp1	syntaxin binding protein 1	25558
P62747	Rhob	ras homolog family member B	64373
P62836	Rap1a	RAP1A, member of RAS oncogene family	295347
P63025	Vamp3	vesicle-associated membrane protein 3	29528
P63322	Rala	RAS like proto-oncogene A	81757
P70490	Mfge8	milk fat globule-EGF factor 8 protein	25277
Q4V8H8	Ehd2	EH-domain containing 2	361512
Q568Z6	Ist1	IST1, ESCRT-III associated factor	307833
Q63258	Itga7	integrin subunit alpha 7	81008
Q9EPF2	Mcam	melanoma cell adhesion molecule	78967
Q9JJ19	Slc9a3r1	SLC9A3 regulator 1	59114

Q9QZK5	Htra1	HtrA serine peptidase 1	65164
Q9Z1E1	Flot1	flotillin 1	64665

Regulation of transport

User ID	Gene Symbol	Gene Name	Entrez Gene ID
P04897	Gnai2	G protein subunit alpha i2	81664
P06685	Atp1a1	ATPase Na+/K+ transporting subunit alpha 1	24211
P35280	Rab8a	RAB8A, member RAS oncogene family	117103
P53987	Slc16a1	solute carrier family 16 member 1	25027
P61765	Stxbp1	syntaxin binding protein 1	25558
P62836	Rap1a	RAP1A, member of RAS oncogene family	295347
P63025	Vamp3	vesicle-associated membrane protein 3	29528
P63036	Dnaja1	DnaJ heat shock protein family (Hsp40) member A1	65028
P63322	Rala	RAS like proto-oncogene A	81757
P97829	Cd47	Cd47 molecule	29364
Q4V8H8	Ehd2	EH-domain containing 2	361512
Q62636	Rap1b	RAP1B, member of RAS oncogene family	171337
Q63377	Atp1b3	ATPase Na+/K+ transporting subunit beta 3	25390
Q99P74	Rab27b	RAB27B, member RAS oncogene family	84590
Q9JJ19	Slc9a3r1	SLC9A3 regulator 1	59114
Q9Z1E1	Flot1	flotillin 1	64665

Regulation of localization

User ID	Gene Symbol	Gene Name	Entrez Gene ID
D3Z8L7	Rras	RAS related	361568
D4A208	Srgap2	SLIT-ROBO Rho GTPase activating protein 2	360840
G3V7W1	Pdcd6	programmed cell death 6	308061
P04897	Gnai2	G protein subunit alpha i2	81664
P06685	Atp1a1	ATPase Na+/K+ transporting subunit alpha 1	24211
P35280	Rab8a	RAB8A, member RAS oncogene family	117103
P40241	Cd9	CD9 molecule	24936
P53987	Slc16a1	solute carrier family 16 member 1	25027
P61765	Stxbp1	syntaxin binding protein 1	25558
P62747	Rhob	ras homolog family member B	64373
P62836	Rap1a	RAP1A, member of RAS oncogene family	295347
P63025	Vamp3	vesicle-associated membrane protein 3	29528
P63036	Dnaja1	DnaJ heat shock protein family (Hsp40) member A1	65028
P63322	Rala	RAS like proto-oncogene A	81757
P97829	Cd47	Cd47 molecule	29364

Q4V8H8	Ehd2	EH-domain containing 2	361512
Q62636	Rap1b	RAP1B, member of RAS oncogene family	171337
Q63377	Atp1b3	ATPase Na+/K+ transporting subunit beta 3	25390
Q99P74	Rab27b	RAB27B, member RAS oncogene family	84590
Q9EPF2	Mcam	melanoma cell adhesion molecule	78967
Q9JJ19	Slc9a3r1	SLC9A3 regulator 1	59114
Q9Z1E1	Flot1	flotillin 1	64665

Table A.S3B. GO Analysis Cellular Component

Phagocytic vesicle			
User ID	Gene Symbol	Gene Name	Entrez Gene ID
D4A208	Srgap2	SLIT-ROBO Rho GTPase activating protein 2	360840
P35280	Rab8a	RAB8A, member RAS oncogene family	117103
P61765	Stxbp1	syntaxin binding protein 1	25558
P62836	Rap1a	RAP1A, member of RAS oncogene family	295347
P63025	Vamp3	vesicle-associated membrane protein 3	29528
Endocytic vesicle			
User ID	Gene Symbol	Gene Name	Entrez Gene ID
D4A208	Srgap2	SLIT-ROBO Rho GTPase activating protein 2	360840
P35280	Rab8a	RAB8A, member RAS oncogene family	117103
P61765	Stxbp1	syntaxin binding protein 1	25558
P62836	Rap1a	RAP1A, member of RAS oncogene family	295347
P63025	Vamp3	vesicle-associated membrane protein 3	29528
P63322	Rala	RAS like proto-oncogene A	81757
Membrane raft			
User ID	Gene Symbol	Gene Name	Entrez Gene ID
P04897	Gnai2	G protein subunit alpha i2	81664
P06685	Atp1a1	ATPase Na+/K+ transporting subunit alpha 1	24211
P11505	Atp2b1	ATPase plasma membrane Ca2+ transporting 1	29598
P18614	Itga1	integrin subunit alpha 1	25118
Q4V8H8	Ehd2	EH-domain containing 2	361512
Q63377	Atp1b3	ATPase Na+/K+ transporting subunit beta 3	25390
Q9JJ19	Slc9a3r1	SLC9A3 regulator 1	59114
Q9Z1E1	Flot1	flotillin 1	64665

Endosome

User ID	Gene Symbol	Gene Name	Entrez Gene ID
G3V7W1	Pdcd6	programmed cell death 6	308061
P06685	Atp1a1	ATPase Na+/K+ transporting subunit alpha 1	24211
P0C0A1	Vps25	vacuolar protein sorting 25 homolog	681059
P35280	Rab8a	RAB8A, member RAS oncogene family	117103
P62747	Rhob	ras homolog family member B	64373
P62836	Rap1a	RAP1A, member of RAS oncogene family	295347
P63025	Vamp3	vesicle-associated membrane protein 3	29528
Q4V8H8	Ehd2	EH-domain containing 2	361512
Q6AY20	LOC100909548	cation-dependent mannose-6-phosphate receptor-like	1.01E+08
Q99P74	Rab27b	RAB27B, member RAS oncogene family	84590
Q9Z1E1	Flot1	flotillin 1	64665

Plasma membrane region

User ID	Gene Symbol	Gene Name	Entrez Gene ID
D4A208	Srgap2	SLIT-ROBO Rho GTPase activating protein 2	360840
F1LYQ8	Farp1	FERM, ARH/RhoGEF and pleckstrin domain protein 1	306183
P06685	Atp1a1	ATPase Na+/K+ transporting subunit alpha 1	24211
P11505	Atp2b1	ATPase plasma membrane Ca2+ transporting 1	29598
P40241	Cd9	CD9 molecule	24936
P61765	Stxbp1	syntaxin binding protein 1	25558
P62747	Rhob	ras homolog family member B	64373
P63025	Vamp3	vesicle-associated membrane protein 3	29528
P63322	Rala	RAS like proto-oncogene A	81757
Q4V8H8	Ehd2	EH-domain containing 2	361512
Q63016	Slc7a5	solute carrier family 7 member 5	50719
Q63377	Atp1b3	ATPase Na+/K+ transporting subunit beta 3	25390
Q99P74	Rab27b	RAB27B, member RAS oncogene family	84590
Q9JJ19	Slc9a3r1	SLC9A3 regulator 1	59114
Q9Z1E1	Flot1	flotillin 1	64665

Whole membrane

User ID	Gene Symbol	Gene Name	Entrez Gene ID
G3V7W1	Pdcd6	programmed cell death 6	308061
P04897	Gnai2	G protein subunit alpha i2	81664

P06685	Atp1a1	ATPase Na+/K+ transporting subunit alpha 1	24211
P0C0A1	Vps25	vacuolar protein sorting 25 homolog	681059
P11505	Atp2b1	ATPase plasma membrane Ca2+ transporting 1	29598
P18614	Itga1	integrin subunit alpha 1	25118
P35280	Rab8a	RAB8A, member RAS oncogene family	117103
P62747	Rhob	ras homolog family member B	64373
P63025	Vamp3	vesicle-associated membrane protein 3	29528
Q4V8H8	Ehd2	EH-domain containing 2	361512
Q63377	Atp1b3	ATPase Na+/K+ transporting subunit beta 3	25390
Q6AY20	LOC100909548	cation-dependent mannose-6-phosphate receptor-like	1.01E+08
Q99P74	Rab27b	RAB27B, member RAS oncogene family	84590
Q9JJ19	Slc9a3r1	SLC9A3 regulator 1	59114
Q9Z1E1	Flot1	flotillin 1	64665

Vesicle

User ID	Gene Symbol	Gene Name	Entrez Gene ID
D4A208	Srgap2	SLIT-ROBO Rho GTPase activating protein 2	360840
G3V7W1	Pdcd6	programmed cell death 6	308061
P06685	Atp1a1	ATPase Na+/K+ transporting subunit alpha 1	24211
P0C0A1	Vps25	vacuolar protein sorting 25 homolog	681059
P18614	Itga1	integrin subunit alpha 1	25118
P35280	Rab8a	RAB8A, member RAS oncogene family	117103
P40241	Cd9	CD9 molecule	24936
P61765	Stxbp1	syntaxin binding protein 1	25558
P62747	Rhob	ras homolog family member B	64373
P62836	Rap1a	RAP1A, member of RAS oncogene family	295347
P63025	Vamp3	vesicle-associated membrane protein 3	29528
P63322	Rala	RAS like proto-oncogene A	81757
P97829	Cd47	Cd47 molecule	29364
Q4V8H8	Ehd2	EH-domain containing 2	361512
Q568Z6	Ist1	IST1, ESCRT-III associated factor	307833

Q63377	Atp1b3	ATPase Na+/K+ transporting subunit beta 3	25390
Q6AY20	LOC100909548	cation-dependent mannose-6-phosphate receptor-like	1.01E+08
Q99P74	Rab27b	RAB27B, member RAS oncogene family	84590
Q9Z1E1	Flot1	flotillin 1	64665

Cytoplasmic vesicle

User ID	Gene Symbol	Gene Name	Entrez Gene ID
D4A208	Srgap2	SLIT-ROBO Rho GTPase activating protein 2	360840
G3V7W1	Pdcd6	programmed cell death 6	308061
P06685	Atp1a1	ATPase Na+/K+ transporting subunit alpha 1	24211
P0C0A1	Vps25	vacuolar protein sorting 25 homolog	681059
P18614	Itga1	integrin subunit alpha 1	25118
P35280	Rab8a	RAB8A, member RAS oncogene family	117103
P61765	Stxbp1	syntaxin binding protein 1	25558
P62747	Rhob	ras homolog family member B	64373
P62836	Rap1a	RAP1A, member of RAS oncogene family	295347
P63025	Vamp3	vesicle-associated membrane protein 3	29528
P63322	Rala	RAS like proto-oncogene A	81757
Q4V8H8	Ehd2	EH-domain containing 2	361512
Q568Z6	Ist1	IST1, ESCRT-III associated factor	307833
Q63377	Atp1b3	ATPase Na+/K+ transporting subunit beta 3	25390
Q6AY20	LOC100909548	cation-dependent mannose-6-phosphate receptor-like	1.01E+08
Q99P74	Rab27b	RAB27B, member RAS oncogene family	84590
Q9Z1E1	Flot1	flotillin 1	64665

Intracellular vesicle

User ID	Gene Symbol	Gene Name	Entrez Gene ID
D4A208	Srgap2	SLIT-ROBO Rho GTPase activating protein 2	360840
G3V7W1	Pdcd6	programmed cell death 6	308061
P06685	Atp1a1	ATPase Na+/K+ transporting subunit alpha 1	24211
P0C0A1	Vps25	vacuolar protein sorting 25 homolog	681059
P18614	Itga1	integrin subunit alpha 1	25118
P35280	Rab8a	RAB8A, member RAS oncogene family	117103
P61765	Stxbp1	syntaxin binding protein 1	25558

P62747	Rhob	ras homolog family member B	64373
P62836	Rap1a	RAP1A, member of RAS oncogene family	295347
P63025	Vamp3	vesicle-associated membrane protein 3	29528
P63322	Rala	RAS like proto-oncogene A	81757
Q4V8H8	Ehd2	EH-domain containing 2	361512
Q568Z6	Ist1	IST1, ESCRT-III associated factor	307833
Q63377	Atp1b3	ATPase Na+/K+ transporting subunit beta 3	25390
Q6AY20	LOC100909548	cation-dependent mannose-6-phosphate receptor-like	1.01E+08
Q99P74	Rab27b	RAB27B, member RAS oncogene family	84590
Q9Z1E1	Flot1	flotillin 1	64665

Plasma membrane part

User ID	Gene Symbol	Gene Name	Entrez Gene ID
D4A208	Srgap2	SLIT-ROBO Rho GTPase activating protein 2	360840
F1LYQ8	Farp1	FERM, ARH/RhoGEF and pleckstrin domain protein 1	306183
O35112	Alcam	activated leukocyte cell adhesion molecule	79559
P04897	Gnai2	G protein subunit alpha i2	81664
P06685	Atp1a1	ATPase Na+/K+ transporting subunit alpha 1	24211
P11505	Atp2b1	ATPase plasma membrane Ca2+ transporting 1	29598
P18614	Itga1	integrin subunit alpha 1	25118
P40241	Cd9	CD9 molecule	24936
P53987	Slc16a1	solute carrier family 16 member 1	25027
P61765	Stxbp1	syntaxin binding protein 1	25558
P62747	Rhob	ras homolog family member B	64373
P63025	Vamp3	vesicle-associated membrane protein 3	29528
P63322	Rala	RAS like proto-oncogene A	81757
P97829	Cd47	Cd47 molecule	29364
Q4V8H8	Ehd2	EH-domain containing 2	361512
Q63016	Slc7a5	solute carrier family 7 member 5	50719
Q63258	Itga7	integrin subunit alpha 7	81008
Q63377	Atp1b3	ATPase Na+/K+ transporting subunit beta 3	25390
Q99P74	Rab27b	RAB27B, member RAS oncogene family	84590
Q9EPF2	Mcam	melanoma cell adhesion molecule	78967

Q9JJ19	Slc9a3r1	SLC9A3 regulator 1	59114
Q9QZA6	LOC100911730	CD151 antigen-like	1.01E+08
Q9Z1E1	Flot1	flotillin 1	64665

Table A.S3C. GO Analysis Molecular Process

GDP binding			
User ID	Gene Symbol	Gene Name	Entrez Gene ID
D3Z8L7	Rras	RAS related	361568
P35280	Rab8a	RAB8A, member RAS oncogene family	117103
P62747	Rhob	ras homolog family member B	64373
P63322	Rala	RAS like proto-oncogene A	81757
Q62636	Rap1b	RAP1B, member of RAS oncogene family	171337
Q99P74	Rab27b	RAB27B, member RAS oncogene family	84590
GTPase activity			
User ID	Gene Symbol	Gene Name	Entrez Gene ID
D3Z8L7	Rras	RAS related	361568
P04897	Gnai2	G protein subunit alpha i2	81664
P35280	Rab8a	RAB8A, member RAS oncogene family	117103
P62747	Rhob	ras homolog family member B	64373
P62836	Rap1a	RAP1A, member of RAS oncogene family	295347
P63322	Rala	RAS like proto-oncogene A	81757
Q04970	Nras	NRAS proto-oncogene, GTPase	24605
Q62636	Rap1b	RAP1B, member of RAS oncogene family	171337
Q99P74	Rab27b	RAB27B, member RAS oncogene family	84590
GTP binding			
User ID	Gene Symbol	Gene Name	Entrez Gene ID
D3Z8L7	Rras	RAS related	361568
P04897	Gnai2	G protein subunit alpha i2	81664

P35280	Rab8a	RAB8A, member RAS oncogene family	117103
P62747	Rhob	ras homolog family member B	64373
P62836	Rap1a	RAP1A, member of RAS oncogene family	295347
P63322	Rala	RAS like proto-oncogene A	81757
Q04970	Nras	NRAS proto-oncogene, GTPase	24605
Q4V8H8	Ehd2	EH-domain containing 2	361512
Q62636	Rap1b	RAP1B, member of RAS oncogene family	171337
Q99P74	Rab27b	RAB27B, member RAS oncogene family	84590

Purine ribonucleoside binding

User ID	Gene Symbol	Gene Name	Entrez Gene ID
D3Z8L7	Rras	RAS related	361568
P04897	Gnai2	G protein subunit alpha i2	81664
P35280	Rab8a	RAB8A, member RAS oncogene family	117103
P62747	Rhob	ras homolog family member B	64373
P62836	Rap1a	RAP1A, member of RAS oncogene family	295347
P63322	Rala	RAS like proto-oncogene A	81757
Q04970	Nras	NRAS proto-oncogene, GTPase	24605
Q4V8H8	Ehd2	EH-domain containing 2	361512
Q62636	Rap1b	RAP1B, member of RAS oncogene family	171337
Q99P74	Rab27b	RAB27B, member RAS oncogene family	84590

Purine nucleoside binding

User ID	Gene Symbol	Gene Name	Entrez Gene ID
D3Z8L7	Rras	RAS related	361568
P04897	Gnai2	G protein subunit alpha i2	81664
P35280	Rab8a	RAB8A, member RAS oncogene family	117103
P62747	Rhob	ras homolog family member B	64373
P62836	Rap1a	RAP1A, member of RAS oncogene family	295347
P63322	Rala	RAS like proto-oncogene A	81757
Q04970	Nras	NRAS proto-oncogene, GTPase	24605
Q4V8H8	Ehd2	EH-domain containing 2	361512
Q62636	Rap1b	RAP1B, member of RAS oncogene family	171337

Q99P74	Rab27b	RAB27B, member RAS oncogene family	84590
Ribonucleoside binding			
User ID	Gene Symbol	Gene Name	Entrez Gene ID
D3Z8L7	Rras	RAS related	361568
P04897	Gnai2	G protein subunit alpha i2	81664
P35280	Rab8a	RAB8A, member RAS oncogene family	117103
P62747	Rhob	ras homolog family member B	64373
P62836	Rap1a	RAP1A, member of RAS oncogene family	295347
P63322	Rala	RAS like proto-oncogene A	81757
Q04970	Nras	NRAS proto-oncogene, GTPase	24605
Q4V8H8	Ehd2	EH-domain containing 2	361512
Q62636	Rap1b	RAP1B, member of RAS oncogene family	171337
Q99P74	Rab27b	RAB27B, member RAS oncogene family	84590
Nucleoside binding			
User ID	Gene Symbol	Gene Name	Entrez Gene ID
D3Z8L7	Rras	RAS related	361568
P04897	Gnai2	G protein subunit alpha i2	81664
P35280	Rab8a	RAB8A, member RAS oncogene family	117103
P62747	Rhob	ras homolog family member B	64373
P62836	Rap1a	RAP1A, member of RAS oncogene family	295347
P63322	Rala	RAS like proto-oncogene A	81757
Q04970	Nras	NRAS proto-oncogene, GTPase	24605
Q4V8H8	Ehd2	EH-domain containing 2	361512
Q62636	Rap1b	RAP1B, member of RAS oncogene family	171337
Q99P74	Rab27b	RAB27B, member RAS oncogene family	84590
Guanyl ribonucleotide binding			
User ID	Gene Symbol	Gene Name	Entrez Gene ID
D3Z8L7	Rras	RAS related	361568
P04897	Gnai2	G protein subunit alpha i2	81664
P35280	Rab8a	RAB8A, member RAS oncogene family	117103
P62747	Rhob	ras homolog family member B	64373
P62836	Rap1a	RAP1A, member of RAS oncogene family	295347
P63322	Rala	RAS like proto-oncogene A	81757

Q04970	Nras	NRAS proto-oncogene, GTPase	24605
Q4V8H8	Ehd2	EH-domain containing 2	361512
Q62636	Rap1b	RAP1B, member of RAS oncogene family	171337
Q99P74	Rab27b	RAB27B, member RAS oncogene family	84590
Guanyl nucleotide binding			
User ID	Gene Symbol	Gene Name	Entrez Gene ID
D3Z8L7	Rras	RAS related	361568
P04897	Gnai2	G protein subunit alpha i2	81664
P35280	Rab8a	RAB8A, member RAS oncogene family	117103
P62747	Rhob	ras homolog family member B	64373
P62836	Rap1a	RAP1A, member of RAS oncogene family	295347
P63322	Rala	RAS like proto-oncogene A	81757
Q04970	Nras	NRAS proto-oncogene, GTPase	24605
Q4V8H8	Ehd2	EH-domain containing 2	361512
Q62636	Rap1b	RAP1B, member of RAS oncogene family	171337
Q99P74	Rab27b	RAB27B, member RAS oncogene family	84590
Nucleoside-triphosphatase activity			
User ID	Gene Symbol	Gene Name	Entrez Gene ID
D3Z8L7	Rras	RAS related	361568
P04897	Gnai2	G protein subunit alpha i2	81664
P06685	Atp1a1	ATPase Na+/K+ transporting subunit alpha 1	24211
P11505	Atp2b1	ATPase plasma membrane Ca2+ transporting 1	29598
P35280	Rab8a	RAB8A, member RAS oncogene family	117103
P62747	Rhob	ras homolog family member B	64373
P62836	Rap1a	RAP1A, member of RAS oncogene family	295347
P63322	Rala	RAS like proto-oncogene A	81757
Q04970	Nras	NRAS proto-oncogene, GTPase	24605
Q62636	Rap1b	RAP1B, member of RAS oncogene family	171337
Q63377	Atp1b3	ATPase Na+/K+ transporting subunit beta 3	25390
Q99P74	Rab27b	RAB27B, member RAS oncogene family	84590

Table A.S3A-C. Gene Ontology of P2 sEV Enriched Proteins. Gene ontology analysis was performed on proteomics data using WebGestalt (Liao et al., 2019). Only proteins enriched in P2 sEVs with a value greater than 2 were compared using Over-Representation Analysis (ORA) set to the genome protein-coding reference set. All groups were significant with an FDR < 0.05.

References

ADAMS, J. M. & CORY, S. 1975. Modified nucleosides and bizarre 5'-termini in mouse myeloma mRNA. *Nature,* 255**,** 28-33.

AHMAD, I., DEL DEBBIO, C. B., DAS, A. V. & PARAMESWARAN, S. 2011. Müller glia: a promising target for therapeutic regeneration. *Investigative ophthalmology & visual science,* 52**,** 5758-64.

ALARCON, C. R., GOODARZI, H., LEE, H., LIU, X., TAVAZOIE, S. & TAVAZOIE, S. F. 2015a. HNRNPA2B1 Is a Mediator of m(6)A-Dependent Nuclear RNA Processing Events. *Cell,* 162**,** 1299-308.

ALARCON, C. R., LEE, H., GOODARZI, H., HALBERG, N. & TAVAZOIE, S. F. 2015b. N6-methyladenosine marks primary microRNAs for processing. *Nature,* 519**,** 482-5.

ALLEN, R. M., ZHAO, S., RAMIREZ SOLANO, M. A., ZHU, W., MICHELL, D. L., WANG, Y., SHYR, Y., SETHUPATHY, P., LINTON, M. F., GRAF, G. A., SHENG, Q. & VICKERS, K. C. 2018. Bioinformatic analysis of endogenous and exogenous small RNAs on lipoproteins. *J Extracell Vesicles,* 7**,** 1506198.

ALSOP, K., FEREDAY, S., MELDRUM, C., DEFAZIO, A., EMMANUEL, C., GEORGE, J., DOBROVIC, A., BIRRER, M. J., WEBB, P. M., STEWART, C., FRIEDLANDER, M., FOX, S., BOWTELL, D. & MITCHELL, G. 2012. BRCA mutation frequency and patterns of treatment response in BRCA mutation-positive women with ovarian cancer: a report from the Australian Ovarian Cancer Study Group. *J Clin Oncol,* 30**,** 2654-63.

ALVAREZ-GARCIA, I. & MISKA, E. A. 2005. MicroRNA functions in animal development and human disease. *Development,* 132**,** 4653-62.

ARENA, S., BELLOSILLO, B., SIRAVEGNA, G., MARTINEZ, A., CANADAS, I., LAZZARI, L., FERRUZ, N., RUSSO, M., MISALE, S., GONZALEZ, I., IGLESIAS, M., GAVILAN, E., CORTI, G., HOBOR, S., CRISAFULLI, G., SALIDO, M., SANCHEZ, J., DALMASES, A., BELLMUNT, J., DE FABRITIIS, G., ROVIRA, A., DI NICOLANTONIO, F., ALBANELL, J., BARDELLI, A. & MONTAGUT, C. 2015. Emergence of Multiple EGFR Extracellular Mutations during Cetuximab Treatment in Colorectal Cancer. *Clin Cancer Res,* 21**,** 2157-66.

ARROYO, J. D., CHEVILLET, J. R., KROH, E. M., RUF, I. K., PRITCHARD, C. C., GIBSON, D. F., MITCHELL, P. S., BENNETT, C. F., POGOSOVA-AGADJANYAN, E. L., STIREWALT, D. L., TAIT, J. F. & TEWARI, M. 2011. Argonaute2 complexes carry a population of circulating microRNAs independent of vesicles in human plasma. *Proc Natl Acad Sci U S A,* 108**,** 5003-8.

AU YEUNG, C. L., CO, N.-N., TSURUGA, T., YEUNG, T.-L., KWAN, S.-Y., LEUNG, C. S., LI, Y., LU, E. S., KWAN, K., WONG, K.-K., SCHMANDT, R., LU, K. H. & MOK, S. C. 2016. Exosomal Transfer of Stroma-Derived MiR21 Confers Paclitaxel Resistance in Ovarian Cancer Cells through Targeting APAF1. *Nat Commun,* 7.

BARBIERI, I. & KOUZARIDES, T. 2020. Role of RNA modifications in cancer. *Nat Rev Cancer,* 20**,** 303-322.

BARDELLI, A. & SIENA, S. 2010. Molecular mechanisms of resistance to cetuximab and panitumumab in colorectal cancer. *J Clin Oncol,* 28**,** 1254-61.

BARTEL, D. P. 2018. Metazoan MicroRNAs. *Cell,* 173**,** 20-51.
BATAGOV, A. O., KUZNETSOV, V. A. & KUROCHKIN, I. V. 2011. Identification of nucleotide patterns enriched in secreted RNAs as putative cis-acting elements targeting them to exosome nano-vesicles. *BMC Genomics,* 12 Suppl 3**,** S18.
BERNARDOS, R. L., BARTHEL, L. K., MEYERS, J. R. & RAYMOND, P. A. 2007. Late-stage neuronal progenitors in the retina are radial Müller glia that function as retinal stem cells. *The Journal of neuroscience : the official journal of the Society for Neuroscience,* 27**,** 7028-40.
BERNARDOS, R. L. & RAYMOND, P. A. 2006. GFAP transgenic zebrafish. *Gene Expr Patterns,* 6**,** 1007-13.
BERULAVA, T., RAHMANN, S., RADEMACHER, K., KLEIN-HITPASS, L. & HORSTHEMKE, B. 2015. N6-adenosine methylation in MiRNAs. *PLoS One,* 10**,** e0118438.
BEVERS, E. M., COMFURIUS, P., DEKKERS, D. W. & ZWAAL, R. F. 1999. Lipid translocation across the plasma membrane of mammalian cells. *Biochim Biophys Acta,* 1439**,** 317-30.
BHAN, A., SOLEIMANI, M. & MANDAL, S. S. 2017. Long Noncoding RNA and Cancer: A New Paradigm. *Cancer Research,* 77**,** 3965-3981.
BIAN, B., ZHAO, C., HE, X., GONG, Y., REN, C., GE, L., ZENG, Y., LI, Q., CHEN, M., WENG, C., HE, J., FANG, Y., XU, H. & YIN, Z. Q. 2020. Exosomes derived from neural progenitor cells preserve photoreceptors during retinal degeneration by inactivating microglia. *J Extracell Vesicles,* 9**,** 1748931.
BINENBAUM, Y., FRIDMAN, E., YAARI, Z., MILMAN, N., SCHROEDER, A., BEN DAVID, G., SHLOMI, T. & GIL, Z. 2018. Transfer of miRNA in Macrophage-Derived Exosomes Induces Drug Resistance in Pancreatic Adenocarcinoma. *Cancer Res,* 78**,** 5287-5299.
BOELENS, M. C., WU, T. J., NABET, B. Y., XU, B., QIU, Y., YOON, T., AZZAM, D. J., TWYMAN-SAINT VICTOR, C., WIEMANN, B. Z., ISHWARAN, H., TER BRUGGE, P. J., JONKERS, J., SLINGERLAND, J. & MINN, A. J. 2014. Exosome transfer from stromal to breast cancer cells regulates therapy resistance pathways. *Cell,* 159**,** 499-513.
BOKAR, J. A., RATH-SHAMBAUGH, M. E., LUDWICZAK, R., NARAYAN, P. & ROTTMAN, F. 1994. Characterization and partial purification of mRNA N6-adenosine methyltransferase from HeLa cell nuclei. Internal mRNA methylation requires a multisubunit complex. *J Biol Chem,* 269**,** 17697-704.
BOKAR, J. A., SHAMBAUGH, M. E., POLAYES, D., MATERA, A. G. & ROTTMAN, F. M. 1997. Purification and cDNA cloning of the AdoMet-binding subunit of the human mRNA (N6-adenosine)-methyltransferase. *RNA,* 3**,** 1233-47.
BOLUKBASI, M. F., MIZRAK, A., OZDENER, G. B., MADLENER, S., STRÖBEL, T., ERKAN, E. P., FAN, J.-B., BREAKEFIELD, X. O. & SAYDAM, O. 2012. miR-1289 and "Zipcode"-like Sequence Enrich mRNAs in Microvesicles. *Molecular Therapy — Nucleic Acids,* 1**,** e10.
BOOTH, A. M., FANG, Y., FALLON, J. K., YANG, J. M., HILDRETH, J. E. & GOULD, S. J. 2006. Exosomes and HIV Gag bud from endosome-like domains of the T cell plasma membrane. *J Cell Biol,* 172**,** 923-35.
BORIACK-SJODIN, P. A., RIBICH, S. & COPELAND, R. A. 2018. RNA-modifying proteins as anticancer drug targets. *Nat Rev Drug Discov,* 17**,** 435-453.
BOROWICZ, S., VAN SCOYK, M., AVASARALA, S., KARUPPUSAMY RATHINAM, M. K., TAULER, J., BIKKAVILLI, R. K. & WINN, R. A. 2014. The soft agar colony formation assay. *J Vis Exp***,** e51998.

BRAND, T. M., IIDA, M. & WHEELER, D. L. 2011. Molecular mechanisms of resistance to the EGFR monoclonal antibody cetuximab. *Cancer Biol Ther,* 11**,** 777-92.

BRINGMANN, A., PANNICKE, T., GROSCHE, J., FRANCKE, M., WIEDEMANN, P., SKATCHKOV, S. N., OSBORNE, N. N. & REICHENBACH, A. 2006. Müller cells in the healthy and diseased retina. *Progress in retinal and eye research,* 25**,** 397-424.

BUSCHOW, S. I., NOLTE-'T HOEN, E. N., VAN NIEL, G., POLS, M. S., TEN BROEKE, T., LAUWEN, M., OSSENDORP, F., MELIEF, C. J., RAPOSO, G., WUBBOLTS, R., WAUBEN, M. H. & STOORVOGEL, W. 2009. MHC II in dendritic cells is targeted to lysosomes or T cell-induced exosomes via distinct multivesicular body pathways. *Traffic,* 10**,** 1528-42.

CAPOZZI, M. E., MCCOLLUM, G. W. & PENN, J. S. 2014. The role of cytochrome P450 epoxygenases in retinal angiogenesis. *Invest Ophthalmol Vis Sci,* 55**,** 4253-60.

CARDONA, A. F., ARRIETA, O., ZAPATA, M. I., ROJAS, L., WILLS, B., REGUART, N., KARACHALIOU, N., CARRANZA, H., VARGAS, C., OTERO, J., ARCHILA, P., MARTIN, C., CORRALES, L., CUELLO, M., ORTIZ, C., PINO, L. E., ROSELL, R., ZATARAIN-BARRON, Z. L. & CLICAP 2017. Acquired Resistance to Erlotinib in EGFR Mutation-Positive Lung Adenocarcinoma among Hispanics (CLICaP). *Target Oncol,* 12**,** 513-523.

CEHAJIC-KAPETANOVIC, J., ELEFTHERIOU, C., ALLEN, A. E., MILOSAVLJEVIC, N., PIENAAR, A., BEDFORD, R., DAVIS, K. E., BISHOP, P. N. & LUCAS, R. J. 2015. Restoration of Vision with Ectopic Expression of Human Rod Opsin. *Curr Biol,* 25**,** 2111-22.

CHA, D. J., FRANKLIN, J. L., DOU, Y., LIU, Q., HIGGINBOTHAM, J. N., DEMORY BECKLER, M., WEAVER, A. M., VICKERS, K., PRASAD, N., LEVY, S., ZHANG, B., COFFEY, R. J. & PATTON, J. G. 2015. KRAS-dependent sorting of miRNA to exosomes. *Elife,* 4**,** e07197.

CHAI, Y., LIU, J., ZHANG, Z. & LIU, L. 2016. HuR-regulated lncRNA NEAT1 stability in tumorigenesis and progression of ovarian cancer. *Cancer Med,* 5**,** 1588-98.

CHAIROUNGDUA, A., SMITH, D. L., POCHARD, P., HULL, M. & CAPLAN, M. J. 2010. Exosome release of beta-catenin: a novel mechanism that antagonizes Wnt signaling. *J Cell Biol,* 190**,** 1079-91.

CHELLAMUTHU, A. & GRAY, S. G. 2020. The RNA Methyltransferase NSUN2 and Its Potential Roles in Cancer. *Cells,* 9.

CHEN, G., HUANG, A. C., ZHANG, W., ZHANG, G., WU, M., XU, W., YU, Z., YANG, J., WANG, B., SUN, H., XIA, H., MAN, Q., ZHONG, W., ANTELO, L. F., WU, B., XIONG, X., LIU, X., GUAN, L., LI, T., LIU, S., YANG, R., LU, Y., DONG, L., MCGETTIGAN, S., SOMASUNDARAM, R., RADHAKRISHNAN, R., MILLS, G., LU, Y., KIM, J., CHEN, Y. H., DONG, H., ZHAO, Y., KARAKOUSIS, G. C., MITCHELL, T. C., SCHUCHTER, L. M., HERLYN, M., WHERRY, E. J., XU, X. & GUO, W. 2018. Exosomal PD-L1 contributes to immunosuppression and is associated with anti-PD-1 response. *Nature,* 560**,** 382-386.

CHEN, J., BRUNNER, A. D., COGAN, J. Z., NUNEZ, J. K., FIELDS, A. P., ADAMSON, B., ITZHAK, D. N., LI, J. Y., MANN, M., LEONETTI, M. D. & WEISSMAN, J. S. 2020. Pervasive functional translation of noncanonical human open reading frames. *Science,* 367**,** 1140-1146.

CHEN, P., XI, Q., WANG, Q. & WEI, P. 2014a. Downregulation of MicroRNA-100 Correlates with Tumor Progression and Poor Prognosis in Colorectal Cancer. *Med. Oncol.,* 31**,** 235.

CHEN, W. X., CAI, Y. Q., LV, M. M., CHEN, L., ZHONG, S. L., MA, T. F., ZHAO, J. H. & TANG, J. H. 2014b. Exosomes from docetaxel-resistant breast cancer cells alter chemosensitivity by delivering microRNAs. *Tumour Biol,* 35**,** 9649-59.

CHEN, W. X., LIU, X. M., LV, M. M., CHEN, L., ZHAO, J. H., ZHONG, S. L., JI, M. H., HU, Q., LUO, Z., WU, J. Z. & TANG, J. H. 2014c. Exosomes from drug-resistant breast cancer cells transmit chemoresistance by a horizontal transfer of microRNAs. *PLoS One,* 9**,** e95240.

CHERRADI, N. 2016. MicroRNAs as Potential Biomarkers in Adrenocortical Cancer: Progress and Challenges. *Front. Endocrinol.,* 6.

CHEVILLET, J. R., KANG, Q., RUF, I. K., BRIGGS, H. A., VOJTECH, L. N., HUGHES, S. M., CHENG, H. H., ARROYO, J. D., MEREDITH, E. K., GALLICHOTTE, E. N., POGOSOVA-AGADJANYAN, E. L., MORRISSEY, C., STIREWALT, D. L., HLADIK, F., YU, E. Y., HIGANO, C. S. & TEWARI, M. 2014. Quantitative and stoichiometric analysis of the microRNA content of exosomes. *Proc Natl Acad Sci U S A,* 111**,** 14888-93.

CHRISTIAN, T., LAHOUD, G., LIU, C., HOFFMANN, K., PERONA, J. J. & HOU, Y. M. 2010. Mechanism of N-methylation by the tRNA m1G37 methyltransferase Trm5. *RNA,* 16**,** 2484-92.

COHN, W. E. 1960. Pseudouridine, a carbon-carbon linked ribonucleoside in ribonucleic acids: isolation, structure, and chemical characteristics. *J Biol Chem,* 235**,** 1488-98.

COLOMBO, M., MOITA, C., NIEL, G. V., KOWAL, J., VIGNERON, J., BENAROCH, P., MANEL, N., MOITA, L. F., THÉRY, C. & RAPOSO, G. 2013. Analysis of ESCRT functions in exosome biogenesis, composition and secretion highlights the heterogeneity of extracellular vesicles. *J Cell Sci,* 126**,** 5553-5565.

COLOMBO, M., RAPOSO, G. & THERY, C. 2014. Biogenesis, secretion, and intercellular interactions of exosomes and other extracellular vesicles. *Annu Rev Cell Dev Biol,* 30**,** 255-89.

CONEDERA, F. M., POUSA, A. M. Q., MERCADER, N., TSCHOPP, M. & ENZMANN, V. 2019. Retinal microglia signaling affects Muller cell behavior in the zebrafish following laser injury induction. *Glia,* 67**,** 1150-1166.

CORTEZ, M. A., BUESO-RAMOS, C., FERDIN, J., LOPEZ-BERESTEIN, G., SOOD, A. K. & CALIN, G. A. 2011. MicroRNAs in body fluids--the mix of hormones and biomarkers. *Nat Rev Clin Oncol,* 8**,** 467-77.

CRESCITELLI, R., LASSER, C., SZABO, T. G., KITTEL, A., ELDH, M., DIANZANI, I., BUZAS, E. I. & LOTVALL, J. 2013. Distinct RNA profiles in subpopulations of extracellular vesicles: apoptotic bodies, microvesicles and exosomes. *J Extracell Vesicles,* 2.

D'SOUZA-SCHOREY, C. & CLANCY, J. W. 2012. Tumor-derived microvesicles: shedding light on novel microenvironment modulators and prospective cancer biomarkers. *Genes & Development,* 26**,** 1287-1299.

D'SOUZA-SCHOREY, C. & SCHOREY, J. S. 2018. Regulation and mechanisms of extracellular vesicle biogenesis and secretion. *Essays Biochem,* 62**,** 125-133.

DEMORY BECKLER, M., HIGGINBOTHAM, J. N., FRANKLIN, J. L., HAM, A. J., HALVEY, P. J., IMASUEN, I. E., WHITWELL, C., LI, M., LIEBLER, D. C. & COFFEY, R. J. 2013. Proteomic analysis of exosomes from mutant KRAS colon cancer cells identifies intercellular transfer of mutant KRAS. *Mol Cell Proteomics,* 12**,** 343-55.

DENG, X., SU, R., WENG, H., HUANG, H., LI, Z. & CHEN, J. 2018. RNA N(6)-methyladenosine modification in cancers: current status and perspectives. *Cell Res,* 28**,** 507-517.

DESROSIERS, R., FRIDERICI, K. & ROTTMAN, F. 1974. Identification of methylated nucleosides in messenger RNA from Novikoff hepatoma cells. *Proc Natl Acad Sci U S A,* 71**,** 3971-5.

DIDIANO, D., ABNER, J. J., HINGER, S. A., FLICKINGER, Z., KENT, M., CLEMENT, M. A., BALAIYA, S., LIU, Q., DAI, X., LEVINE, E. M. & PATTON, J. G. 2020. Induction of a proliferative response in the zebrafish retina by injection of extracellular vesicles. *Exp Eye Res,* 200**,** 108254.

DOMINISSINI, D., MOSHITCH-MOSHKOVITZ, S., SCHWARTZ, S., SALMON-DIVON, M., UNGAR, L., OSENBERG, S., CESARKAS, K., JACOB-HIRSCH, J., AMARIGLIO, N., KUPIEC, M., SOREK, R. & RECHAVI, G. 2012. Topology of the human and mouse m6A RNA methylomes revealed by m6A-seq. *Nature,* 485**,** 201-6.

DOU, Y., CHA, D. J., FRANKLIN, J. L., HIGGINBOTHAM, J. N., JEPPESEN, D. K., WEAVER, A. M., PRASAD, N., LEVY, S., COFFEY, R. J., PATTON, J. G. & ZHANG, B. 2016. Circular RNAs are down-regulated in KRAS mutant colon cancer cells and can be transferred to exosomes. *Sci Rep,* 6**,** 37982.

EMMRICH, S., RASCHE, M., SCHONING, J., REIMER, C., KEIHANI, S., MAROZ, A., XIE, Y., LI, Z., SCHAMBACH, A., REINHARDT, D. & KLUSMANN, J. H. 2014. miR-99a/100~125b tricistrons regulate hematopoietic stem and progenitor cell homeostasis by shifting the balance between TGFbeta and Wnt signaling. *Genes Dev,* 28**,** 858-74.

ENSSLIN, M. A. & SHUR, B. D. 2007. The EGF repeat and discoidin domain protein, SED1/MFG-E8, is required for mammary gland branching morphogenesis. *Proc Natl Acad Sci U S A,* 104**,** 2715-20.

FABBRI, M., PAONE, A., CALORE, F., GALLI, R. & CROCE, C. M. 2013. A new role for microRNAs, as ligands of Toll-like receptors. *RNA Biol,* 10**,** 169-74.

FAN, Y.-X., BIAN, X.-H., QIAN, P.-D., CHEN, Z.-Z., WEN, J., LUO, Y.-H., YAN, P.-W. & ZHANG, Q. 2018. MicroRNA-125b Inhibits Cell Proliferation and Induces Cell Apoptosis in Esophageal Squamous Cell Carcinoma by Targeting BMF. *Oncol. Rep.,* 40**,** 61-72.

FANG, Y. & FULLWOOD, M. J. 2016. Roles, Functions, and Mechanisms of Long Non-coding RNAs in Cancer. *Genomics Proteomics Bioinformatics,* 14**,** 42-54.

FANG, Y., ZHOU, W., RONG, Y., KUANG, T., XU, X., WU, W., WANG, D. & LOU, W. 2019. Exosomal MiRNA-106b from Cancer-Associated Fibroblast Promotes Gemcitabine Resistance in Pancreatic Cancer. *Exp Cell Res,* 383**,** 111543.

FARBER, D. B. & KATSMAN, D. 2016. Embryonic Stem Cell-Derived Microvesicles: Could They be Used for Retinal Regeneration? *Adv Exp Med Biol,* 854**,** 563-9.

FAUSETT, B. V. & GOLDMAN, D. 2006. A role for alpha1 tubulin-expressing Muller glia in regeneration of the injured zebrafish retina. *Journal of Neuroscience,* 26**,** 6303-13.

FAUSETT, B. V., GUMERSON, J. D. & GOLDMAN, D. 2008. The proneural basic helix-loop-helix gene ascl1a is required for retina regeneration. *Journal of Neuroscience,* 28**,** 1109-17.

FELICIANO, A., CASTELLVI, J., ARTERO-CASTRO, A., LEAL, J. A., ROMAGOSA, C., HERNANDEZ-LOSA, J., PEG, V., FABRA, A., VIDAL, F., KONDOH, H., CAJAL, S. R. Y. & LLEONART, M. E. 2013. MiR-125b Acts as a Tumor Suppressor in Breast Tumorigenesis via Its Novel Direct Targets ENPEP, CK2-α, CCNJ, and MEGF9. *PLOS ONE,* 8**,** e76247.

FILIPOWICZ, W. 2005. RNAi: the nuts and bolts of the RISC machine. *Cell,* 122**,** 17-20.

FISCHER, A. J., BOSSE, J. L. & EL-HODIRI, H. M. 2013. The ciliary marginal zone (CMZ) in development and regeneration of the vertebrate eye. *Exp Eye Res,* 116**,** 199-204.

FLETCHER, J. I., WILLIAMS, R. T., HENDERSON, M. J., NORRIS, M. D. & HABER, M. 2016. ABC transporters as mediators of drug resistance and contributors to cancer cell biology. *Drug Resist Updat,* 26**,** 1-9.

FONG, M. Y., ZHOU, W., LIU, L., ALONTAGA, A. Y., CHANDRA, M., ASHBY, J., CHOW, A., O'CONNOR, S. T., LI, S., CHIN, A. R., SOMLO, G., PALOMARES, M., LI, Z., TREMBLAY, J. R., TSUYADA, A., SUN, G., REID, M. A., WU, X., SWIDERSKI, P., REN, X., SHI, Y., KONG, M., ZHONG, W., CHEN, Y. & WANG, S. E. 2015. Breast-cancer-secreted miR-122 reprograms glucose metabolism in premetastatic niche to promote metastasis. *Nat Cell Biol,* 17**,** 183-94.

FOZZATTI, L. & CHENG, S. Y. 2020. Tumor Cells and Cancer-Associated Fibroblasts: A Synergistic Crosstalk to Promote Thyroid Cancer. *Endocrinol Metab (Seoul),* 35**,** 673-680.

FREEDMAN, J. E., GERSTEIN, M., MICK, E., ROZOWSKY, J., LEVY, D., KITCHEN, R., DAS, S., SHAH, R., DANIELSON, K., BEAULIEU, L., NAVARRO, F. C., WANG, Y., GALEEV, T. R., HOLMAN, A., KWONG, R. Y., MURTHY, V., TANRIVERDI, S. E., KOUPENOVA-ZAMOR, M., MIKHALEV, E. & TANRIVERDI, K. 2016. Diverse human extracellular RNAs are widely detected in human plasma. *Nat Commun,* 7**,** 11106.

FUJINO, Y., TAKEISHI, S., NISHIDA, K., OKAMOTO, K., MUGURUMA, N., KIMURA, T., KITAMURA, S., MIYAMOTO, H., FUJIMOTO, A., HIGASHIJIMA, J., SHIMADA, M., ROKUTAN, K. & TAKAYAMA, T. 2017. Downregulation of MicroRNA-100/MicroRNA-125b is Associated with Lymph Node Metastasis in Early Colorectal Cancer with Submucosal Invasion. *Cancer Sci.,* 108**,** 390-397.

FUTTER, C. E., PEARSE, A., HEWLETT, L. J. & HOPKINS, C. R. 1996. Multivesicular endosomes containing internalized EGF-EGF receptor complexes mature and then fuse directly with lysosomes. *J Cell Biol,* 132**,** 1011-23.

GEBERT, L. F. R. & MACRAE, I. J. 2019. Regulation of microRNA function in animals. *Nat Rev Mol Cell Biol,* 20**,** 21-37.

GEULA, S., MOSHITCH-MOSHKOVITZ, S., DOMINISSINI, D., MANSOUR, A. A., KOL, N., SALMON-DIVON, M., HERSHKOVITZ, V., PEER, E., MOR, N., MANOR, Y. S., BEN-HAIM, M. S., EYAL, E., YUNGER, S., PINTO, Y., JAITIN, D. A., VIUKOV, S., RAIS, Y., KRUPALNIK, V., CHOMSKY, E., ZERBIB, M., MAZA, I., RECHAVI, Y., MASSARWA, R., HANNA, S., AMIT, I., LEVANON, E. Y., AMARIGLIO, N., STERN-GINOSSAR, N., NOVERSHTERN, N., RECHAVI, G. & HANNA, J. H. 2015. Stem cells. m6A mRNA methylation facilitates resolution of naive pluripotency toward differentiation. *Science,* 347**,** 1002-6.

GIBBINGS, D. J., CIAUDO, C., ERHARDT, M. & VOINNET, O. 2009. Multivesicular bodies associate with components of miRNA effector complexes and modulate miRNA activity. *Nat Cell Biol,* 11**,** 1143-9.

GIRALDEZ, A. J., MISHIMA, Y., RIHEL, J., GROCOCK, R. J., VAN DONGEN, S., INOUE, K., ENRIGHT, A. J. & SCHIER, A. F. 2006. Zebrafish MiR-430 Promotes Deadenylation and Clearance of Maternal mRNAs. *Science,* 312**,** 75-79.

GOMES, S. E., SIMOES, A. E., PEREIRA, D. M., CASTRO, R. E., RODRIGUES, C. M. & BORRALHO, P. M. 2016. miR-143 or miR-145 overexpression increases cetuximab-mediated antibody-dependent cellular cytotoxicity in human colon cancer cells. *Oncotarget,* 7**,** 9368-87.

GONG, Y., HE, T., YANG, L., YANG, G., CHEN, Y. & ZHANG, X. 2015. The Role of MiR-100 in Regulating Apoptosis of Breast Cancer Cells. *Sci. Rep.,* 5.

GOULD, G. W. & LIPPINCOTT-SCHWARTZ, J. 2009. New roles for endosomes: from vesicular carriers to multi-purpose platforms. *Nat Rev Mol Cell Biol,* 10**,** 287-92.

GROBBEN, B., DE DEYN, P. P. & SLEGERS, H. 2002. Rat C6 glioma as experimental model system for the study of glioblastoma growth and invasion. *Cell Tissue Res,* 310**,** 257-70.
GROSJEAN, H., KEITH, G. & DROOGMANS, L. 2004. Detection and quantification of modified nucleotides in RNA using thin-layer chromatography. *Methods Mol Biol,* 265**,** 357-91.
GUO, H., INGOLIA, N. T., WEISSMAN, J. S. & BARTEL, D. P. 2010. Mammalian microRNAs predominantly act to decrease target mRNA levels. *Nature,* 466**,** 835-40.
GUO, Q., WANG, H., YAN, Y., LIU, Y., SU, C., CHEN, H., YAN, Y., ADHIKARI, R., WU, Q. & ZHANG, J. 2020. The Role of Exosomal microRNA in Cancer Drug Resistance. *Frontiers in Oncology,* 10.
GUTIERREZ-VAZQUEZ, C., VILLARROYA-BELTRI, C., MITTELBRUNN, M. & SANCHEZ-MADRID, F. 2013. Transfer of extracellular vesicles during immune cell-cell interactions. *Immunol Rev,* 251**,** 125-42.
HAAG, S., WARDA, A. S., KRETSCHMER, J., GUNNIGMANN, M. A., HOBARTNER, C. & BOHNSACK, M. T. 2015. NSUN6 is a human RNA methyltransferase that catalyzes formation of m5C72 in specific tRNAs. *RNA,* 21**,** 1532-43.
HADERK, F., SCHULZ, R., ISKAR, M., CID, L. L., WORST, T., WILLMUND, K. V., SCHULZ, A., WARNKEN, U., SEILER, J., BENNER, A., NESSLING, M., ZENZ, T., GOBEL, M., DURIG, J., DIEDERICHS, S., PAGGETTI, J., MOUSSAY, E., STILGENBAUER, S., ZAPATKA, M., LICHTER, P. & SEIFFERT, M. 2017. Tumor-derived exosomes modulate PD-L1 expression in monocytes. *Sci Immunol,* 2.
HAN, L., LAM, E. W. & SUN, Y. 2019. Extracellular vesicles in the tumor microenvironment: old stories, but new tales. *Mol Cancer,* 18**,** 59.
HANAYAMA, R., TANAKA, M., MIWA, K., SHINOHARA, A., IWAMATSU, A. & NAGATA, S. 2002. Identification of a factor that links apoptotic cells to phagocytes. *Nature,* 417**,** 182-7.
HANGAUER, M. J., VAUGHN, I. W. & MCMANUS, M. T. 2013. Pervasive transcription of the human genome produces thousands of previously unidentified long intergenic noncoding RNAs. *PLoS Genet,* 9**,** e1003569.
HARCOURT, E. M., KIETRYS, A. M. & KOOL, E. T. 2017. Chemical and structural effects of base modifications in messenger RNA. *Nature,* 541**,** 339-346.
HARDING, C., HEUSER, J. & STAHL, P. 1983. Receptor-mediated endocytosis of transferrin and recycling of the transferrin receptor in rat reticulocytes. *J Cell Biol,* 97**,** 329-39.
HECK, A. M., RUSSO, J., WILUSZ, J., NISHIMURA, E. O. & WILUSZ, C. J. 2020. YTHDF2 destabilizes m(6)A-modified neural-specific RNAs to restrain differentiation in induced pluripotent stem cells. *RNA,* 26**,** 739-755.
HIGGINBOTHAM, JAMES N., DEMORY BECKLER, M., GEPHART, JONATHAN D., FRANKLIN, JEFFREY L., BOGATCHEVA, G., KREMERS, G.-J., PISTON, DAVID W., AYERS, GREGORY D., MCCONNELL, RUSSELL E., TYSKA, MATTHEW J. & COFFEY, ROBERT J. 2011. Amphiregulin Exosomes Increase Cancer Cell Invasion. *Current Biology,* 21**,** 779-786.
HINGER, S. A., ABNER, J. J., FRANKLIN, J. L., JEPPESEN, D. K., COFFEY, R. J. & PATTON, J. G. 2020. Rab13 regulates sEV secretion in mutant KRAS colorectal cancer cells. *Sci Rep,* 10**,** 15804.
HINGER, S. A., CHA, D. J., FRANKLIN, J. L., HIGGINBOTHAM, J. N., DOU, Y., PING, J., SHU, L., PRASAD, N., LEVY, S., ZHANG, B., LIU, Q., WEAVER, A. M., COFFEY, R. J. & PATTON, J. G.

2018. Diverse Long RNAs Are Differentially Sorted into Extracellular Vesicles Secreted by Colorectal Cancer Cells. *Cell Rep,* 25**,** 715-725 e4.

HOLLEY, R. W., EVERETT, G. A., MADISON, J. T. & ZAMIR, A. 1965. Nucleotide Sequences in the Yeast Alanine Transfer Ribonucleic Acid. *J Biol Chem,* 240**,** 2122-8.

HOLOCH, D. & MOAZED, D. 2015. RNA-mediated epigenetic regulation of gene expression. *Nat Rev Genet,* 16**,** 71-84.

HOSHINO, D., KIRKBRIDE, K. C., COSTELLO, K., CLARK, E. S., SINHA, S., GREGA-LARSON, N., TYSKA, M. J. & WEAVER, A. M. 2013. Exosome Secretion Is Enhanced by Invadopodia and Drives Invasive Behavior. *Cell Reports,* 5**,** 1159-1168.

HU, G., ZHAO, X., WANG, J., LV, L., WANG, C., FENG, L., SHEN, L. & REN, W. 2018. MiR-125b Regulates the Drug-Resistance of Breast Cancer Cells to Doxorubicin by Targeting HAX-1. *Oncol. Lett.,* 15**,** 1621-1629.

HU, W., LIU, C., BI, Z. Y., ZHOU, Q., ZHANG, H., LI, L. L., ZHANG, J., ZHU, W., SONG, Y. Y., ZHANG, F., YANG, H. M., BI, Y. Y., HE, Q. Q., TAN, G. J., SUN, C. C. & LI, D. J. 2020. Comprehensive landscape of extracellular vesicle-derived RNAs in cancer initiation, progression, metastasis and cancer immunology. *Mol Cancer,* 19**,** 102.

HUANG, H., WENG, H., SUN, W., QIN, X., SHI, H., WU, H., ZHAO, B. S., MESQUITA, A., LIU, C., YUAN, C. L., HU, Y. C., HUTTELMAIER, S., SKIBBE, J. R., SU, R., DENG, X., DONG, L., SUN, M., LI, C., NACHTERGAELE, S., WANG, Y., HU, C., FERCHEN, K., GREIS, K. D., JIANG, X., WEI, M., QU, L., GUAN, J. L., HE, C., YANG, J. & CHEN, J. 2018. Recognition of RNA N(6)-methyladenosine by IGF2BP proteins enhances mRNA stability and translation. *Nat Cell Biol,* 20**,** 285-295.

HUGEL, B., MARTINEZ, M. C., KUNZELMANN, C. & FREYSSINET, J. M. 2005. Membrane microparticles: two sides of the coin. *Physiology (Bethesda),* 20**,** 22-7.

JAISWAL, J. K., ANDREWS, N. W. & SIMON, S. M. 2002. Membrane proximal lysosomes are the major vesicles responsible for calcium-dependent exocytosis in nonsecretory cells. *J Cell Biol,* 159**,** 625-35.

JAISWAL, R., GONG, J., SAMBASIVAM, S., COMBES, V., MATHYS, J. M., DAVEY, R., GRAU, G. E. & BEBAWY, M. 2012. Microparticle-associated nucleic acids mediate trait dominance in cancer. *FASEB J,* 26**,** 420-9.

JEPPESEN, D. K., FENIX, A. M., FRANKLIN, J. L., HIGGINBOTHAM, J. N., ZHANG, Q., ZIMMERMAN, L. J., LIEBLER, D. C., PING, J., LIU, Q., EVANS, R., FISSELL, W. H., PATTON, J. G., ROME, L. H., BURNETTE, D. T. & COFFEY, R. J. 2019. Reassessment of Exosome Composition. *Cell,* 177**,** 428-445 e18.

JIA, G., FU, Y., ZHAO, X., DAI, Q., ZHENG, G., YANG, Y., YI, C., LINDAHL, T., PAN, T., YANG, Y. G. & HE, C. 2011. N6-methyladenosine in nuclear RNA is a major substrate of the obesity-associated FTO. *Nat Chem Biol,* 7**,** 885-7.

JIANG, Q., HE, M., GUAN, S., MA, M., WU, H., YU, Z., JIANG, L., WANG, Y., ZONG, X., JIN, F. & WEI, M. 2016. MicroRNA-100 Suppresses the Migration and Invasion of Breast Cancer Cells by Targeting FZD-8 and Inhibiting Wnt/β-Catenin Signaling Pathway. *Tumor Biol.,* 37**,** 5001-5011.

JOHNSTONE, R. M., ADAM, M., HAMMOND, J. R., ORR, L. & TURBIDE, C. 1987. Vesicle formation during reticulocyte maturation. Association of plasma membrane activities with released vesicles (exosomes). *J Biol Chem,* 262**,** 9412-20.

JONKHOUT, N., TRAN, J., SMITH, M. A., SCHONROCK, N., MATTICK, J. S. & NOVOA, E. M. 2017. The RNA modification landscape in human disease. *RNA,* 23**,** 1754-1769.

JORSTAD, N. L., WILKEN, M. S., GRIMES, W. N., WOHL, S. G., VANDENBOSCH, L. S., YOSHIMATSU, T., WONG, R. O., RIEKE, F. & REH, T. A. 2017. Stimulation of functional neuronal regeneration from Muller glia in adult mice. *Nature,* 548**,** 103-107.

KALLURI, R. 2016. The biology and function of exosomes in cancer. *J Clin Invest,* 126**,** 1208-15.

KALRA, H., SIMPSON, R. J., JI, H., AIKAWA, E., ALTEVOGT, P., ASKENASE, P., BOND, V. C., BORRAS, F. E., BREAKEFIELD, X., BUDNIK, V., BUZAS, E., CAMUSSI, G., CLAYTON, A., COCUCCI, E., FALCON-PEREZ, J. M., GABRIELSSON, S., GHO, Y. S., GUPTA, D., HARSHA, H. C., HENDRIX, A., HILL, A. F., INAL, J. M., JENSTER, G., KRAMER-ALBERS, E. M., LIM, S. K., LLORENTE, A., LOTVALL, J., MARCILLA, A., MINCHEVA-NILSSON, L., NAZARENKO, I., NIEUWLAND, R., NOLTE-'T HOEN, E. N., PANDEY, A., PATEL, T., PIPER, M. G., PLUCHINO, S., PRASAD, T. S., RAJENDRAN, L., RAPOSO, G., RECORD, M., REID, G. E., SANCHEZ-MADRID, F., SCHIFFELERS, R. M., SILJANDER, P., STENSBALLE, A., STOORVOGEL, W., TAYLOR, D., THERY, C., VALADI, H., VAN BALKOM, B. W., VAZQUEZ, J., VIDAL, M., WAUBEN, M. H., YANEZ-MO, M., ZOELLER, M. & MATHIVANAN, S. 2012. Vesiclepedia: a compendium for extracellular vesicles with continuous community annotation. *PLoS Biol,* 10**,** e1001450.

KAPLAN, R. N., RIBA, R. D., ZACHAROULIS, S., BRAMLEY, A. H., VINCENT, L., COSTA, C., MACDONALD, D. D., JIN, D. K., SHIDO, K., KERNS, S. A., ZHU, Z., HICKLIN, D., WU, Y., PORT, J. L., ALTORKI, N., PORT, E. R., RUGGERO, D., SHMELKOV, S. V., JENSEN, K. K., RAFII, S. & LYDEN, D. 2005. VEGFR1-positive haematopoietic bone marrow progenitors initiate the pre-metastatic niche. *Nature,* 438**,** 820-7.

KARL, M. O. & REH, T. A. 2010. Regenerative medicine for retinal diseases: activating endogenous repair mechanisms. *Trends Mol Med,* 16**,** 193-202.

KATSMAN, D., STACKPOLE, E. J., DOMIN, D. R. & FARBER, D. B. 2012. Embryonic stem cell-derived microvesicles induce gene expression changes in Muller cells of the retina. *PLoS One,* 7**,** e50417.

KE, S., ALEMU, E. A., MERTENS, C., GANTMAN, E. C., FAK, J. J., MELE, A., HARIPAL, B., ZUCKER-SCHARFF, I., MOORE, M. J., PARK, C. Y., VAGBO, C. B., KUSSNIERCZYK, A., KLUNGLAND, A., DARNELL, J. E., JR. & DARNELL, R. B. 2015. A majority of m6A residues are in the last exons, allowing the potential for 3' UTR regulation. *Genes Dev,* 29**,** 2037-53.

KE, S., PANDYA-JONES, A., SAITO, Y., FAK, J. J., VAGBO, C. B., GEULA, S., HANNA, J. H., BLACK, D. L., DARNELL, J. E., JR. & DARNELL, R. B. 2017. m(6)A mRNA modifications are deposited in nascent pre-mRNA and are not required for splicing but do specify cytoplasmic turnover. *Genes Dev,* 31**,** 990-1006.

KIM, V. 2005. MicroRNA biogenesis: coordinated cropping and dicing. *Nat Rev Mol Cell Biol,* 6**,** 376-385.

KONNO, M., KOSEKI, J., ASAI, A., YAMAGATA, A., SHIMAMURA, T., MOTOOKA, D., OKUZAKI, D., KAWAMOTO, K., MIZUSHIMA, T., EGUCHI, H., TAKIGUCHI, S., SATOH, T., MIMORI, K., OCHIYA, T., DOKI, Y., OFUSA, K., MORI, M. & ISHII, H. 2019. Distinct methylation levels of mature microRNAs in gastrointestinal cancers. *Nat Commun,* 10**,** 3888.

KOPP, F. & MENDELL, J. T. 2018. Functional Classification and Experimental Dissection of Long Noncoding RNAs. *Cell,* 172**,** 393-407.

KOSAKA, N., IGUCHI, H., YOSHIOKA, Y., TAKESHITA, F., MATSUKI, Y. & OCHIYA, T. 2010. Secretory mechanisms and intercellular transfer of microRNAs in living cells. *J Biol Chem,* 285**,** 17442-52.

KOSSINOVA, O. A., GOPANENKO, A. V., TAMKOVICH, S. N., KRASHENININA, O. A., TUPIKIN, A. E., KISELEVA, E., YANSHINA, D. D., MALYGIN, A. A., VEN'YAMINOVA, A. G., KABILOV, M. R. & KARPOVA, G. G. 2017. Cytosolic YB-1 and NSUN2 are the only proteins recognizing specific motifs present in mRNAs enriched in exosomes. *Biochim Biophys Acta,* 1865**,** 664-673.

KOWAL, J., ARRAS, G., COLOMBO, M., JOUVE, M., MORATH, J. P., PRIMDAL-BENGTSON, B., DINGLI, F., LOEW, D., TKACH, M. & THERY, C. 2016. Proteomic comparison defines novel markers to characterize heterogeneous populations of extracellular vesicle subtypes. *Proc Natl Acad Sci U S A,* 113**,** E968-77.

KROL, J., LOEDIGE, I. & FILIPOWICZ, W. 2010. The widespread regulation of microRNA biogenesis, function and decay. *Nat Rev Genet,* 11**,** 597-610.

KUNADT, M., ECKERMANN, K., STUENDL, A., GONG, J., RUSSO, B., STRAUSS, K., RAI, S., KUGLER, S., FALOMIR LOCKHART, L., SCHWALBE, M., KRUMOVA, P., OLIVEIRA, L. M., BAHR, M., MOBIUS, W., LEVIN, J., GIESE, A., KRUSE, N., MOLLENHAUER, B., GEISS-FRIEDLANDER, R., LUDOLPH, A. C., FREISCHMIDT, A., FEILER, M. S., DANZER, K. M., ZWECKSTETTER, M., JOVIN, T. M., SIMONS, M., WEISHAUPT, J. H. & SCHNEIDER, A. 2015. Extracellular vesicle sorting of alpha-Synuclein is regulated by sumoylation. *Acta Neuropathol,* 129**,** 695-713.

LASMAN, L., KRUPALNIK, V., VIUKOV, S., MOR, N., AGUILERA-CASTREJON, A., SCHNEIR, D., BAYERL, J., MIZRAHI, O., PELES, S., TAWIL, S., SATHE, S., NACHSHON, A., SHANI, T., ZERBIB, M., KILIMNIK, I., AIGNER, S., SHANKAR, A., MUELLER, J. R., SCHWARTZ, S., STERN-GINOSSAR, N., YEO, G. W., GEULA, S., NOVERSHTERN, N. & HANNA, J. H. 2020. Context-dependent functional compensation between Ythdf m(6)A reader proteins. *Genes Dev,* 34**,** 1373-1391.

LAURENT-PUIG, P., GRISONI, M. L., HEINEMANN, V., LIEBAERT, F., NEUREITER, D., JUNG, A., MONTESTRUC, F., GASTON-MATHE, Y., THIEBAUT, R. & STINTZING, S. 2019. Validation of miR-31-3p Expression to Predict Cetuximab Efficacy When Used as First-Line Treatment in RAS Wild-Type Metastatic Colorectal Cancer. *Clin Cancer Res,* 25**,** 134-141.

LEI, Y., GUO, W., CHEN, B., CHEN, L., GONG, J. & LI, W. 2018. Tumorreleased lncRNA H19 promotes gefitinib resistance via packaging into exosomes in nonsmall cell lung cancer. *Oncol Rep,* 40**,** 3438-3446.

LENKOWSKI, J. R. & RAYMOND, P. A. 2014. Muller glia: Stem cells for generation and regeneration of retinal neurons in teleost fish. *Prog Retin Eye Res,* 40**,** 94-123.

LI, F., ZHAO, D., WU, J. & SHI, Y. 2014. Structure of the YTH domain of human YTHDF2 in complex with an m(6)A mononucleotide reveals an aromatic cage for m(6)A recognition. *Cell Res,* 24**,** 1490-2.

LI, K., WONG, D. K., HONG, K. Y. & RAFFAI, R. L. 2018. Cushioned-Density Gradient Ultracentrifugation (C-DGUC): A Refined and High Performance Method for the Isolation, Characterization, and Use of Exosomes. *Methods Mol Biol,* 1740**,** 69-83.

LI, Y., YE, Y., FENG, B. & QI, Y. 2017. Long Noncoding RNA lncARSR Promotes Doxorubicin Resistance in Hepatocellular Carcinoma via Modulating PTEN-PI3K/Akt Pathway. *J Cell Biochem,* 118**,** 4498-4507.

LIAO, Y., WANG, J., JAEHNIG, E. J., SHI, Z. & ZHANG, B. 2019. WebGestalt 2019: gene set analysis toolkit with revamped UIs and APIs. *Nucleic Acids Res,* 47**,** W199-W205.

LIU, J., DOU, X., CHEN, C., CHEN, C., LIU, C., XU, M. M., ZHAO, S., SHEN, B., GAO, Y., HAN, D. & HE, C. 2020. N (6)-methyladenosine of chromosome-associated regulatory RNA regulates chromatin state and transcription. *Science,* 367**,** 580-586.

LIU, J., YUE, Y., HAN, D., WANG, X., FU, Y., ZHANG, L., JIA, G., YU, M., LU, Z., DENG, X., DAI, Q., CHEN, W. & HE, C. 2014. A METTL3-METTL14 complex mediates mammalian nuclear RNA N6-adenosine methylation. *Nat Chem Biol,* 10**,** 93-5.

LIU, N., DAI, Q., ZHENG, G., HE, C., PARISIEN, M. & PAN, T. 2015. N(6)-methyladenosine-dependent RNA structural switches regulate RNA-protein interactions. *Nature,* 518**,** 560-4.

LIU, W., HU, J., ZHOU, K., CHEN, F., WANG, Z., LIAO, B., DAI, Z., CAO, Y., FAN, J. & ZHOU, J. 2017. Serum exosomal miR-125b is a novel prognostic marker for hepatocellular carcinoma. *Onco Targets Ther,* 10**,** 3843-3851.

LU, Y., ZHAO, X., LIU, Q., LI, C., GRAVES-DEAL, R., CAO, Z., SINGH, B., FRANKLIN, J. L., WANG, J., HU, H., YANG, M., YEATMAN, T. J., LEE, E., SAITO-DIAZ, K., HINGER, S., PATTON, J. G., CHUNG, C. H., EMMRICH, S., KLUSMANN, J.-H., FAN, D. & COFFEY, R. J. 2017. lncRNA MIR100HG-derived miR-100 and miR-125b mediate Cetuximab resistance via Wnt/beta catenin signaling. *Nature Medicine,* 23**,** 1331-1341.

LUNDBERG, I. V., WIKBERG, M. L., LJUSLINDER, I., LI, X., MYTE, R., ZINGMARK, C., LÖFGREN-BURSTRÖM, A., EDIN, S. & PALMQVIST, R. 2018. MicroRNA Expression in KRAS- and BRAF-Mutated Colorectal Cancers. *Anticancer Res.,* 38**,** 677-683.

LUO, Y., WANG, X., NIU, W., WANG, H., WEN, Q., FAN, S., ZHAO, R., LI, Z., XIONG, W., PENG, S., ZENG, Z., LI, X., LI, G., TAN, M. & ZHOU, M. 2017. Elevated MicroRNA-125b Levels Predict a Worse Prognosis in HER2-Positive Breast Cancer Patients. *Oncol. Lett.,* 13**,** 867-874.

MAAS, S. L. N., BREAKEFIELD, X. O. & WEAVER, A. M. 2017. Extracellular Vesicles: Unique Intercellular Delivery Vehicles. *Trends in Cell Biology,* 27**,** 172-188.

MACLAREN, R. E., PEARSON, R. A., MACNEIL, A., DOUGLAS, R. H., SALT, T. E., AKIMOTO, M., SWAROOP, A., SOWDEN, J. C. & ALI, R. R. 2006. Retinal repair by transplantation of photoreceptor precursors. *Nature,* 444**,** 203-7.

MADAMANCHI, A., CAPOZZI, M., GENG, L., LI, Z., FRIEDMAN, R. D., DICKESON, S. K., PENN, J. S. & ZUTTER, M. M. 2014. Mitigation of oxygen-induced retinopathy in alpha2beta1 integrin-deficient mice. *Invest Ophthalmol Vis Sci,* 55**,** 4338-47.

MAIA, J., CAJA, S., STRANO MORAES, M. C., COUTO, N. & COSTA-SILVA, B. 2018. Exosome-Based Cell-Cell Communication in the Tumor Microenvironment. *Front Cell Dev Biol,* 6**,** 18.

MATEESCU, B., KOWAL, E. J., VAN BALKOM, B. W., BARTEL, S., BHATTACHARYYA, S. N., BUZAS, E. I., BUCK, A. H., DE CANDIA, P., CHOW, F. W., DAS, S., DRIEDONKS, T. A., FERNANDEZ-MESSINA, L., HADERK, F., HILL, A. F., JONES, J. C., VAN KEUREN-JENSEN, K. R., LAI, C. P., LASSER, C., LIEGRO, I. D., LUNAVAT, T. R., LORENOWICZ, M. J., MAAS, S. L., MAGER, I., MITTELBRUNN, M., MOMMA, S., MUKHERJEE, K., NAWAZ, M., PEGTEL, D. M., PFAFFL, M. W., SCHIFFELERS, R. M., TAHARA, H., THERY, C., TOSAR, J. P., WAUBEN, M. H., WITWER, K. W. & NOLTE-'T HOEN, E. N. 2017. Obstacles and opportunities in the functional analysis of extracellular vesicle RNA - an ISEV position paper. *J Extracell Vesicles,* 6**,** 1286095.

MATSUO, H., CHEVALLIER, J., MAYRAN, N., LE BLANC, I., FERGUSON, C., FAURE, J., BLANC, N. S., MATILE, S., DUBOCHET, J., SADOUL, R., PARTON, R. G., VILBOIS, F. & GRUENBERG, J. 2004. Role of LBPA and Alix in multivesicular liposome formation and endosome organization. *Science,* 303**,** 531-4.

MAUER, J., LUO, X., BLANJOIE, A., JIAO, X., GROZHIK, A. V., PATIL, D. P., LINDER, B., PICKERING, B. F., VASSEUR, J. J., CHEN, Q., GROSS, S. S., ELEMENTO, O., DEBART, F., KILEDJIAN, M. & JAFFREY, S. R. 2017. Reversible methylation of m(6)Am in the 5' cap controls mRNA stability. *Nature,* 541**,** 371-375.

MCALLISTER, S. S. & WEINBERG, R. A. 2014. The tumour-induced systemic environment as a critical regulator of cancer progression and metastasis. *Nat Cell Biol,* 16**,** 717-27.

MCGOUGH, I. J. & VINCENT, J. P. 2016. Exosomes in developmental signalling. *Development,* 143**,** 2482-93.

MCKENZIE, A. J., HOSHINO, D., CHA, D. J., FRANKLIN, J. L., COFFEY, R. J., PATTON, J. G. & WEAVER, A. M. 2016. KRAS-MEK signaling controls Ago2 and miRNA sorting into exosomes. *Cell Reports,* 15**,** 978-987.

MEAD, B. & TOMAREV, S. 2017. Bone Marrow-Derived Mesenchymal Stem Cells-Derived Exosomes Promote Survival of Retinal Ganglion Cells Through miRNA-Dependent Mechanisms. *Stem Cells Transl Med,* 6**,** 1273-1285.

MELO, S. A., SUGIMOTO, H., O'CONNELL, J. T., KATO, N., VILLANUEVA, A., VIDAL, A., QIU, L., VITKIN, E., PERELMAN, L. T., MELO, C. A., LUCCI, A., IVAN, C., CALIN, G. A. & KALLURI, R. 2014. Cancer exosomes perform cell-independent microRNA biogenesis and promote tumorigenesis. *Cancer Cell,* 26**,** 707-21.

MEYER, K. D. & JAFFREY, S. R. 2014. The dynamic epitranscriptome: N6-methyladenosine and gene expression control. *Nat Rev Mol Cell Biol,* 15**,** 313-26.

MEYER, K. D., SALETORE, Y., ZUMBO, P., ELEMENTO, O., MASON, C. E. & JAFFREY, S. R. 2012. Comprehensive analysis of mRNA methylation reveals enrichment in 3' UTRs and near stop codons. *Cell,* 149**,** 1635-46.

MITCHELL, D. M., LOVEL, A. G. & STENKAMP, D. L. 2018. Dynamic changes in microglial and macrophage characteristics during degeneration and regeneration of the zebrafish retina. *J Neuroinflammation,* 15**,** 163.

MITCHELL, D. M., SUN, C., HUNTER, S. S., NEW, D. D. & STENKAMP, D. L. 2019. Regeneration associated transcriptional signature of retinal microglia and macrophages. *Sci Rep,* 9**,** 4768.

MONTAGUT, C., DALMASES, A., BELLOSILLO, B., CRESPO, M., PAIRET, S., IGLESIAS, M., SALIDO, M., GALLEN, M., MARSTERS, S., TSAI, S. P., MINOCHE, A., SESHAGIRI, S., SERRANO, S., HIMMELBAUER, H., BELLMUNT, J., ROVIRA, A., SETTLEMAN, J., BOSCH, F. & ALBANELL, J. 2012. Identification of a mutation in the extracellular domain of the Epidermal Growth Factor Receptor conferring cetuximab resistance in colorectal cancer. *Nat Med,* 18**,** 221-3.

MURPHY, D. E., DE JONG, O. G., BROUWER, M., WOOD, M. J., LAVIEU, G., SCHIFFELERS, R. M. & VADER, P. 2019. Extracellular vesicle-based therapeutics: natural versus engineered targeting and trafficking. *Exp Mol Med,* 51**,** 32.

NACHTERGAELE, S. & HE, C. 2018. Chemical Modifications in the Life of an mRNA Transcript. *Annu Rev Genet,* 52**,** 349-372.

NANDROT, E. F., ANAND, M., ALMEIDA, D., ATABAI, K., SHEPPARD, D. & FINNEMANN, S. C. 2007. Essential role for MFG-E8 as ligand for alphavbeta5 integrin in diurnal retinal phagocytosis. *Proc Natl Acad Sci U S A,* 104**,** 12005-10.

NEELY, M. D., DAVISON, C. A., ASCHNER, M. & BOWMAN, A. B. 2017. From the Cover: Manganese and Rotenone-Induced Oxidative Stress Signatures Differ in iPSC-Derived Human Dopamine Neurons. *Toxicological Sciences,* 159**,** 366-379.

NIENTIEDT, C., HELLER, M., ENDRIS, V., VOLCKMAR, A. L., ZSCHABITZ, S., TAPIA-LALIENA, M. A., DUENSING, A., JAGER, D., SCHIRMACHER, P., SULTMANN, H., STENZINGER, A., HOHENFELLNER, M., GRULLICH, C. & DUENSING, S. 2017. Mutations in BRCA2 and taxane resistance in prostate cancer. *Sci Rep,* 7**,** 4574.

NISHIDA, N., YOKOBORI, T., MIMORI, K., SUDO, T., TANAKA, F., SHIBATA, K., ISHII, H., DOKI, Y., KUWANO, H. & MORI, M. 2011. MicroRNA MiR-125b is a Prognostic Marker in Human Colorectal Cancer. *Int. J. Oncol.,* 38**,** 1437-1443.

OSHIMA, K., AOKI, N., KATO, T., KITAJIMA, K. & MATSUDA, T. 2002. Secretion of a peripheral membrane protein, MFG-E8, as a complex with membrane vesicles. *Eur J Biochem,* 269**,** 1209-18.

OSTENFELD, M. S., JEPPESEN, D. K., LAURBERG, J. R., BOYSEN, A. T., BRAMSEN, J. B., PRIMDAL-BENGTSON, B., HENDRIX, A., LAMY, P., DAGNAES-HANSEN, F., RASMUSSEN, M. H., BUI, K. H., FRISTRUP, N., CHRISTENSEN, E. I., NORDENTOFT, I., MORTH, J. P., JENSEN, J. B., PEDERSEN, J. S., BECK, M., THEODORESCU, D., BORRE, M., HOWARD, K. A., DYRSKJOT, L. & ORNTOFT, T. F. 2014. Cellular disposal of miR23b by RAB27-dependent exosome release is linked to acquisition of metastatic properties. *Cancer Res,* 74**,** 5758-71.

OTTAVIANI, S., STEBBING, J., FRAMPTON, A. E., ZAGORAC, S., KRELL, J., DE GIORGIO, A., TRABULO, S. M., NGUYEN, V. T. M., MAGNANI, L., FENG, H., GIOVANNETTI, E., FUNEL, N., GRESS, T. M., JIAO, L. R., LOMBARDO, Y., LEMOINE, N. R., HEESCHEN, C. & CASTELLANO, L. 2018. TGF-beta induces miR-100 and miR-125b but blocks let-7a through LIN28B controlling PDAC progression. *Nat Commun,* 9**,** 1845.

OTTESON, D. C., CIRENZA, P. F. & HITCHCOCK, P. F. 2002. Persistent neurogenesis in the teleost retina: evidence for regulation by the growth-hormone/insulin-like growth factor-I axis. *Mechanisms of Development,* 117**,** 137-49.

PAGET, S. 1889. The Distribution of Secondary Growths in Cancer of the Breast. *The Lancet,* 133**,** 571-573.

PAN, B. T., TENG, K., WU, C., ADAM, M. & JOHNSTONE, R. M. 1985. Electron microscopic evidence for externalization of the transferrin receptor in vesicular form in sheep reticulocytes. *J Cell Biol,* 101**,** 942-8.

PAN, T. 2018. Modifications and functional genomics of human transfer RNA. *Cell Res,* 28**,** 395-404.

PANNEERDOSS, S., EEDUNURI, V. K., YADAV, P., TIMILSINA, S., RAJAMANICKAM, S., VISWANADHAPALLI, S., ABDELFATTAH, N., ONYEAGUCHA, B. C., CUI, X., LAI, Z., MOHAMMAD, T. A., GUPTA, Y. K., HUANG, T. H., HUANG, Y., CHEN, Y. & RAO, M. K. 2018. Cross-talk among writers, readers, and erasers of m(6)A regulates cancer growth and progression. *Sci Adv,* 4**,** eaar8263.

PATTERSON, E. E., HOLLOWAY, A. K., WENG, J., FOJO, T. & KEBEBEW, E. 2011. MicroRNA profiling of adrenocortical tumors reveals miR-483 as a marker of malignancy. *Cancer,* 117**,** 1630-9.

PATTON, J. G., FRANKLIN, J. L., WEAVER, A. M., VICKERS, K., ZHANG, B., COFFEY, R. J., ANSEL, K. M., BLELLOCH, R., GOGA, A., HUANG, B., L'ETOILLE, N., RAFFAI, R. L., LAI, C. P., KRICHEVSKY, A. M., MATEESCU, B., GREINER, V. J., HUNTER, C., VOINNET, O. & MCMANUS, M. T. 2015. Biogenesis, delivery, and function of extracellular RNA. *J Extracell Vesicles,* 4**,** 27494.

PEARSON, R. A., BARBER, A. C., RIZZI, M., HIPPERT, C., XUE, T., WEST, E. L., DURAN, Y., SMITH, A. J., CHUANG, J. Z., AZAM, S. A., LUHMANN, U. F. O., BENUCCI, A., SUNG, C. H., BAINBRIDGE, J. W., CARANDINI, M., YAU, K.-W., SOWDEN, J. C. & ALI, R. R. 2012. Restoration of vision after transplantation of photoreceptors. *Nature,* 485**,** 99-103.

PEARSON, R. A., GONZALEZ-CORDERO, A., WEST, E. L., RIBEIRO, J. R., AGHAIZU, N., GOH, D., SAMPSON, R. D., GEORGIADIS, A., WALDRON, P. V., DURAN, Y., NAEEM, A., KLOC, M., CRISTANTE, E., KRUCZEK, K., WARRE-CORNISH, K., SOWDEN, J. C., SMITH, A. J. & ALI, R. R. 2016. Donor and host photoreceptors engage in material transfer following transplantation of post-mitotic photoreceptor precursors. *Nat Commun,* 7**,** 13029.

PEINADO, H., ALECKOVIC, M., LAVOTSHKIN, S., MATEI, I., COSTA-SILVA, B., MORENO-BUENO, G., HERGUETA-REDONDO, M., WILLIAMS, C., GARCIA-SANTOS, G., GHAJAR, C., NITADORI-HOSHINO, A., HOFFMAN, C., BADAL, K., GARCIA, B. A., CALLAHAN, M. K., YUAN, J., MARTINS, V. R., SKOG, J., KAPLAN, R. N., BRADY, M. S., WOLCHOK, J. D., CHAPMAN, P. B., KANG, Y., BROMBERG, J. & LYDEN, D. 2012. Melanoma exosomes educate bone marrow progenitor cells toward a pro-metastatic phenotype through MET. *Nat Med,* 18**,** 883-91.

PEINADO, H., ZHANG, H., MATEI, I. R., COSTA-SILVA, B., HOSHINO, A., RODRIGUES, G., PSAILA, B., KAPLAN, R. N., BROMBERG, J. F., KANG, Y., BISSELL, M. J., COX, T. R., GIACCIA, A. J., ERLER, J. T., HIRATSUKA, S., GHAJAR, C. M. & LYDEN, D. 2017. Pre-metastatic niches: organ-specific homes for metastases. *Nat Rev Cancer,* 17**,** 302-317.

PENG, Y., BAULIER, E., KE, Y., YOUNG, A., AHMEDLI, N. B., SCHWARTZ, S. D. & FARBER, D. B. 2018. Human embryonic stem cells extracellular vesicles and their effects on immortalized human retinal Muller cells. *PLoS One,* 13**,** e0194004.

POGGIO, M., HU, T., PAI, C. C., CHU, B., BELAIR, C. D., CHANG, A., MONTABANA, E., LANG, U. E., FU, Q., FONG, L. & BLELLOCH, R. 2019. Suppression of Exosomal PD-L1 Induces Systemic Anti-tumor Immunity and Memory. *Cell,* 177**,** 414-427 e13.

QIN, X., GUO, H., WANG, X., ZHU, X., YAN, M., WANG, X., XU, Q., SHI, J., LU, E., CHEN, W. & ZHANG, J. 2019. Exosomal MiR-196a Derived from Cancer-Associated Fibroblasts Confers Cisplatin Resistance in Head and Neck Cancer through Targeting CDKN1B and ING5. *Genome Biol,* 20**,** 12.

QU, L., DING, J., CHEN, C., WU, Z. J., LIU, B., GAO, Y., CHEN, W., LIU, F., SUN, W., LI, X. F., WANG, X., WANG, Y., XU, Z. Y., GAO, L., YANG, Q., XU, B., LI, Y. M., FANG, Z. Y., XU, Z. P., BAO, Y., WU, D. S., MIAO, X., SUN, H. Y., SUN, Y. H., WANG, H. Y. & WANG, L. H. 2016. Exosome-Transmitted lncARSR Promotes Sunitinib Resistance in Renal Cancer by Acting as a Competing Endogenous RNA. *Cancer Cell,* 29**,** 653-668.

RAJARAM, K., HARDING, R. L., HYDE, D. R. & PATTON, J. G. 2014. miR-203 regulates progenitor cell proliferation during adult zebrafish retina regeneration. *Dev Biol,* 392**,** 393-403.
RAMACHANDRAN, R., FAUSETT, B. V. & GOLDMAN, D. 2010. Ascl1a regulates Müller glia dedifferentiation and retinal regeneration through a Lin-28-dependent, let-7 microRNA signalling pathway. *Nature cell biology,* 12**,** 1101-7.
RAMACHANDRAN, R., ZHAO, X.-F. & GOLDMAN, D. 2012. Insm1a-mediated gene repression is essential for the formation and differentiation of Müller glia-derived progenitors in the injured retina. *Nature cell biology,* 14**,** 1013-23.
RAMACHANDRAN, R., ZHAO, X. F. & GOLDMAN, D. 2011. Ascl1a/Dkk/beta-catenin signaling pathway is necessary and glycogen synthase kinase-3beta inhibition is sufficient for zebrafish retina regeneration. *Proc Natl Acad Sci U S A,* 108**,** 15858-63.
RAO, M. B., DIDIANO, D. & PATTON, J. G. 2017. Neurotransmitter-Regulated Regeneration in the Zebrafish Retina. *Stem Cell Reports,* 8**,** 831-842.
RAPOSO, G., NIJMAN, H. W., STOORVOGEL, W., LIEJENDEKKER, R., HARDING, C. V., MELIEF, C. J. & GEUZE, H. J. 1996. B lymphocytes secrete antigen-presenting vesicles. *J Exp Med,* 183**,** 1161-72.
RAPOSO, G. & STAHL, P. D. 2019. Extracellular vesicles: a new communication paradigm? *Nat Rev Mol Cell Biol,* 20**,** 509-510.
RAPOSO, G. & STOORVOGEL, W. 2013. Extracellular vesicles: exosomes, microvesicles, and friends. *J Cell Biol,* 200**,** 373-83.
RAYMOND, P. A., BARTHEL, L. K., BERNARDOS, R. L. & PERKOWSKI, J. J. 2006. Molecular characterization of retinal stem cells and their niches in adult zebrafish. *BMC Developmental Biology,* 6**,** 36.
RICHARDS, K. E., ZELENIAK, A. E., FISHEL, M. L., WU, J., LITTLEPAGE, L. E. & HILL, R. 2017. Cancer-Associated Fibroblast Exosomes Regulate Survival and Proliferation of Pancreatic Cancer Cells. *Oncogene,* 36**,** 1770-1778.
RIES, R. J., ZACCARA, S., KLEIN, P., OLARERIN-GEORGE, A., NAMKOONG, S., PICKERING, B. F., PATIL, D. P., KWAK, H., LEE, J. H. & JAFFREY, S. R. 2019. m(6)A enhances the phase separation potential of mRNA. *Nature,* 571**,** 424-428.
RINN, J. L. & CHANG, H. Y. 2012. Genome Regulation by Long Noncoding RNAs. *Annual Review of Biochemistry, Vol 81,* 81**,** 145-166.
ROBBINS, P. D. & MORELLI, A. E. 2014. Regulation of immune responses by extracellular vesicles. *Nat Rev Immunol,* 14**,** 195-208.
RODRIGUEZ, A., GRIFFITHS-JONES, S., ASHURST, J. L. & BRADLEY, A. 2004. Identification of mammalian microRNA host genes and transcription units. *Genome Res,* 14**,** 1902-10.
ROSKA, B. & SAHEL, J. A. 2018. Restoring vision. *Nature,* 557**,** 359-367.
ROUNDTREE, I. A., EVANS, M. E., PAN, T. & HE, C. 2017. Dynamic RNA Modifications in Gene Expression Regulation. *Cell,* 169**,** 1187-1200.
S, E. L. A., MAGER, I., BREAKEFIELD, X. O. & WOOD, M. J. 2013. Extracellular vesicles: biology and emerging therapeutic opportunities. *Nat Rev Drug Discov,* 12**,** 347-57.
SADIK, N., CRUZ, L., GURTNER, A., RODOSTHENOUS, R. S., DUSOSWA, S. A., ZIEGLER, O., VAN SOLINGE, T. S., WEI, Z., SALVADOR-GARICANO, A. M., GYORGY, B., BROEKMAN, M. & BALAJ, L. 2018. Extracellular RNAs: A New Awareness of Old Perspectives. *Methods Mol Biol,* 1740**,** 1-15.

SAKAI, W., SWISHER, E. M., KARLAN, B. Y., AGARWAL, M. K., HIGGINS, J., FRIEDMAN, C., VILLEGAS, E., JACQUEMONT, C., FARRUGIA, D. J., COUCH, F. J., URBAN, N. & TANIGUCHI, T. 2008. Secondary mutations as a mechanism of cisplatin resistance in BRCA2-mutated cancers. *Nature,* 451**,** 1116-20.

SANTANGELO, L., GIURATO, G., CICCHINI, C., MONTALDO, C., MANCONE, C., TARALLO, R., BATTISTELLI, C., ALONZI, T., WEISZ, A. & TRIPODI, M. 2016. The RNA-Binding Protein SYNCRIP Is a Component of the Hepatocyte Exosomal Machinery Controlling MicroRNA Sorting. *Cell Rep,* 17**,** 799-808.

SANTOS, M. F., RAPPA, G., KARBANOVA, J., KURTH, T., CORBEIL, D. & LORICO, A. 2018. VAMP-associated protein-A and oxysterol-binding protein-related protein 3 promote the entry of late endosomes into the nucleoplasmic reticulum. *J Biol Chem,* 293**,** 13834-13848.

SANTOS, P. & ALMEIDA, F. 2020. Role of Exosomal MiRNAs and the Tumor Microenvironment in Drug Resistance. *Cells,* 9**,** 1450.

SANTOS-FERREIRA, T., LLONCH, S., BORSCH, O., POSTEL, K., HAAS, J. & ADER, M. 2016. Retinal transplantation of photoreceptors results in donor-host cytoplasmic exchange. *Nat Commun,* 7**,** 13028.

SCHAEFER, M., KAPOOR, U. & JANTSCH, M. F. 2017. Understanding RNA modifications: the promises and technological bottlenecks of the 'epitranscriptome'. *Open Biol,* 7.

SCHMIDT, O. & TEIS, D. 2012. The ESCRT machinery. *Curr Biol,* 22**,** R116-20.

SCHMITT, A. M. & CHANG, H. Y. 2016. Long Noncoding RNAs in Cancer Pathways. *Cancer Cell,* 29**,** 452-463.

SHIFRIN, D. A., JR., DEMORY BECKLER, M., COFFEY, R. J. & TYSKA, M. J. 2013. Extracellular vesicles: communication, coercion, and conditioning. *Mol Biol Cell,* 24**,** 1253-9.

SHIRASAWA, S., FURUSE, M., YOKOYAMA, N. & SASAZUKI, T. 1993. Altered growth of human colon cancer cell lines disrupted at activated Ki-ras. *Science,* 260**,** 85-8.

SHURTLEFF, M. J., TEMOCHE-DIAZ, M. M., KARFILIS, K. V., RI, S. & SCHEKMAN, R. 2016. Y-box protein 1 is required to sort microRNAs into exosomes in cells and in a cell-free reaction. *Elife,* 5**,** e19276.

SHURTLEFF, M. J., TEMOCHE-DIAZ, M. M. & SCHEKMAN, R. 2018. Extracellular Vesicles and Cancer: Caveat Lector. *Annual Review of Cancer Biology,* 2**,** 395-411.

SHURTLEFF, M. J., YAO, J., QIN, Y., NOTTINGHAM, R. M., TEMOCHE-DIAZ, M. M., SCHEKMAN, R. & LAMBOWITZ, A. M. 2017. Broad role for YBX1 in defining the small noncoding RNA composition of exosomes. *Proc Natl Acad Sci U S A,* 114**,** E8987-E8995.

SIBBRITT, T., PATEL, H. R. & PREISS, T. 2013. Mapping and significance of the mRNA methylome. *Wiley Interdiscip Rev RNA,* 4**,** 397-422.

SILVA, A. K., LUCIANI, N., GAZEAU, F., AUBERTIN, K., BONNEAU, S., CHAUVIERRE, C., LETOURNEUR, D. & WILHELM, C. 2015. Combining magnetic nanoparticles with cell derived microvesicles for drug loading and targeting. *Nanomedicine,* 11**,** 645-55.

SIMONS, M. & RAPOSO, G. 2009. Exosomes--vesicular carriers for intercellular communication. *Curr Opin Cell Biol,* 21**,** 575-81.

SINGH, B. & COFFEY, R. J. 2014. Trafficking of epidermal growth factor receptor ligands in polarized epithelial cells. *Annu Rev Physiol,* 76**,** 275-300.

SINGH, M. S., BALMER, J., BARNARD, A. R., ASLAM, S. A., MORALLI, D., GREEN, C. M., BARNEA-CRAMER, A., DUNCAN, I. & MACLAREN, R. E. 2016. Transplanted photoreceptor

precursors transfer proteins to host photoreceptors by a mechanism of cytoplasmic fusion. *Nat Commun,* 7**,** 13537.

SKOG, J., WÜRDINGER, T., VAN RIJN, S., MEIJER, D. H., GAINCHE, L., SENA-ESTEVES, M., CURRY, W. T., CARTER, B. S., KRICHEVSKY, A. M. & BREAKEFIELD, X. O. 2008. Glioblastoma microvesicles transport RNA and proteins that promote tumour growth and provide diagnostic biomarkers. *Nature cell biology,* 10**,** 1470-6.

SLOAN, K. E., WARDA, A. S., SHARMA, S., ENTIAN, K. D., LAFONTAINE, D. L. J. & BOHNSACK, M. T. 2017. Tuning the ribosome: The influence of rRNA modification on eukaryotic ribosome biogenesis and function. *RNA Biol,* 14**,** 1138-1152.

SOMMER, S., LAVI, U. & DARNELL, J. E., JR. 1978. The absolute frequency of labeled N-6-methyladenosine in HeLa cell messenger RNA decreases with label time. *J Mol Biol,* 124**,** 487-99.

SON, B., LEE, S., YOUN, H., KIM, E., KIM, W. & YOUN, B. 2016. The Role of the Tumor Microenvironment in Therapeutic Resistance. *Oncotarget* 8**,** 3933-3945.

SQUADRITO, M. L., BAER, C., BURDET, F., MADERNA, C., GILFILLAN, G. D., LYLE, R., IBBERSON, M. & DE PALMA, M. 2014. Endogenous RNAs Modulate MicroRNA Sorting to Exosomes and Transfer to Acceptor Cells. *Cell Rep,* 8**,** 1432-46.

STATELLO, L., MAUGERI, M., GARRE, E., NAWAZ, M., WAHLGREN, J., PAPADIMITRIOU, A., LUNDQVIST, C., LINDFORS, L., COLLEN, A., SUNNERHAGEN, P., RAGUSA, M., PURRELLO, M., DI PIETRO, C., TIGUE, N. & VALADI, H. 2018. Identification of RNA-binding proteins in exosomes capable of interacting with different types of RNA: RBP-facilitated transport of RNAs into exosomes. *PLoS One,* 13**,** e0195969.

STENKAMP, D. L. 2007. Neurogenesis in the fish retina. *International Review of Cytology,* 259**,** 173-224.

STERN, J. H., TIAN, Y., FUNDERBURGH, J., PELLEGRINI, G., ZHANG, K., GOLDBERG, J. L., ALI, R. R., YOUNG, M., XIE, Y. & TEMPLE, S. 2018. Regenerating Eye Tissues to Preserve and Restore Vision. *Cell Stem Cell,* 22**,** 834-849.

STUBBS, J. D., LEKUTIS, C., SINGER, K. L., BUI, A., YUZUKI, D., SRINIVASAN, U. & PARRY, G. 1990. cDNA cloning of a mouse mammary epithelial cell surface protein reveals the existence of epidermal growth factor-like domains linked to factor VIII-like sequences. *Proc Natl Acad Sci U S A,* 87**,** 8417-21.

SUN, L., FANG, Y., WANG, X., HAN, Y., DU, F., LI, C., HU, H., LIU, H., LIU, Q., WANG, J., LIANG, J., CHEN, P., YANG, H., NIE, Y., WU, K., FAN, D., COFFEY, R. J., LU, Y., ZHAO, X. & WANG, X. 2019. miR-302a Inhibits Metastasis and Cetuximab Resistance in Colorectal Cancer by Targeting NFIB and CD44. *Theranostics,* 9**,** 8409-8425.

TAYLOR, M. R., COUTO, J. R., SCALLAN, C. D., CERIANI, R. L. & PETERSON, J. A. 1997. Lactadherin (formerly BA46), a membrane-associated glycoprotein expressed in human milk and breast carcinomas, promotes Arg-Gly-Asp (RGD)-dependent cell adhesion. *DNA Cell Biol,* 16**,** 861-9.

THERY, C. 2011. Exosomes: secreted vesicles and intercellular communications. *F1000 Biol Rep,* 3**,** 15.

THERY, C., BOUSSAC, M., VERON, P., RICCIARDI-CASTAGNOLI, P., RAPOSO, G., GARIN, J. & AMIGORENA, S. 2001. Proteomic analysis of dendritic cell-derived exosomes: a secreted subcellular compartment distinct from apoptotic vesicles. *J Immunol,* 166**,** 7309-18.

THERY, C., REGNAULT, A., GARIN, J., WOLFERS, J., ZITVOGEL, L., RICCIARDI-CASTAGNOLI, P., RAPOSO, G. & AMIGORENA, S. 1999. Molecular characterization of dendritic cell-derived exosomes. Selective accumulation of the heat shock protein hsc73. *J Cell Biol,* 147**,** 599-610.

THERY, C., WITWER, K. W., AIKAWA, E., ALCARAZ, M. J., ANDERSON, J. D., ANDRIANTSITOHAINA, R., ANTONIOU, A., ARAB, T., ARCHER, F., ATKIN-SMITH, G. K., AYRE, D. C., BACH, J. M., BACHURSKI, D., BAHARVAND, H., BALAJ, L., BALDACCHINO, S., BAUER, N. N., BAXTER, A. A., BEBAWY, M., BECKHAM, C., BEDINA ZAVEC, A., BENMOUSSA, A., BERARDI, A. C., BERGESE, P., BIELSKA, E., BLENKIRON, C., BOBIS-WOZOWICZ, S., BOILARD, E., BOIREAU, W., BONGIOVANNI, A., BORRAS, F. E., BOSCH, S., BOULANGER, C. M., BREAKEFIELD, X., BREGLIO, A. M., BRENNAN, M. A., BRIGSTOCK, D. R., BRISSON, A., BROEKMAN, M. L., BROMBERG, J. F., BRYL-GORECKA, P., BUCH, S., BUCK, A. H., BURGER, D., BUSATTO, S., BUSCHMANN, D., BUSSOLATI, B., BUZAS, E. I., BYRD, J. B., CAMUSSI, G., CARTER, D. R., CARUSO, S., CHAMLEY, L. W., CHANG, Y. T., CHEN, C., CHEN, S., CHENG, L., CHIN, A. R., CLAYTON, A., CLERICI, S. P., COCKS, A., COCUCCI, E., COFFEY, R. J., CORDEIRO-DA-SILVA, A., COUCH, Y., COUMANS, F. A., COYLE, B., CRESCITELLI, R., CRIADO, M. F., D'SOUZA-SCHOREY, C., DAS, S., DATTA CHAUDHURI, A., DE CANDIA, P., DE SANTANA, E. F., DE WEVER, O., DEL PORTILLO, H. A., DEMARET, T., DEVILLE, S., DEVITT, A., DHONDT, B., DI VIZIO, D., DIETERICH, L. C., DOLO, V., DOMINGUEZ RUBIO, A. P., DOMINICI, M., DOURADO, M. R., DRIEDONKS, T. A., DUARTE, F. V., DUNCAN, H. M., EICHENBERGER, R. M., EKSTROM, K., EL ANDALOUSSI, S., ELIE-CAILLE, C., ERDBRUGGER, U., FALCON-PEREZ, J. M., FATIMA, F., FISH, J. E., FLORES-BELLVER, M., FORSONITS, A., FRELET-BARRAND, A., et al. 2018. Minimal information for studies of extracellular vesicles 2018 (MISEV2018): a position statement of the International Society for Extracellular Vesicles and update of the MISEV2014 guidelines. *J Extracell Vesicles,* 7**,** 1535750.

THUMMEL, R., KASSEN, S. C., MONTGOMERY, J. E., ENRIGHT, J. M. & HYDE, D. R. 2008. Inhibition of Muller glial cell division blocks regeneration of the light-damaged zebrafish retina. *Developmental Neurobiology,* 68**,** 392-408.

TKACH, M. & THERY, C. 2016. Communication by Extracellular Vesicles: Where We Are and Where We Need to Go. *Cell,* 164**,** 1226-32.

TRAJKOVIC, K., HSU, C., CHIANTIA, S., RAJENDRAN, L., WENZEL, D., WIELAND, F., SCHWILLE, P., BRUGGER, B. & SIMONS, M. 2008. Ceramide triggers budding of exosome vesicles into multivesicular Endosomes. *Science,* 319**,** 1244-1247.

TURCHINOVICH, A., TONEVITSKY, A. G. & BURWINKEL, B. 2016. Extracellular miRNA: A Collision of Two Paradigms. *Trends Biochem Sci,* 41**,** 883-92.

VALADI, H., EKSTROM, K., BOSSIOS, A., SJOSTRAND, M., LEE, J. J. & LOTVALL, J. O. 2007. Exosome-mediated transfer of mRNAs and microRNAs is a novel mechanism of genetic exchange between cells. *Nat Cell Biol,* 9**,** 654-9.

VAN NIEL, G., BERGAM, P., DI CICCO, A., HURBAIN, I., LO CICERO, A., DINGLI, F., PALMULLI, R., FORT, C., POTIER, M. C., SCHURGERS, L. J., LOEW, D., LEVY, D. & RAPOSO, G. 2015. Apolipoprotein E Regulates Amyloid Formation within Endosomes of Pigment Cells. *Cell Rep,* 13**,** 43-51.

VAN NIEL, G., D'ANGELO, G. & RAPOSO, G. 2018. Shedding light on the cell biology of extracellular vesicles. *Nat Rev Mol Cell Biol,* 19**,** 213-228.

VERON, P., SEGURA, E., SUGANO, G., AMIGORENA, S. & THERY, C. 2005. Accumulation of MFG-E8/lactadherin on exosomes from immature dendritic cells. *Blood Cells Mol Dis,* 35**,** 81-8.

VICKERS, K. C., PALMISANO, B. T., SHOUCRI, B. M., SHAMBUREK, R. D. & REMALEY, A. T. 2011. MicroRNAs are transported in plasma and delivered to recipient cells by high-density lipoproteins. *Nat Cell Biol,* 13**,** 423-33.

VIHTELIC, T. S. & HYDE, D. R. 2000. Light-induced rod and cone cell death and regeneration in the adult albino zebrafish (Danio rerio) retina. *J Neurobiol,* 44**,** 289-307.

VILLARROYA-BELTRI, C., GUTIERREZ-VAZQUEZ, C., SANCHEZ-CABO, F., PEREZ-HERNANDEZ, D., VAZQUEZ, J., MARTIN-COFRECES, N., MARTINEZ-HERRERA, D. J., PASCUAL-MONTANO, A., MITTELBRUNN, M. & SANCHEZ-MADRID, F. 2013. Sumoylated hnRNPA2B1 controls the sorting of miRNAs into exosomes through binding to specific motifs. *Nat Commun,* 4**,** 2980.

WALDRON, P. V., DI MARCO, F., KRUCZEK, K., RIBEIRO, J., GRACA, A. B., HIPPERT, C., AGHAIZU, N. D., KALARGYROU, A. A., BARBER, A. C., GRIMALDI, G., DURAN, Y., BLACKFORD, S. J. I., KLOC, M., GOH, D., ZABALA ALDUNATE, E., SAMPSON, R. D., BAINBRIDGE, J. W. B., SMITH, A. J., GONZALEZ-CORDERO, A., SOWDEN, J. C., ALI, R. R. & PEARSON, R. A. 2018. Transplanted Donor- or Stem Cell-Derived Cone Photoreceptors Can Both Integrate and Undergo Material Transfer in an Environment-Dependent Manner. *Stem Cell Reports,* 10**,** 406-421.

WAN, J. & GOLDMAN, D. 2016. Retina regeneration in zebrafish. *Current Opinion in Genetics and Development,* 40**,** 41-47.

WANG, R., DONG, L.-D., MENG, X.-B., SHI, Q. & SUN, W.-Y. 2015. Unique MicroRNA Signatures Associated with Early Coronary Atherosclerotic Plaques. *Biochem. Biophys. Res. Commun.,* 464**,** 574-579.

WANG, X., LU, Z., GOMEZ, A., HON, G. C., YUE, Y., HAN, D., FU, Y., PARISIEN, M., DAI, Q., JIA, G., REN, B., PAN, T. & HE, C. 2014. N6-methyladenosine-dependent regulation of messenger RNA stability. *Nature,* 505**,** 117-20.

WASSMER, S. J., CARVALHO, L. S., GYORGY, B., VANDENBERGHE, L. H. & MAGUIRE, C. A. 2017. Exosome-associated AAV2 vector mediates robust gene delivery into the murine retina upon intravitreal injection. *Sci Rep,* 7**,** 45329.

WEI, Y., LAI, X., YU, S., CHEN, S., MA, Y., ZHANG, Y., LI, H., ZHU, X., YAO, L. & ZHANG, J. 2014. Exosomal miR-221/222 enhances tamoxifen resistance in recipient ER-positive breast cancer cells. *Breast Cancer Res Treat,* 147**,** 423-31.

WEI, Z. Y., BATAGOV, A. O., SCHINELLI, S., WANG, J. T., WANG, Y., EL FATIMY, R., RABINOVSKY, R., BALAJ, L., CHEN, C. C., HOCHBERG, F., CARTER, B., BREAKEFIELD, X. O. & KRICHEVSKY, A. M. 2017. Coding and noncoding landscape of extracellular RNA released by human glioma stem cells. *Nature Communications,* 8**,** 1145.

WEN, S. W., LIMA, L. G., LOBB, R. J., NORRIS, E. L., HASTIE, M. L., KRUMEICH, S. & MOLLER, A. 2019. Breast Cancer-Derived Exosomes Reflect the Cell-of-Origin Phenotype. *Proteomics,* 19**,** e1800180.

WIKLANDER, O. P. B., BRENNAN, M. A., LOTVALL, J., BREAKEFIELD, X. O. & EL ANDALOUSSI, S. 2019. Advances in therapeutic applications of extracellular vesicles. *Sci Transl Med,* 11.

WILLMS, E., CABANAS, C., MAGER, I., WOOD, M. J. A. & VADER, P. 2018. Extracellular Vesicle Heterogeneity: Subpopulations, Isolation Techniques, and Diverse Functions in Cancer Progression. *Front Immunol,* 9**,** 738.

WINKLER, J., ABISOYE-OGUNNIYAN, A., METCALF, K. J. & WERB, Z. 2020. Concepts of extracellular matrix remodelling in tumour progression and metastasis. *Nat Commun,* 11**,** 5120.

WOHL, S. G., HOOPER, M. J. & REH, T. A. 2019. MicroRNAs miR-25, let-7 and miR-124 regulate the neurogenic potential of Muller glia in mice. *Development,* 146.

WORTZEL, I., DROR, S., KENIFIC, C. M. & LYDEN, D. 2019. Exosome-Mediated Metastasis: Communication from a Distance. *Dev Cell,* 49**,** 347-360.

WU, B., SU, S., PATIL, D. P., LIU, H., GAN, J., JAFFREY, S. R. & MA, J. 2018a. Molecular basis for the specific and multivariant recognitions of RNA substrates by human hnRNP A2/B1. *Nat Commun,* 9**,** 420.

WU, Y., XIE, L., WANG, M., XIONG, Q., GUO, Y., LIANG, Y., LI, J., SHENG, R., DENG, P., WANG, Y., ZHENG, R., JIANG, Y., YE, L., CHEN, Q., ZHOU, X., LIN, S. & YUAN, Q. 2018b. Mettl3-mediated m(6)A RNA methylation regulates the fate of bone marrow mesenchymal stem cells and osteoporosis. *Nat Commun,* 9**,** 4772.

WYLES, J. P., MCMASTER, C. R. & RIDGWAY, N. D. 2002. Vesicle-associated membrane protein-associated protein-A (VAP-A) interacts with the oxysterol-binding protein to modify export from the endoplasmic reticulum. *J Biol Chem,* 277**,** 29908-18.

XING, Q., LI, R., XU, A., QIN, Z., TANG, J., ZHANG, L., TANG, M., HAN, P., WANG, W., QIN, C. & DU, M. 2019. Genetic variants in a long noncoding RNA related to Sunitinib Resistance predict risk and survival of patients with renal cell carcinoma. *Cancer Medicine,* 8**,** 2886-2896.

XU, C., WANG, X., LIU, K., ROUNDTREE, I. A., TEMPEL, W., LI, Y., LU, Z., HE, C. & MIN, J. 2014. Structural basis for selective binding of m6A RNA by the YTHDC1 YTH domain. *Nat Chem Biol,* 10**,** 927-9.

XU, J., CHEN, Q., TIAN, K., LIANG, R., CHEN, T., GONG, A., MATHY, N. W., YU, T. & CHEN, X. 2020. m6A methyltransferase METTL3 maintains colon cancer tumorigenicity by suppressing SOCS2 to promote cell proliferation. *Oncol Rep,* 44**,** 973-986.

YAMADA, A., HORIMATSU, T., OKUGAWA, Y., NISHIDA, N., HONJO, H., IDA, H., KOU, T., KUSAKA, T., SASAKI, Y., YAGI, M., HIGURASHI, T., YUKAWA, N., AMANUMA, Y., KIKUCHI, O., MUTO, M., UENO, Y., NAKAJIMA, A., CHIBA, T., BOLAND, C. R. & GOEL, A. 2015. Serum MiR-21, MiR-29a, and MiR-125b Are Promising Biomarkers for the Early Detection of Colorectal Neoplasia. *Clin. Cancer Res.,* 21**,** 4234-4242.

YAO, K., QIU, S., TIAN, L., SNIDER, W. D., FLANNERY, J. G., SCHAFFER, D. V. & CHEN, B. 2016. Wnt Regulates Proliferation and Neurogenic Potential of Müller Glial Cells via a Lin28/let-7 miRNA-Dependent Pathway in Adult Mammalian Retinas. *Cell Reports,* 17**,** 165-178.

YAO, K., QIU, S., WANG, Y. V., PARK, S. J. H., MOHNS, E. J., MEHTA, B., LIU, X., CHANG, B., ZENISEK, D., CRAIR, M. C., DEMB, J. B. & CHEN, B. 2018. Restoration of vision after de novo genesis of rod photoreceptors in mammalian retinas. *Nature,* 560**,** 484-488.

YUAN, S., TANG, H., XING, J., FAN, X., CAI, X., LI, Q., HAN, P., LUO, Y., ZHANG, Z., JIANG, B., DOU, Y., GOROSPE, M. & WANG, W. 2014. Methylation by NSun2 represses the levels and function of microRNA 125b. *Mol Cell Biol,* 34**,** 3630-41.

ZACCARA, S., RIES, R. J. & JAFFREY, S. R. 2019. Reading, writing and erasing mRNA methylation. *Nat Rev Mol Cell Biol,* 20**,** 608-624.

ZHANG, W., CAI, X., YU, J., LU, X., QIAN, Q. & QIAN, W. 2018a. Exosome-mediated transfer of lncRNA RP11838N2.4 promotes erlotinib resistance in non-small cell lung cancer. *Int J Oncol,* 53**,** 527-538.

ZHANG, Y., LI, M. & HU, C. 2018b. Exosomal transfer of miR-214 mediates gefitinib resistance in non-small cell lung cancer. *Biochem Biophys Res Commun,* 507**,** 457-464.

ZHANG, Z., XING, T., CHEN, Y. & XIAO, J. 2018c. Exosome-mediated miR-200b promotes colorectal cancer proliferation upon TGF-beta1 exposure. *Biomed Pharmacother,* 106**,** 1135-1143.

ZHAO, B. S., WANG, X., BEADELL, A. V., LU, Z., SHI, H., KUUSPALU, A., HO, R. K. & HE, C. 2017. m(6)A-dependent maternal mRNA clearance facilitates zebrafish maternal-to-zygotic transition. *Nature,* 542**,** 475-478.

ZHAO, Y., LI, H., FANG, S., KANG, Y., WU, W., HAO, Y., LI, Z., BU, D., SUN, N., ZHANG, M. Q. & CHEN, R. 2016. NONCODE 2016: an informative and valuable data source of long non-coding RNAs. *Nucleic Acids Res.,* 44**,** D203-D208.

ZHENG, G., DAHL, J. A., NIU, Y., FEDORCSAK, P., HUANG, C. M., LI, C. J., VAGBO, C. B., SHI, Y., WANG, W. L., SONG, S. H., LU, Z., BOSMANS, R. P., DAI, Q., HAO, Y. J., YANG, X., ZHAO, W. M., TONG, W. M., WANG, X. J., BOGDAN, F., FURU, K., FU, Y., JIA, G., ZHAO, X., LIU, J., KROKAN, H. E., KLUNGLAND, A., YANG, Y. G. & HE, C. 2013. ALKBH5 is a mammalian RNA demethylase that impacts RNA metabolism and mouse fertility. *Mol Cell,* 49**,** 18-29.

ZHENG, P., CHEN, L., YUAN, X., LUO, Q., LIU, Y., XIE, G., MA, Y. & SHEN, L. 2017. Exosomal transfer of tumor-associated macrophage-derived miR-21 confers cisplatin resistance in gastric cancer cells. *J Exp Clin Cancer Res,* 36**,** 53.

ZHOU, H., SU, J., HU, X., ZHOU, C., LI, H., CHEN, Z., XIAO, Q., WANG, B., WU, W., SUN, Y., ZHOU, Y., TANG, C., LIU, F., WANG, L., FENG, C., LIU, M., LI, S., ZHANG, Y., XU, H., YAO, H., SHI, L. & YANG, H. 2020. Glia-to-Neuron Conversion by CRISPR-CasRx Alleviates Symptoms of Neurological Disease in Mice. *Cell,* 181**,** 590-603 e16.

ZHOU, J., BENITO-MARTIN, A., MIGHTY, J., CHANG, L., GHOROGHI, S., WU, H., WONG, M., GUARIGLIA, S., BARANOV, P., YOUNG, M., GHARBARAN, R., EMERSON, M., MARK, M. T., MOLINA, H., CANTO-SOLER, M. V., SELGAS, H. P. & REDENTI, S. 2018. Retinal progenitor cells release extracellular vesicles containing developmental transcription factors, microRNA and membrane proteins. *Sci Rep,* 8**,** 2823.

ZHOU, J., WAN, J., GAO, X., ZHANG, X., JAFFREY, S. R. & QIAN, S. B. 2015. Dynamic m(6)A mRNA methylation directs translational control of heat shock response. *Nature,* 526**,** 591-4.

ZHU, X., SHEN, H., YIN, X., YANG, M., WEI, H., CHEN, Q., FENG, F., LIU, Y., XU, W. & LI, Y. 2019. Macrophages derived exosomes deliver miR-223 to epithelial ovarian cancer cells to elicit a chemoresistant phenotype. *J Exp Clin Cancer Res,* 38**,** 81.

ZITVOGEL, L., REGNAULT, A., LOZIER, A., WOLFERS, J., FLAMENT, C., TENZA, D., RICCIARDI-CASTAGNOLI, P., RAPOSO, G. & AMIGORENA, S. 1998. Eradication of established murine

tumors using a novel cell-free vaccine: dendritic cell-derived exosomes. *Nat Med,* 4**,** 594-600.

ZOU, F., TU, R., DUAN, B., YANG, Z., PING, Z., SONG, X., CHEN, S., PRICE, A., LI, H., SCOTT, A., PERERA, A., LI, S. & XIE, T. 2020. Drosophila YBX1 homolog YPS promotes ovarian germ line stem cell development by preferentially recognizing 5-methylcytosine RNAs. *Proc Natl Acad Sci U S A,* 117**,** 3603-3609.